Author:
Wiseman, Beth E

Title:
LC3-associated phagocytosis and its potential neuroinflammatory role in Parkinson's Disease

University of BRISTOL

LC3-associated phagocytosis and its potential neuroinflammatory role in Parkinson's Disease

Bethan Wiseman

August 2023

A dissertation submitted to the University of Bristol in accordance with the requirements for award of the degree of MSc by Research in the School of Biochemistry, Faculty of Life Sciences.

Word count: 16,104

Abstract

Parkinson's disease (PD) is a neurodegenerative movement disorder characterised by the progressive loss of dopaminergic neurons (vmDANs) in the ventral midbrain. Post-mortem studies have determined that neuroinflammation- orchestrated by glial cells (astrocytes, microglia)- accompanies PD and that chronic glial reactivity in a pro-inflammatory environment is a key contributing factor. LC3-associated phagocytosis (LAP) directs phagocytic cargo to degradative lysosomes using selective components of the autophagy machinery, and is dependent on the actions of Rubicon. LAP dampens macrophages inflammation via suppression of pro-inflammatory cytokines (e.g IL-6, IL-1β, CXCL10), with Rubicon depletion concomitantly causing elevated inflammation. Whilst there is emerging evidence that glia use LAP to remove axon debris in models of CNS injury, its potential involvement in neuroinflammatory PD (patho)physiology has not been explored. The current study used vmDANs, ventral midbrain astrocytes (vmAstros) and midbrain conditioned microglia (vmMicroglia) derived from human induced pluripotent stem cells to model neuronal debris clearance and the inflammatory response in PD. As proof of concept, we showed that vmAstros and vmMicroglia phagocytosed zymosan into $LC3^{+ve}$ LAPosomes. Additionally, when vmAstros were activated to a pro-inflammatory phenotype characteristic of PD, the rate of canonical phagocytosis was not influenced by vmAstro reactive status; however, the number of $LC3^{+ve}$ LAPosomes after LAP induction with zymosan significantly decreased. This suggests our inflammatory vmAstros were LAP-deficient which could have important implications to local midbrain pathology. vmDAN fragments were also employed as physiologically relevant phagocytic cargo to monitor the LAP response in our PD-like model. However, no pro- or anti-inflammatory response was detected in wild-type or Rubicon-deficient vmAstros challenged with vmDAN corpses. These results indicate several amendments to our *in vitro* model of human neuroinflammation are required to fully characterise the protective roles of LAP and the consequence of LAP-deficiency in the ventral midbrain and in the context of PD.

Acknowledgements

I would like to start by thanking my supervisor Professor Jon Lane for opening up his resources to allow me to participate in this extremely interesting area of research and for providing constant guidance and encouragement over the past year.

I would also like to thank Avijit Nair for dedicating his time to teach me so many of the techniques that I present here in this report. I would also like to thank Shiza Shaikh and Annie Dewitz for providing me with invaluable cell culture training and expertise. Finally, I would like to thank the remaining members of the Lane lab Dr Madhu Kollardy, Becky Sipthorpe, and David Alliband for always being available to assist me with any issues and answer any questions.

I have learnt a great deal in this past year and I look forward to my ongoing journey in research and academia.

Author declaration

I declare that the work in this dissertation was carried out in accordance with the requirements of the University's *Regulations and Code of Practice for Research Degree Programmes* and that it has not been submitted for any other academic award. Except were indicated by specific reference in the text, the work is the candidate's own work. Work done in collaboration with, or with the assistance of, other, is indicated as such. Any views expressed in the dissertation are those of the author.

SIGNED: …Bethan Wiseman…….. DATE: …15/08/23……

Contents

Table of figures

Table of tables

Abbreviations

ACM	Astrocyte conditioned media
AML	Acute myeloid leukemia
APS	Ammonium persulfate
ATG	Autophagy-related
BafA1	Bafilomycin A1
BBB	Blood brain barrier
BDNF	Brain-derived neurotrophic factor
BMM	Bone marrow macrophages
BMP	Bone morphogenetic protein
BSA	Bovine serum albumin
CASM	Conjugation of ATG8s to single membrane
CMA	Chaperone-mediated autophagy
CNS	Central nervous system
DABCO	4-diazabicylo[2.2.2]octane
DAMPs	Damage associated molecular patters
db-cAMP	Dibutyryl- cyclic adenosine monophosphate
DTT	Dithiothreitol
E8	Essential 8 Basal media
E8 flex	Essential 8 Flex Basal media
EB	Embroid bodies
EDTA	Ethylenediaminetetraacetic acid
EGF	Epidermal growth factor
EGF	Epidermal growth factor
ELISA	Enzyme-linked immunosorbent assay
ER	Endoplasmic reticulum
ESCs	Embryonic stem cells
FACS	Fluorescent activated cell sorting
FBS	Fetal bovine serum
GABARAP	Gamma-aminobutyric acid receptor-associated protein
GDNF	Glial-derived neurotrophic factor
GFAP	Glial fibrillary acidic protein
h	Hour
HBSS	Hanks balanced salt solution
HD	Huntington’s disease
hiPSCs	Human induced pluripotent stem cells
HRP	Horse-radish peroxidase
HSP	Heat shock protein
IFN	Interferon
IL	Interleukin
IRBD	Idiopathic rapid-eye-movement sleep behavior disorder
ITC	IL-1α, TNF-α, and C1q
LAM	LC3-associated macropinocytosis
LANDO	LC3-associated endocytosis
LAP	LC3-associated phagocytosis
LC3	Light chain 3
LIF	Leukaemia inhibitory factor
LPS	Lipopolysaccharide
MPCs	Microglia-like progenitor cells
MPM	Microglia progenitor medium
MSCF	Macrophage colony stimulating factor

NADPH	Nicotinamide adenine dinucleotide phosphate
NAS2	Normal α-syn
NEAA	Non essential amino acids
NF-κB	Nuclear factor-κB
NMDA	N-methyl-D-aspartate
NOX	NADPH oxidase
ns	Not-significant
NSAIDs	Non-steroidal anti-inflammatory drugs
PBS	Phosphate-buffered saline
PBS-tx	PBS with Triton X-100
PD	Parkinson's disease
PE	Phosphatidylethanolamine
PFA	Paraformaldehyde
PI3KC3	Phosphatidylinositol 3-Kinase Catalytic Subunit Type 3
PI3P	Phosphatidlinosoitol-3-phosphate
POS	Photoreceptor outer segments
PS	Phosphatidylserine
qRT-PCR	Real time quantitative reverse transcription polymerase chain reaction
RIPA	Radioimmunoprecipitation
RISC	RNA-induced silencing
ROS	Reactive oxygen species
RPE	Retinal pigment epithelium
RT	Room temperature
SCF	Stem cell factor
SCNA	α-syn gene
SDS	Sodium Dodecyl sulfate
SHH	Sonic hedgehog
shRNA	Short hair RNA
siRNA	Short interfering RNA
SLE	Systemic lupus erythematosus
SNARE	Soluble NSF attachment protein receptor
SNpc	Substantia nigra pars compacta
TAM	Tumour associated macrophages
TBS-tw	TBS with Tween-20
TEMED	Tetramethylethylenediamine
TGN	*Trans*-golgi network
TH	Tyrosine hydroxylase
TLR	Toll-like receptor
TNF	Tumour necrosis factor
TUJ1	Neuron specific class III beta-tubulin
VEGF	Vascular endothelial growth factor
vmAPCs	Ventral midbrain astrocyte progenitor cells
vmAstros	Ventral midbrain astrocytes
vmDANs	Ventral midbrain dopaminergic neurons
vmMicroglia	Ventral midbrain microglia
vmNPCs	Ventral midbrain neural progenitor clels
α-syn	α-synuclein

1. Introduction

1.1 The aetiology and pathogenesis of Parkinson's disease

Parkinson's disease (PD), first described in 1817 by James Parkinson, is the second most common neurodegenerative disorder estimated to affect more than 10 million people worldwide (Ball *et al*, 2019). PD is a slowing progressing neurological disorder causing motor symptoms that develop and increase in severity over time (Sveinbjornsdottir, 2016; Bloem, Okun & Klein, 2021). The clinical presentation of PD is typified by aberrant motor function with symptoms including rigidity, hypokinesia, and tremor (Sveinbjornsdottir, 2016; Bloem, Okun & Klein, 2021). Other manifestations include dysautonomic symptoms, psychiatric symptoms, and sleep disturbances (Sveinbjornsdottir, 2016; Bloem, Okun & Klein, 2021). While current treatments aim to ameliorate these symptoms, to date, the aetiology of PD is not well understood and there is no cure.

A major hallmark of PD is the loss of ventral midbrain dopaminergic neurons (vmDANs) in the substantia nigra pars compacta (SNpc) (Forno, 1996). vmDANs synthesize the neurotransmitter dopamine which constitutes the major source of dopamine in the CNS: important for voluntary movement as well as emotion-driven behaviour such as motivation and reward (Chinta & Anderson, 2005). vmDANs from the SNpc project to the putamen and caudate nucleus of the dorsal striatum (Moore, 2003). Neural projections to the dorsal striatum contribute to the nigrostriatal pathway, and loss of nigrostriatal dopaminergic innervation is responsible for the motor defects in PD (Fearnley & Lees, 1991). PD has widespread ramifications and neuronal loss spreads to other areas of the brain as the disease progresses (Schapira, Chaudhuri & Jenner, 2017). For example, patient studies identified denervation in serotonergic (Kish *et al*, 2008), cholinergic (Müller & Bohnen, 2013), noradrenergic (Nahimi *et al*, 2018), and pyramidal neurons (MacDonald & Halliday, 2002). Cellular and molecular changes linked to neuronal degeneration include the accumulation of cytoplasmic inclusions of insoluble α-synuclein (α-syn) aggregates, termed Lewy bodies

(Spillantini *et al*, 1998; Polymeropoulos *et al*, 1997), mitochondrial or lysosomal dysfunction (Nguyen *et al*, 2019; Burbulla *et al*, 2017), oxidative stress (Blesa *et al*, 2015; Dias, Junn & Mouradian, 2013) and neuroinflammation (Stokholm *et al*, 2017; Williams-Gray *et al*, 2016; Gelders, Baekelandtan & Van der Perren, 2018; Hall *et al*, 2018) (Fig.1).

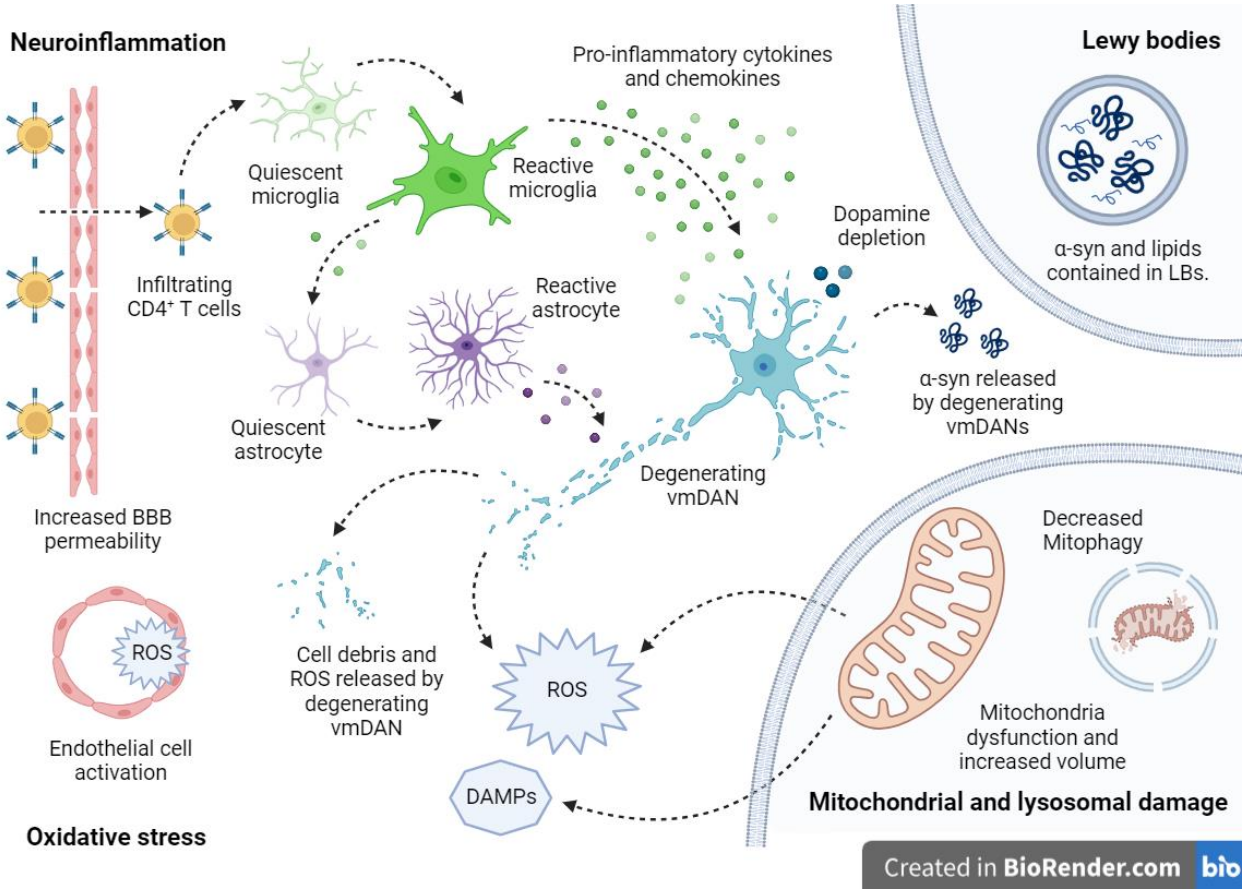

Figure 1. Cellular changes associated with the progression of PD.

Hallmarks of PD at the cellular level include defective mitophagy and mitochondrial dysfunction culminating in increased generation of reactive oxygen species (ROS) release of damage associated molecular patterns (DAMPs). The accumulation of α-syn, ROS and DAMPs can activate glial cells, alongside cells of the innate immune system, prompting neuroinflammatory signalling which can accelerate the loss of vmDANs in PD (adapted from Castillo-Rangel *et al*, 2023).

1.2 Neuroinflammation in PD

Several studies have highlighted an association between PD and neuroinflammation. Neuroinflammation is the nervous system's innate immune response to promote repair following an injury or during disease (Kwon & Koh, 2020). The neuroinflammatory processes are orchestrated by microglia and astrocytes (the "glia") which become activated during disease and display morphological and functional transformation (Fig.2) (Liddelow & Barres, 2017; Sevenich, 2018). Glia activation, or 'gliosis', refers to a phenotypic shift underpinned by changes in gene expression with associated altered glial secretory profiles triggering altered migration, proliferation, and phagocytosis (Liddelow & Barres, 2017; Sevenich, 2018). Patient post-mortem analysis has identified activation of glial cells in the PD brain, while elevated pro-inflammatory signalling molecules are commonly detected in PD patients (McGeer *et al*, 1988). More recently, neuroinflammation was suggested to even contribute to PD pathogenesis. For example, using mouse models it was identified that neuroinflammation can decrease the survival of vmDANs (Koprich *et al*, 2008). Degenerating neurons release cell debris, pro-inflammatory cytokines such as IL-1α, ROS, and α-syn resulting in sustained glial activation fashioning a positive feedback loop between glia reactivity, neuronal loss and chronic neuroinflammation (Arena *et al*, 2022). Therefore, growing interest has been directed toward understanding the role of glia during PD-related pathology.

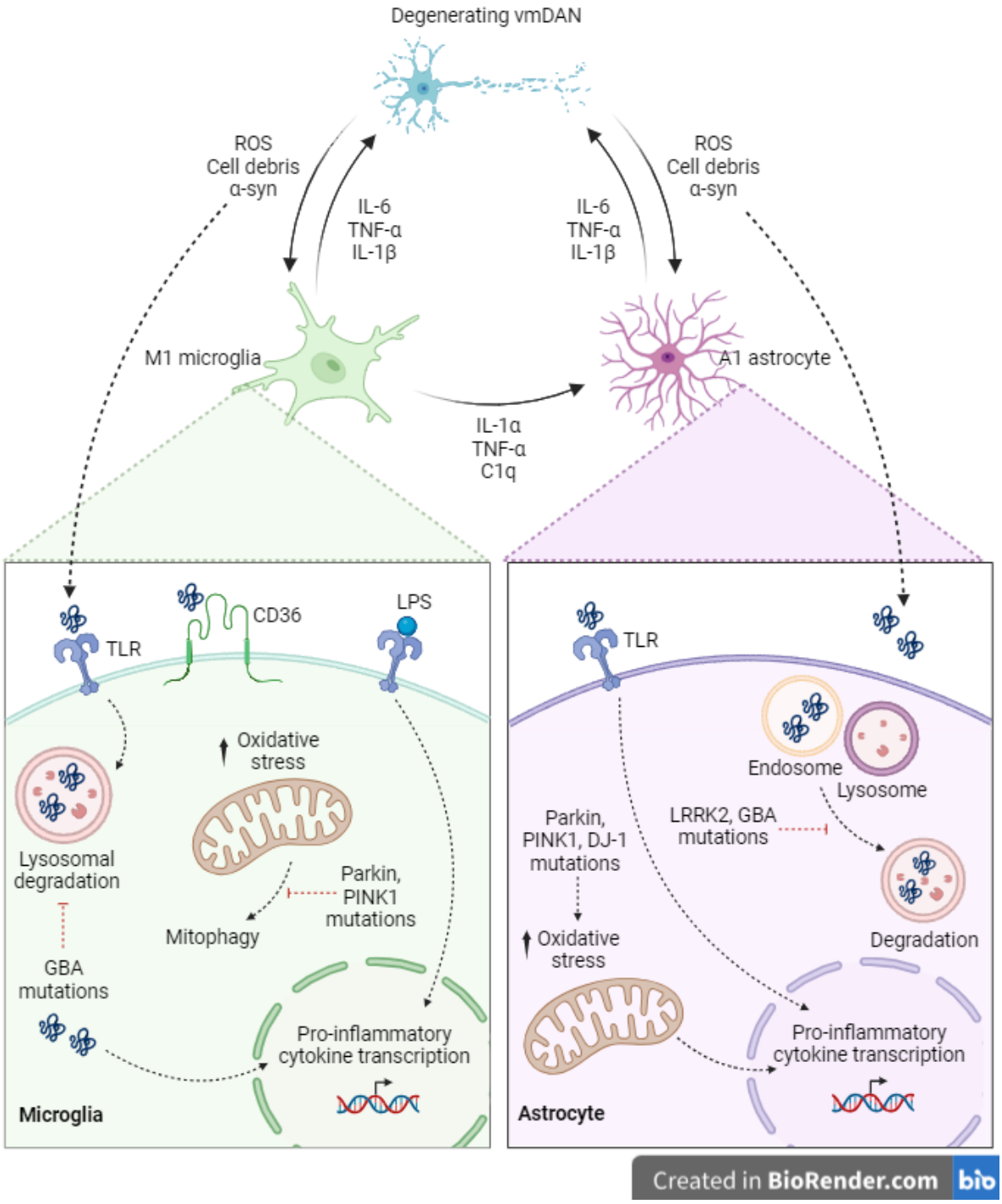

Figure 2. The neuroinflammatory loop in PD.

Activated microglia release pro-inflammatory cytokines which activate astrocytes. Reactive astrocytes and microglia release neurotoxic pro-inflammatory cytokines leading to the loss of vmDANs. Degenerating vmDANs release cell debris, ROS and α-syn which augments the pro-inflammatory signalling cascade orchestrated by glial cells. Astrocytes and microglia are also associated with mutations in lysosomal degradation pathways (GBA and LRRK2 mutations) resulting in inefficient clearance of pathological α-syn released from neurons accelerating the neuroinflammatory response. Furthermore, mutations in PINK1, Parkin and DJ-1 in astrocytes and microglia triggers mitochondrial dysfunction, oxidative stress and enhanced neuroinflammatory signalling in PD (adapted from Kam *et al*, 2020).

1.3 Microglia in PD

Microglia are immunecompetent, phagocytic cells equating to 5-12% of all cells within the central nervous system (CNS) (Lawson *et al*, 1990). Microglia are derived from myeloid progenitors in the primitive yolk sac which migrate to the brain parenchyma during mid-embryonic development (Ginhoux *et al*, 2010). Microglia survey the environment by extending their processes to monitor synaptic function, entry of pathogens and activation of neurons (Hickman *et al*, 2018; Reemst *et al*, 2016; Elmore *et al*, 2018). In health, microglia participate in neuromodulation, synaptic plasticity, learning, and memory formation (Cornell *et al*, 2022).

Microglia can be activated by a variety of stimuli and assume a M1 pro-inflammatory or M2 anti-inflammatory phenotype (Liddelow & Barres, 2017). Activation of the former is observed during PD which accompanies and/or pre-empts vmDAN degeneration (McGeer *et al*, 1993). For example, longitudinal follow up from patients with idiopathic rapid-eye-movement sleep behaviour disorder (IRBD) identified patients with activated microglia and neuroinflammation predisposed for developing parkinsonism (Stokholm *et al*, 2017). Several proinflammatory cytokines including interferon (IFN)-γ and tumour necrosis factor (TNF)-α can polarize microglia and, in turn, microglia secrete neurotoxic pro-inflammatory signalling molecules including interleukin (IL)-6, IL-1β, and TNF-α (Subhramanyam *et al*, 2019). Alternatively, microglia can be activated following exposure to the bacterial endotoxin lipopolysaccharide (LPS) via stimulation of toll-like receptor 4 (TLR4) (Nakamura, Si & Kataoka, 1999; Subhramanyam *et al*, 2019). In rodent models, TNF-α inflammatory signalling caused 23% loss of vmDANs 7 months post LPS injection (Gao *et al*, 2002). Correspondingly, knockout of TLR4 (required for pro-inflammatory LPS signalling) reduced the number of activated microglia in this setting and was neuroprotective against vmDAN degeneration (Noelker *et al*, 2013). This exemplifies the contribution of microglia-mediated neurotoxicity during the progression of PD.

1.4 Astrocytes in PD

Astrocytes are stellate cells equating to 50% of the glia population and between 20-50% of all cells across different brain regions (Montgomery, 1994). Astrocytes are derived from neural progenitor cells migrating from the subventricular zone along radial glia processes to colonize all areas in the CNS (Molofsky & Deneen, 2015). Astrocytes participate in the maintenance of the blood brain barrier (BBB) and exhibit neuroprotective roles via neurotransmitter recycling, guiding axon projections, stimulating neurite growth, and providing trophic support to neurons (Linnerbauer & Rothhammer, 2020). For example, astrocytes secrete various neurotropic molecules including glial-derived neurotrophic factor (GDNF) and brain-derived neurotrophic factor (BDNF), particularly important for the development and survival of vmDANs (Miyazaki & Asanuma, 2020; Booth, Hirst & Wade-Martinis, 2017). Like microglia, astrocytes also possess important phagocytic functions. For example, a recent study demonstrated that astrocytes compensate for phagocytic roles when microglia are impaired (Konishi *et al*, 2020).

Following an insult or during disease, astrocytes can be activated to pro-inflammatory or anti-inflammatory phenotypes (A1 and A2, respectively) contingent on the initial stimulus (Linnerbauer & Rothhammer, 2020). Astrocytes respond via varied mechanisms including phagocytosing synapses (Chung *et al*, 2013) or cellular debris (Tasdemir-Yilmaz & Freeman, 2014), and forming scars to encapsule necrotic lesions (Anderson *et al*, 2016). Several markers have been identified to help distinguish the A2 from the A1 astrocyte phenotype. For example, ICAM1 (a transmembrane glycoprotein) and C3 (an immune complement protein) are preferentially upregulated in A1 astrocytes whereas PTX3 (a pattern recognition molecule) is preferentially upregulated in A2 astrocytes (Fan & Huo, 2021; Dietrich, 2002). In PD, astrocyte A1 activation stimulates proliferation and triggers upregulation of the intermediate filament glial fibrillary acidic protein (GFAP) promoting migration (Miyazaki & Asanuma, 2020). A1 astrocytes lose most normal astrocyte functions and are neurotoxic hindering neuronal survival, growth, and synaptogenesis (Booth, Hirst & Wade-Martinis,

2017; Liddelow & Barres, 2017). Furthermore, astrocytes are responsible for maintenance of the BBB, which has been reported to be disrupted in PD patients (Gray & Woulfe, 2015; Booth, Hirst & Wade-Martinis, 2017). Microglia drive the formation of pro-inflammatory astrocytes via secretion of IL-1α, TNF-α, and C1q (Liddelow *et al*, 2017). A1 activated astrocytes secrete a variety of pro-inflammatory cytokines and chemokines including IL-6, IL-1β, and TNF-α, augmenting neuroinflammation and neurotoxicity (Liddelow & Barres, 2017). Accordingly, blocking microglia-mediated A1 astrocyte conversion is neuroprotective in PD models (Yun *et al*, 2018).

1.5 Glial regional heterogeneity and susceptibility to PD

vmDANs are the first class of neurons that are susceptible to degeneration in PD, stimulating interest in understanding the functional differences in neighbouring midbrain glial cells, as opposed to these residing in other brain regions.

Several studies have revealed regional heterogeneity of astrocytes across the adult brain. For example, a wide array of genes has been found to be differently expressed in midbrain astrocytes, including but not limited to genes encoding glycoproteins (Barbin *et al*, 1988), dopamine receptors (Reuss *et al*, 2000), neuropeptides (Batter & Kessler, 1991), and N-methyl-D-aspartate (NMDA) receptors (Karavanova *et al*, 2007). GFAP, traditionally used as a marker to assess astrocyte reactivity, was found to be expressed more strongly in white matter astrocytes compared to those residing in grey matter (Cahoy *et al*, 2008). The differences in gene expression correspond to functional variations. For example, astrocytes from different brain regions differentially stimulate neurite growth (Garcia *et al*, 1995). Furthermore, it has been shown that astrocytes in the midbrain express specific proteins for communication with local populations of vmDANs (Zhang & Barres, 2010). Therefore, this supports the use of region-specific astrocytes in PD research.

The presence of heterogeneity of microglia across different brain regions is contentious and relatively under investigated. Ideas that microglia might be regionally diverse were largely

overlooked until recent years, given that microglia are motile cells able to migrate to different areas of the brain (Tay *et al*, 2017). One study reported considerable differences in microglia phenotypes across BG nuclei regarding lysosome content, membrane properties, and anatomical features (De Biase *et al*, 2017). Regional differences in microglial transcriptomics have also been reported regarding immune function and sensitivity to aging (Grabert *et al*, 2016). In contrast, similar transcription profiles were recorded in adult microglia expressing homeostatic genes across different brain regions (Li *et al*, 2019). Overall, due to these conflicting reports, the possibility of regional differences in microglia toward disease progression should be considered in PD research.

1.6 Use of hiPSCs for modelling human neuroinflammation

The use of human relevant cellular platforms to study human development and disease is critical for accurate human modelling and for accelerating the discovery of targeted therapies (Nishikawa, Goldstein & Nierras, 2008). Human induced pluripotent stem cells (hiPSCs) were first described in 2006, and have since been used to model a variety of human diseases. HiPSCs are produced from genetic remodelling of human somatic cells, typically fibroblasts, via a cocktail of transcription factors including OCT4, SOX2, MYC and KLF4 (Nishikawa, Goldstein & Nierras, 2008). Characteristically, hiPSCs have embryonic stem (ES) cell fates and can proliferate in their unspecialized state or differentiate into any human cell type (Nishikawa, Goldstein & Nierras, 2008). Hence, in this study, neural and hematopoietic induction of hiPSCs were used to closely recapitulate human neuroinflammation.

HiPSCs provide the opportunity for developing a human *in vitro* model to study neuroinflammation, offering unprecedented advantages over primary human cells which are difficult to isolate and ethically challenging (D'Souza *et al*, 2021). Furthermore, hiPSCs allow investigation of early hallmarks pre-empting PD, unlike patient post-mortem samples which only show end-stage pathology. Efficient and scalable protocols for deriving glial cells and

neurons have been established, and appropriate neural patterning of hiPSCs can generate region-specific populations of cells. Modelling the initial inflammatory changes in PD can be achieved by ventral midbrain induction of hiPSCs, for example. Terminally differentiated glial cells and neurones can be studied in monoculture and co-culture systems, or the culture media transferred between cell types.

Of note, hiPSCs have several limitations particularly for use in age-related models. For example, hiPSCs are epigenetically reverted to embryonic state, and therefore, cannot be easily used for studying diseases associated with ageing, like PD. Few novel techniques have been described, including induced (i)neurons (direct conversion of somatic cells to neurons) which bypass cellular rejuvenation associated with reprogramming somatic cells to hiPSCs; however, more work is required to establish this model for use in glial cells (Mertens *et al*, 2018; Torper *et al*, 2013).

1.7 Autophagy

Autophagy is a catabolic pathway evolutionary conserved from yeast to human (Glick, Barth & Macleod, 2010). Autophagy directs cytoplasmic material to degradative lysosomes and the breakdown products (amino acids and lipids etc.) serve as input for biosynthesis pathways (Glick, Barth & Macleod, 2010). There are three different types of autophagy that have been identified in mammalian cells:

- **Chaperone mediated autophagy (CMA)**: delivers proteins from the cytoplasm to the lysosome in a one-by-one manner (Kaushik & Cuervo, 2018). Proteins that contain the KFERQ-consensus motif can bind to the cytosolic chaperone heat shock protein 70 (HSC70) for internalization by the lysosome (Kaushik & Cuervo, 2018).
- **Microautophagy**: the lysosome directly ingulfs portions of the cytosol by invaginating its membrane forming vesicles that bud into the lysosomal lumen (Li, Li & Bao, 2021).

- **Macroautophagy** (herein referred to as autophagy): delivers portions of the cytoplasm including cytoplasmic components and organelles to lysosomes via autophagosomes (Lamb, Yoshimori & Tooze, 2013).

Autophagy is regulated by the expression of autophagy related genes (ATGs) and currently, over 30 ATGs have been identified in regulating autophagosome formation, maturation and cargo degradation (Mizushima, 2007). Autophagosomes are double membraned vesicles formed de novo via an isolation membrane, termed the phagophore, which expands forming the autophagosome: meanwhile sequestering portions of the cytoplasm (Mizushima, 2007). A subfamily of ATG8 proteins is required for autophagosome formation and maturation by virtue of covalent attachment to phosphatidylethanolamine (PE) on autophagic membranes (Barz *et al*, 2021). Homologues of ATG8s that have been identified in mammals include the microtubule-associated proteins 1A/1B light chain 3 (LC3A, LC3B, LC3C) and the gamma-aminobutyric acid receptor-associated protein subfamily (GABARAP, GABARAPL1, GABARAPL2/GATE-16) (Barz *et al*, 2021). ATG8 lipidation promotes the selection of cargo, closure of the autophagosome, and fusion with the lysosomal membrane (Heckmann & Green, 2019).

Autophagy was initially characterised as a pathway for promoting nutrient recycling in response to starvation (Lamb, Yoshimori & Tooze, 2013). In contrast to bulk degradation, autophagy also contributes to fine-tuned cellular responses rendering it essential for cellular homeostasis (Metcalf *et al*, 2012). For example, autophagy selectively removes abnormal aggregated or misfolded proteins and damaged organelles (Metcalf *et al*, 2012). This autophagy specificity is achieved by autophagic cargo receptors that coordinate synchronized binding of ATG8-family proteins with the relevant cargo: either directly or indirectly via polyubiquitin chains attached to the cargo surface (Zaffagnini & Martens, 2016). Identification of selective autophagic mechanisms have surged over the past decades and depending on the cargo, the process can be termed mitophagy for the selective removal of damaged mitochondria, aggrephagy for the selective degradation of protein aggregates,

endoplasmic reticulum (ER)-phagy for the selective removal of damaged ER, amongst many others (Fimia, Kroemer & Piacentini, 2013).

1.8 Autophagy in PD

Neurons are post-mitotic, and their high metabolic demands render them particularly sensitive to oxidative stress (Ghandi & Abramov, 2012; Maday & Holzbaur, 2016). Therefore, quality control mechanisms, like autophagy, are essential for long-term viability of neurons (Maday & Holzbaur, 2016). Autophagy is spatiotemporally regulated in neurons, commencing with autophagosome formation in the distal axon which then travels to the soma for maturation and fusion with lysosomes (Maday & Holzbaur, 2016). An increased number of autophagosomes were found in the SNpc of PD-patient post-mortem samples (Dehay *et al*, 2010). Therefore, this stimulates interest into how autophagy might be involved in PD pathology.

Accumulating evidence implicates autophagy dysfunction in PD. For example, defective mitophagy has been associated with autosomal recessive forms of early-onset PD (Truban *et al*, 2017). vmDANs are especially sensitive to autophagy deficits, with *in vitro* studies finding that autophagy deficient vmDANs have axonal and dendritic dystrophy and reduced dopamine content (Friedman *et al*, 2012). α-syn, the protein which accumulates in the brains of PD patients, is subject to autophagy degradation and dysfunctional autophagy increases endogenous levels of α-syn in neurons (Sahoo *et al*, 2022; Sato *et al*, 2018). The presence of accumulated α-syn triggers neuronal damage which pre-empts vmDAN loss in PD (Tu *et al*, 2021). Additionally, α-syn can be degraded by CMA, however, mutant forms of α-syn cannot be efficiently degraded by this pathway (Martinez-Vicente *et al*, 2008). In contrast to autophagy dysfunction promoting α-syn accumulation in PD, α-syn has been reported to disrupt degradation of cargo by autophagy. For example, mutant α-syn impedes other substates being degraded via CMA (Martinez-Vicente *et al*, 2008). Furthermore, α-syn was found to suppress microglial autophagy and promote neurodegeneration in a mouse model

of PD (Tu *et al*, 2021). Conversely, upregulating the degradation of α-syn by autophagy protects against α-syn mediated toxicity in PD (Guo *et al*, 2021; Decressac *et al*, 2013). Therefore, dysfunctional autophagy and CMA are closely linked to disrupting CNS homeostasis and promoting PD pathology.

Recent evidence also proposes a relationship between autophagy and neuroinflammation in PD. For example, in a murine model of PD, dysfunctional autophagy triggered activation of the NLRP3 inflammasome which elevated neuroinflammatory signalling (Han *et al*, 2019). In turn, increased expression of pro-inflammatory cytokines, specifically TNF-α, dysregulated autophagy in neurons and microglia (Jin *et al*, 2018). Furthermore, activation of M1 pro-inflammatory microglia can be stimulated by the suppression of autophagy genes (Jin *et al*, 2018). Therefore, autophagy might be involved in regulating microglia activation and promoting neuroinflammatory responses. A recent study also found that activated microglia secrete pro-inflammatory chemokines CCL3, CCL4 and CCL5 which activate the neuronal receptor CCR5 suppressing neuronal autophagy (Festa *et al*, 2023). This suggests that glial-derived inflammation can reciprocally regulate autophagy. Few studies have explored whether this relationship could be exploited therapeutically. For example, inducing phagocytosis and degradation of tissue debris via specialist non-canonical autophagy promoted neuroinflammatory recovery in an experimental autoimmune encephalomyelitis animal model (Berglund *et al*, 2020). Overall, our understanding of the relationship between autophagy and neuroinflammation in PD is growing, however, the mechanisms controlling this interaction are still largely unknown.

1.9 Non-canonical autophagy

Non-canonical variations of autophagy have been identified under specific cellular circumstances. One form of non-canonical autophagy utilises alternative routes during autophagosome formation using only a proportion of the components of the autophagy machinery (Nishida *et al*, 2009). For example, in canonical autophagy, ATG5 and ATG7 are

required during lipidation of ATG8s to the growing phagophore (Nishida *et al*, 2009). However, ATG5/ATG7-independent formation of autophagosomes via Rab9-dependent fusion of vesicles derived from the trans-golgi with late endosomes have been identified (Nishida *et al*, 2009). Therefore, ATG5/ATG7-deficient cells are still able to degrade autophagic cargo (Nishida *et al*, 2009).

Another form of non-canonical autophagy is the conjugation of a subfamily of ATG8s to single membranes (CASM), as opposed to double-membraned autophagosomes in canonical autophagy (Durgan & Florey, 2022). ATG5, ATG12 and ATG16 form the ATG16L complex and membrane localisation of ATG16L is required for ATG8 conjugation in both canonical and non-canonical autophagy (Fujita *et al*, 2008). While CASM shares similarities to canonical autophagy with respect to the ATG8 conjugation step, cumulative work has revealed some key differences in their regulatory triggers and molecular mechanisms. For example, in canonical autophagy, ATG8 lipidation to PE is required for the maturation of double-membraned autophagosomes (Ichimura *et al*, 2000); however, although ATG8-PE conjugation has been reported during CASM (Martinez *et al*, 2015), recent work has determined that the alternative conjugation of ATG8 to phosphatidylserine (PS) is likewise employed (Durgan *et al*, 2021). This provides evidence for diverging mechanisms between these closely related pathways (Durgan *et al*, 2021). During CASM, LC3 lipidated vesicles fuse with late endosomes or lysosomes for the degradation of engulfed material (Durgan & Florey. 2022). A physiological role of CASM was recently reported during the removal of damaged lysosomes which is mechanistically distinct from lysophagy (selective degradation of lysosomes by autophagy) (Cross *et al*, 2023). Furthermore, CASM has been shown to have key roles in restoring plasma membrane integrity in models of membrane stress: a process termed LC3-associated macropinocytosis (LAM) (Kumar, Jia & Derectic, 2021). Other varieties of CASM include LC3-associated endocytosis (LANDO) and LC3-associated phagocytosis (LAP) (Durgan & Florey, 2022).

1.10 LC3-associated phagocytosis (LAP)

LAP is a novel form of non-canonical autophagy which bridges the cellular processes of autophagy and phagocytosis (Heckmann & Green, 2019). LAP uses selective components of the autophagy machinery to conjugate a subfamily of ATG8s (exemplified by LC3) to phagosome membranes (Martinez *et al*, 2011; Sanjuan *et al*, 2007). Whereas a basal level of intracellular clearance by autophagy is required for cellular survival, LAP is activated in response to extracellular phagocytic material (Heckmann & Green, 2019). Engagement of a variety of cell surface receptors have been studied to engage LAP, including the TLR2, the apoptotic body receptor TIM4, Dectin-1, and Fc receptors (Heckmann & Green, 2019). LAP degrades an assortment of cargo including dead cells, pathogens, and immune complexes in a variety of cell and tissue types (Heckmann & Green, 2019).

1.11 Autophagy and LAP mechanisms

Initiation

Autophagy, induced by nutrient signalling, is initiated by nucleation of the phagophore requiring the assembly of the initiation kinase complex composed of ULK1, FIP200, ATG13 and ATG101 (Mizushima, 2010). The ER, *trans*-Golgi network (TGN), recycling endosome, and ATG9 vesicles associated with the latter are major suppliers of lipids for the isolation membrane, which expands to sequester intracellular cargo and seals forming double-membraned autophagosomes (Yamamoto *et al*, 2012; Reggiori, 2006). Rather, LAP commences with development of the phagosome cup, independent of the initiation kinase complex (Heckmann & Green, 2019). In LAP, development and biogenesis of the single membrane phagosome precedes recruitment of the LAP machinery and is instead regulated by mediators of canonical phagocytosis (Heckmann and Green, 2019). Phagocytes are recruited by ‘soluble attractant signals’ or externalised phosphatidylserine which engage with receptors on the phagocyte and instigate cytoskeletal changes in the plasma membrane which mechanically drive the formation of the phagosome (Fazeli & Wehman, 2017).

Autophagosome or phagosome formation

The Phosphatidylinositol 3-Kinase Catalytic Subunit Type 3 (PI3KC3) complex is the first protein complex required for LAP, and is also required for autophagy (Backer, 2016; Heckmann & Green, 2019). Both pathways utilise the scaffolding complex VPS15, the tumour suppressor BECN1, and the lipid kinase VPS34 in their PI3KC3 complex (Heckmann & Green, 2019). VPS34 is a pseudokinase which phosphorylates the inositol ring of phosphotidylinositides to produce phosphatidlinosoitol-3-phosphate (PI3P) required in downstream events (Heckmann & Green, 2019). In autophagy the PI3KC3 requires ATG14, which is dispensable for LAP which instead recruits Rubicon (Heckmann & Green, 2019) Rubicon is a RUN-domain-containing protein which negatively regulates canonical autophagy (Martinez *et al*, 2015). Rubicon binds and stabilises VPS34 in PI3KC3, essential for PI3P generation on the single membrane phagosome; however, it inhibits PI3P generation on double-membraned autophagosomes (Zhong *et al*, 2009). Rubicon competes with ATG14 for interaction with VPS34, thereby promoting the progression of LAP and repressing autophagy (Heckmann & Green, 2019; Martinez *et al*, 2015).

Following PI3KC3 assembly, the nicotinamide adenine dinucleotide phosphate (NADPH) oxidase (NOX) family of enzymes stimulate the production of ROS in the phagosome membrane: essential for the progression of LAP, but not for autophagy (Martinez *et al*, 2015). Although the exact role of ROS in LAP is unclear, ROS could be involved in the oxidation of lipids in the phagosome membrane, which is seen during the early stages of LAP and initiates transmembrane ion imbalance and water influx (Boyle & Randow, 2015).

Membrane lipidation

LC3 lipidation plays fundamental roles in both autophagy and LAP. LC3 lipidation requires the assembly of two ubiquitin-like conjugation systems (Glick, Barth & Macleod, 2010). Firstly, ATG7, an E1-like enzyme, activates and transfers ATG12 to ATG10, an E2-like enzyme (Glick, Barth & Macleod, 2010). ATG12 is conjugated to ATG5 and the ATG5—

ATG12 heterodimer with ATG16L form the ATG5—ATG12-ATG16L complex which behaves as an E3 ligase for the second ubiquitin-like conjugation system (Glick, Barth & Macleod, 2010). A second E1-like enzyme and E2-like enzyme (ATG7 and ATG3, respectively) transfers LC3 from the ATG3-LC3 heterodimer to the ATG5—ATG12-ATG16L complex (Nakatogawa, 2013). The membrane localised PI3P on the phagophore or phagosome attracts the conjugation machinery (Heckmann & Green, 2019). WIP12 associated with ATG16L binds to PI3P in autophagy resulting in membrane labelling at sites of LC3 lipidation (Proikas-Cezanne *et al*, 2015). This, however, is not required in LAP and so the mechanism bridging PI3KC3 to the lipidation system is unclear (Heckmann & Green, 2019). ATG4 is used in autophagy and LAP for cysteine orchestrated cleavage of LC3 producing soluble LC3-I with a glycine residue exposed at the C-terminus for lipidation and generation of membrane-conjugated LC3-II (Fernández, Á. and López-Otín, 2015). LC3 lipidation promotes phagosome-lysosome fusion (LAP) or autophagosome-lysosome fusion (autophagy) required for hydrolytic degradation of engulfed material and recycling (Heckmann & Green, 2019) (Fig.3).

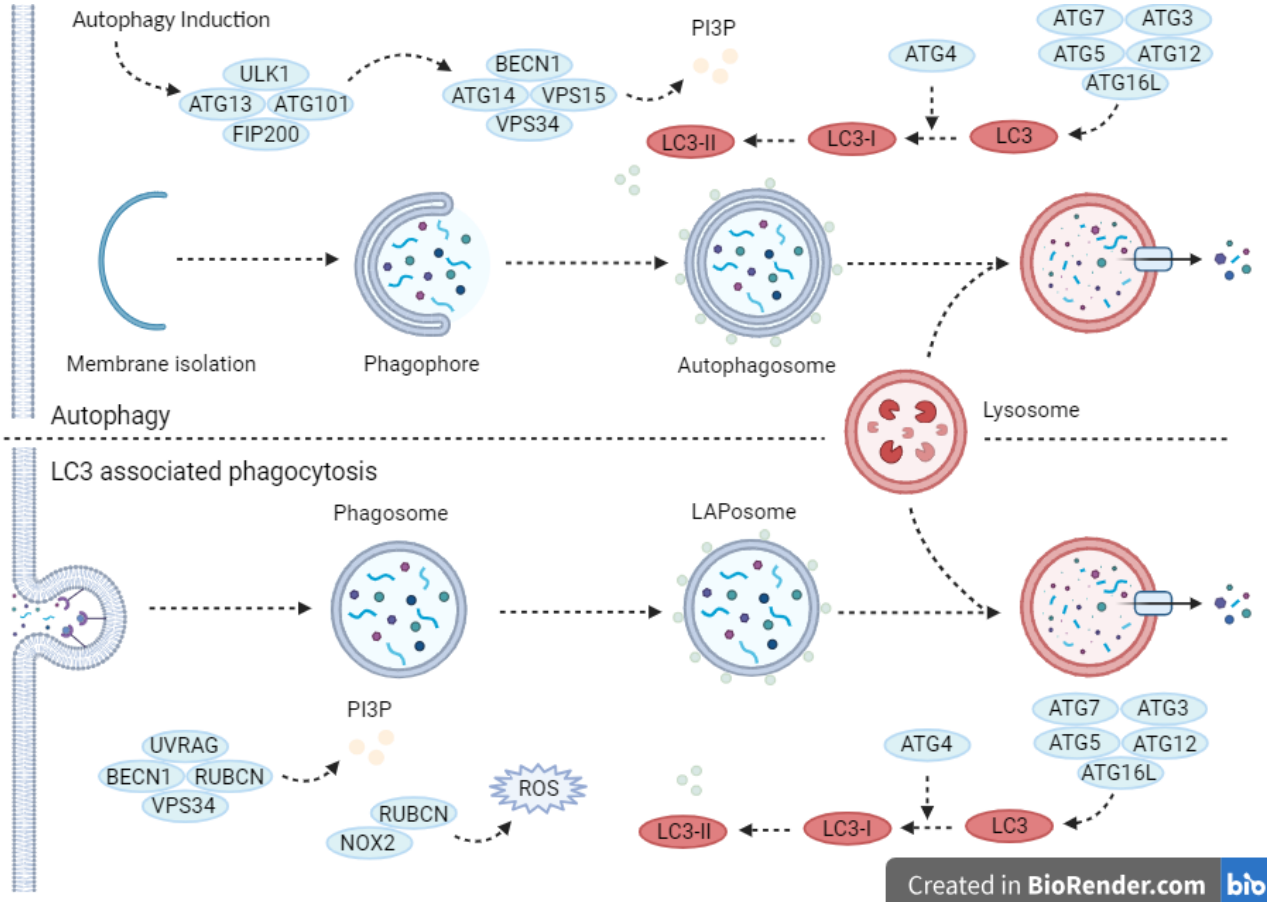

Figure 3. LC3-associated phagocytosis vs autophagy mechanisms.

Illustrated is the core autophagy (top) and LAP (bottom) machinery during the major steps of vesicle formation and maturation. In autophagy, several protein complexes support phagophore nucleation, autophagosome formation and lysosomal fusion. In LAP, similar protein complexes support phagosome maturation and lysosomal fusion.

1.12 LAP during infection and inflammation

LAP assists in preventing infection by degrading infectious cargo via acidic hydrolases in the lysosomal lumen (Heckmann & Green, 2019). Importantly, LAP activation promotes TLR signalling and activation of the type-I interferon response, preventing the development of autoimmunity (Henault *et al*, 2012). LAP is required for efficient recovery after Streptococcus pneumonia (Inomata *et al*, 2020), Salmonella (Masud *et al*, 2019), and Aspergillus fumigates infections (Martinez *et al*, 2015). LAP also shapes the inflammatory response during tissue damage. LAP-deficient mice were unable to restrict A. fumigates

growth post-infection and exhibited increased serum levels of G-CSF, IL-1α, IL-1β, IL-6 (Martinez *et al*, 2015). Notably, elevated levels of IL-1α, IL-1β, IL-6 are commonly reported in PD (Arena *et al*, 2022; Koprich *et al*, 2008). In addition to the degradation of foreign particles, LAP degrades unwanted dying cells and cellular debris of self-origin. For example, macrophages use LAP to clear apoptotic cells which quenches inflammation via suppression of pro-inflammatory cytokines (e.g, IL-6, IL-1β, CXCL-10) (Martinez *et al*, 2011). Abrogation of LAP in this setting results in increased inflammatory signalling and cytokine release (Martinez *et al*, 2011). Therefore, LAP has key roles in shaping the immune response and dampening pro-inflammatory signalling.

1.13 Roles of LAP during disease

Examination of LAP in disease has revealed critical understanding of the protective roles of LAP. For example, LAP is defective in monocytes of patients with liver cirrhosis, and restoring LAP was protective against inflammation-driven pathology (Wan *et al*, 2020). However, LAP has been identified to have cell specific and context dependent effects during cancer. For example, activation of LAP in tumour associated macrophages (TAMs) upon engulfment of dying cells may be detrimental: LAP dampens inflammation which suppresses the recruitment of T lymphocytes and establishes immune tolerance (Cunha *et al*, 2018). Alternatively, in acute myeloid leukaemia (AML) LAP is the predominant method for the clearance dead and dying cells by bone marrow macrophages (BMM) (Moore *et al*, 2022). Inhibiting LAP in this setting resulted in the accumulation of apoptotic cells and accelerated tumour growth (Moore *et al*, 2022). Therefore, the roles of LAP in disease are complex and requires cell-specific examination.

Over recent years, LAP has been increasingly considered as an important player in regulating CNS homeostasis. For example, astrocytes have been found to be dependent on LAP for the clearance of microglia debris (Zhou *et al*, 2022). LAP has also been explored in the context of injury and neurodegeneration. For example, a recent study demonstrated glia

utilise LAP for the clearance of axonal debris to support recovery following CNS injury (Szabó *et al*, 2023). Furthermore, LAP was found to compromised in Huntington's disease (HD) mouse striatal astrocytes (Wakida *et al*, 2022), and in models of subarachnoid haemorrhage, LAP in microglia was impaired (Chen *et al*, 2023). However, LAP's potential involvement in PD pathogenesis has not yet been explored.

1.14 Hypothesis and aims

This study uses human vmDANs, ventral midbrain astrocytes (vmAstros), and midbrain conditioned microglia (vmMicroglia) derived from human induced pluripotent stem cells (hiPSCs) to model neuronal debris clearance and the inflammatory response in PD. HiPSC-derived models are to date the closest available model of human neuroinflammation. As heterogenous brain populations behave differently during disease (Matejuk & Ransohoff, 2020), hiPSCs will be differentiated toward a midbrain phenotype. This produces cells relevant to the area of the brain affected by PD to more accurately recapitulate events happening *in situ*.

Increased neuroinflammatory signalling was identified early in PD and chronic reactivity of glial cells in a proinflammatory environment contributes to vmDAN degeneration (Kwon & Koh, 2020; Koprich *et al*, 2008). LAP is dependent on the action of Rubicon and dampens macrophage inflammation via suppression of pro-inflammatory cytokines (e.g, IL-6, IL-1β, CXCL-10), with Rubicon depletion concomitantly causing elevated inflammation (Inomata *et al*, 2020). I will study the contribution of LAP during the removal of vmDAN fragments and the ensuing inflammatory outcome as an in vitro human model for progressive neuroinflammation and neurotoxicity in PD.

<u>Hypothesis</u>

I hypothesise that midbrain glia use LAP for efficient clearance of vmDAN corpses, and that LAP deficiency accelerates PD via neuroinflammation.

Aims

1. To derive vmAstros, vmDANs, and vmMicroglia from hiPSCs.

2. To test whether LAP occurs in hiPSC-derived ventral midbrain glial cells.

3. To define how LAP shapes the neuroinflammatory response in human PD models.

2. Methods

2.1 Cell culture

2.1.1 Reagents

Reagent	Manufacturer	Catalogue number
Absorbic acid	Sigma-Aldrich	A5960
Accutase	Biolegend	42320
Advanced DMEM-F12	Gibco	12491-015
B27	Gibco	17504-044
β-Mercaptoethanol	Thermo Fisher	31350010
Bone morphogenetic protein 4 (BMP4)	Peprotech	120-05
Complement component C1q	Sigma-Aldrich	80295-33-6
Cyrostor	Merck	C2874
DAPT	Tocris	2634
Dibutyryl- cyclic adenosine monophosphate (db-cAMP)	Sigma-Aldrich	D0627
DMEM-F12 with 1X Glutamax	Themo Fisher	10565018
Fetal Bovine solution (FBS)	Sigma-Aldrich	F7524
Fibronectin	Sigma-Aldrich	FC010/3612225
Essential 8 Basal media (E8)	Gibco	A15169-01
Essential 8 Flex Basal media (E8 Flex)	Gibco	A28583-01
Ethylenediaminetetraacetic acid (EDTA)	Thermo Scientific	R1021 01014882
Epidermal growth factor (EGF)	Peprotech	AF-100-15
Geltrex	Thermo Fisher	A1413302
Glutamax	Gibco	35050-038
BDNF	Peprotech	450-02
GDNF	Peprotech	450-10
IL-1α	Peprotech	200-01A
IL-3	R&D	203-IL
Insulin	Santa Cruz Biotechnology	SC-360248
Laminin	Sigma-Aldrich	L2020
Leukaemia inhibitory factor (LIF)	Themo Fisher Scientific	300-05
LPS Escherichia Coli O55:B5	Sigma-Aldrich	25532-16-4
Macrophage colony stimulating factor (MCSF)	Thermo Fisher	PHC9501
N2	Thermo Fisher	17502-048

Neurobasal media	Gibco	21103-049
Neurobrew	MACs	130-097-263
MEM non essential amino acids (NEAA)	Gibco	11140-035
Penicillin/streptomycin	Sigma-Aldrich	P4333
Dulbecco's phosphate-buffered saline (PBS)	Sigma- Aldrich	D8537
RevitaCell	ThermoFisher	A2644501
Stem cell factor (SCF)	Miltenyi Biotec	130-093-991
TNF-α	Peprotech	300-01A
Vascular endothelial growth factor (VEGF)	Peprotech	100-20
Vitronectin	ThermoFisher	A14700
Lenti-X Concentrator	Clontech	631232
Polybrene	Sigma-Aldrich	TR-1003
Lipofectamine 2000	Thermo Fisher	11668027
Puromycin Dihydrochloride	Thermo Fisher	A1113802
Lenti-X Packaging single shots	Takara	631278
Opti-MEM	Thermo Fisher	31985057
XVivo-15	TheraPEAK	BE02-060Q

Table 1. List of reagents for cell culture.

2.1.2 Media

Media	**Composition**
RPE1, HEK293T media	DMEM-F12 with Glutamax supplemented with 10% FBS.
N2B27 complete media	Neurobasal media (48%) and DMEM-F12 with Glutamax (48%) supplemented with: N2 (1/200), B27 (1/100), 1mM Glutamax, 5µg/ml human insulin, NEAA (1/100), 75µM β-Mercaptoethanol, 0.2mM ascorbic acid (AA), 20ng/mL GDNF and 20ng/mL BDNF.
N2B27 maturation media	Neurobasal media (48%) and DMEM-F12 with Glutamax (48%) supplemented with: N2 (1/200), B27 (1/100), 1mM Glutamax, 5µg/ml human insulin, NEAA (1/100), 75µM β-Mercaptoethanol, 0.2mM ascorbic acid (AA), 20ng/mL GDNF and 20ng/mL BDNF, 500µM db-cAMP and 10µM DAPT.
ASTRO complete media	Advanced DMEM/F12 (96%) supplemented with: NEAA (1%), Glutamax (1%), N2 (1%), B27 (0.4%), 20µg/mL LIF and 20µg/mL EGF.

ASTRO maturation media	Advanced DMEM/F12 (96%) supplemented with: NEAA (1%), Glutamax (1%), N2 (1%), B27 (0.4%), 20 µg/mL LIF and 20µg/mL BMP4.
3G induction media	E8 flex media supplemented with: 50ng/ml VEGF, 50ng/ml BMP4 and 20ng/ml SCF.
Microglia-like progenitor medium (MPM)	XVivo-15 supplemented with: 1X Glutamax, 1X Pen/Strep, 50nM βME, 50ng/ml MCSF and 50ng/ml IL-3.
Astrocyte conditioned media (ACM)	Advanced DMEM-F12 (96%) supplemented with: 1X Pen/Strep, 1X Glutamax, 20ng/ml FGF, 20ng/ml EGF and Neurobrew with Vitamin A.
Microglia maturation medium	ACM (49%) and Advanced DMEM-F12 (49%) supplemented with: 1X Pen/Strep and N2 (1/100).

Table 2. List of media composition for cell culture.

2.1.3 Immortalised cell lines

YFP-LC3B RPE1s and HEK293T cells

Thawing

Frozen cryovials were removed from -80ºC or liquid nitrogen and thawed briefly in a 37ºC water bath. YFP-LC3B RPE1s or HEK293T cells were suspended in 10mL of media (see composition in table 1) then pelleted by centrifuge at 150 x*g* for 3 minutes. Cells were resuspended in the 10mL of media in 10cm dishes and incubated at 37ºC 5% CO_2.

Passaging

YFP-LC3B RPE1 and HEK293T cells were grown at 37ºC 5% CO_2 until 90-100% confluency. Cells were washed once with PBS before dissociating with trypsin-EDTA for 3 minutes at 37ºC 5% CO_2. The trypsin-EDTA activity was quenched with media and cells were split in a 1:4-1:12 ratio.

Freezing

YFP-LC3B RPE1 and HEK293T cells were pelleted by centrifuge at 150 x*g* for 3 minutes and resuspended in FBS supplemented with 10% DMSO in cryovials. The cryovials were slowly frozen overnight in a “Mr. Frosty” (Jencons Scientific Ltd) at -80ºC.

2.1.4 Maintenance and cryopreservation of hiPSCs

Normal α-synuclein (NAS2) and AST23 hiPSCs were gifted from Dr Tilo Kunath, Centre of Regenerative Medicine, University of Edinburgh.

Thawing

1 hour (h) prior to thawing, 5µg/mL vitronectin coated 6-well plates were prepared at room temperature (RT). Frozen cryovials of NAS2 iPSCs were removed from -80ºC or liquid nitrogen and thawed briefly in a 37ºC water bath. HiPSCs were suspended in 10mL of E8 media then pelleted by centrifuge at 150 x*g* for 3 minutes. Cells were resuspended in the appropriate volume of E8 media supplemented with RevitaCell (1/100) on vitronectin coated plates and incubated at 37ºC 5% CO_2.

Passaging

HiPSCs were grown to 70-80% confluency then 1h prior to splitting, vitronectin coated 6-well plates were prepared and hiPSCs had their media replaced and supplemented with RevitaCell (1/100). HiPSCs were dissociated with EDTA for 3 minutes at 37ºC 5% CO_2 then were resuspended in E8 or E8 Flex media supplemented with RevitaCell (1/100) in a 1:4-1:10 splitting ratio. After 24hrs, RevitaCell was removed from E8 and media was replenished daily or E8 flex media was replenished every two days.

Freezing

HiPSCs were pelleted by centrifuge at 150 x*g* for 3 minutes and resuspended in 700uL of CyroStor in cryovials. The cryovials were slowly frozen overnight in a “Mr. Frosty” at -80ºC.

2.1.5 Maintenance and cryopreservation of vmNPC

Thawing

1h prior to thawing, 12-well or 6-well 0.25X Geltrex coated plates were prepared at 37ºC 5% CO_2. Frozen cryovials of ventral midbrain neural progenitor cells (vmNPCs) were removed from -80ºC or liquid nitrogen and briefly thawed in a 37ºC water bath. Cells were suspended in 5mL of N2B27 media then pelleted by centrifuge at 150 x*g* for 3 minutes. Cells were resuspended in the appropriate volume of N2B27 complete media on 0.25X Geltrex coated plates and incubated at 37ºC 5% CO_2.

Passaging

vmNPCs were grown up until day 40 and split at 100% confluency. 1h prior to splitting, 0.25X Geltrex coated plates were prepared and vmNPCs had their N2B27 complete media supplemented with RevitaCell (1/100). vmNPCs were dissociated with accutase for 3-5 minutes at 37ºC 5% CO_2. The accutase was aspirated and vmNPCs were resuspended in N2B27 complete media supplemented with RevitaCell (1/100) and split in a 1:2 or 1:3 ratio. Media was replenished every 1-2 days as needed.

Freezing

vmNPCs were pelleted by centrifuge at 150 x*g* for 3 minutes and resuspended in 700uL of CyroStor in cryovials. The cryovials were slowly frozen overnight in a “Mr. Frosty” at -80ºC.

2.1.6 Terminal differentiation of vmNPCs to vmDANs

vmNPCs were terminally differentiated to vmDANs between days 25-40 post neuralization as previously described (Fig.4) (Stathakos *et al*, 2021). vmNPCs had there N2B27 complete media replaced with N2B27 maturation media (see media composition in table 2). On the third day of terminal differentiation, 10µM DAPT was removed from the N2B27 maturation media. Cells were maintained at 37ºC 5% CO_2 and fed every 1-3 days as needed for two weeks.

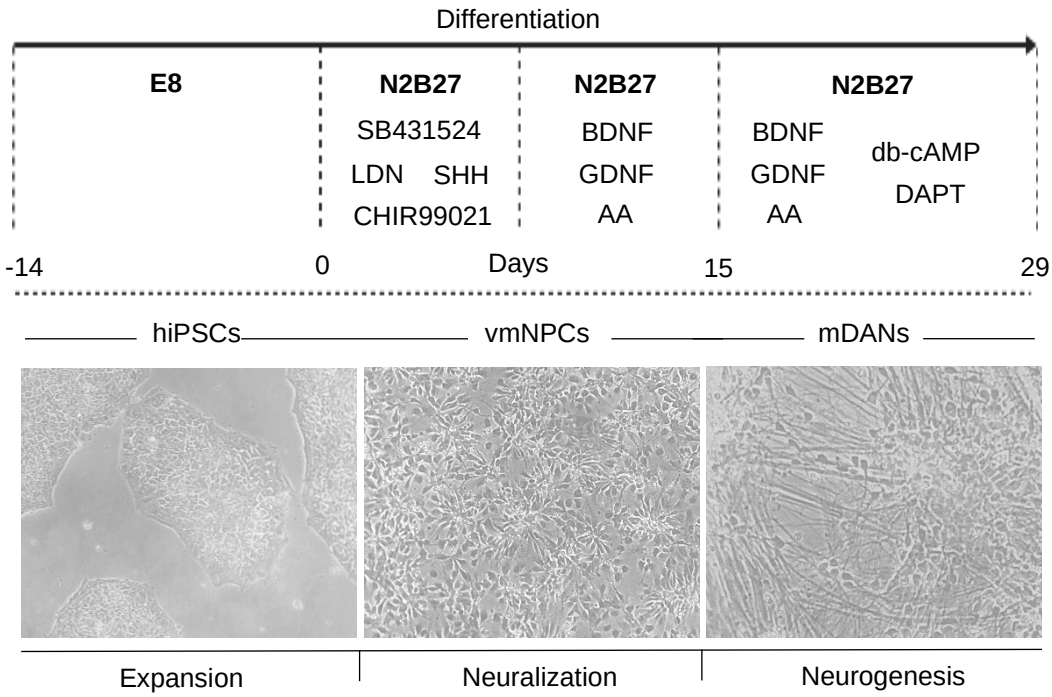

Figure 4. Protocol for generating vmNPCs and mDANs from hiPSCs.

2.1.7 Maintenance and cryopreservation of vmAPCs

Thawing

vmAPCs were grown on 0.25X Geltrex coated flasks in ASTRO complete media (see media composition in table 2). 1h prior to thawing, 0.25X Geltrex coated T25, T75 or T175 flasks were prepared at 37ºC 5% CO_2. Frozen cryovials were removed from -80ºC or liquid nitrogen and briefly thawed in a 37ºC water bath. vmAPCs were suspended in 10mL of ASTRO media then pelleted by centrifuge at 150 x*g* for 3 minutes. Cells were resuspended in the appropriate volume of ASTRO complete media on 0.25X Geltrex coated flasks and incubated at 37ºC 5% CO_2.

Passaging

Cells were grown to 70-90% confluency and 1h prior to splitting 0.25X Geltrex flasks were prepared at 37ºC 5% CO_2. vmAPCs were dissociated with accutase for 3-5 minutes at 37ºC 5% CO_2. The accutase was quenched with ASTRO media and cells were pelleted by

centrifuge at 150 x*g* for 3 minutes. VmAPCs were resuspended in ASTRO complete media as per 1:2-1:4 splitting ratio. vmAPCs were expanded no longer than day 110 after neutralization.

Freezing

vmAPCs were pelleted by centrifuge at 150 x*g* for 3 minutes and resuspended in 700uL of CyroStor in cryovials. The cryovials were slowly frozen overnight in a “Mr. Frosty” at -80ºC.

2.1.8 Terminal differentiation of vmAPCs to vmAstros

From day 90 post-neuralization, vmAPCs were terminally differentiated to vmAstros as previously described (Fig.5) (Crompton *et al*, 2021). If splitting prior to differentiation, vmAPCs were dissociated with accutase and pelleted by centrifuge at 150 x*g* for 3 minutes. VmAPCs were resuspended in ASTRO maturation media (see media composition table 2). If splitting was not carried out before terminal differentiation, vmAPCs were washed 3x with Advanced DMEM/F12 before addition of the ASTRO maturation media. Cells were maintained at 37ºC 5% CO_2. On day 3, cells had a 50% media change and on day 6, cells had a full media change. After 10 days of maturation 20 µg/mL LIF and 20µg/mL BMP4 was permanently removed from the ASTRO media. ASTRO media was replenished every 5-7 days and vmAstros were maintained in culture up until day 120.

2.1.9 vmAstro activation

Terminally differentiated vmAstros were maintained for at least three days in ASTRO media post-differentiation on 0.25X Geltrex coated plates. vmAstros were seeded to 650,000 cells/well of a 6-well plate and treated with either (1) non-redox media (control) or (2) non-redox media supplemented with 30 ng/ml TNF-α, 400 ng/ml C1q, and 3 ng/ml IL-1α for 24hrs at 37ºC 5% CO_2.

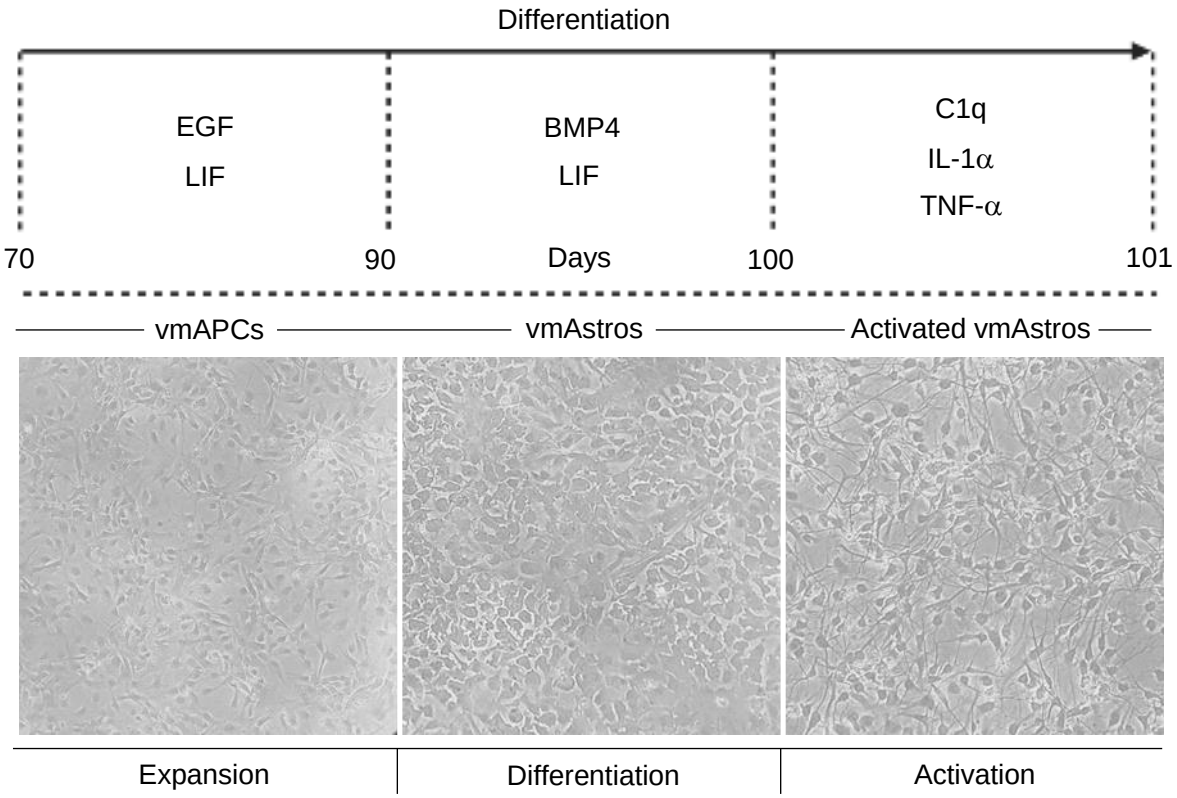

Figure 5. Protocol for generating vmAstros and reactive vmAstros from vmAPCs.

2.1.10 Differentiation of hiPSCs to macrophage precursor cells (MPCs)

HiPSCs were differentiated to vmMicroglia by adapting previously established protocols (Fig.6) (Haenseler *et al*, 2017). HiPSCs were grown to around 80% confluency in E8 medium in 6-well vitronectin coated plates as previously described (see section 2.1.4). On the day of embryoid body (EB) induction, cells were treated for 1h at 37ºC 5% CO_2 with RevitaCell (1/100). HiPSCs were washed with PBS before dissociating with accutase for 3-5 minutes at 37ºC 5% CO_2. Dissociated hiPSCs were pelleted by centrifugation at 150 x*g* for 3 minutes. HiPSCs were resuspended in 3G induction medium and seeded in a 96-well ultra-low attachment plate at a density of 10,000 cells/well. Briefly, cells were aggregated by centrifugation and maintained at 37ºC 5% CO_2. On day 2 cells had a 50% media change and

on day 4, EBs were transferred to a 6 well plate in MPM medium (see media composition table 2) with 2/3rd media changes every 5 days.

2.1.11 Terminal differentiation of MPCs to vmMicroglia

1 week prior to harvesting the MPCs, vmAPCs were cultured for preparing conditioned medium for 48hrs (see media composition table 2). 1h prior to harvesting MPCs, 7.5 µg/mL fibronectin coated 12-well plates or coverslips were prepared for 2hrs at RT.

Between days 30-70 MPCs were harvested and pelleted at 150 x*g* for 3 minutes. Cells were resuspended microglia maturation medium (see media composition table 2) and cultured on fibronectin coated coverslips or 12-well plates for two weeks to generate midbrain conditioned microglia (vmMicroglia). On the first week, media was topped as needed and on the second week, 50% media change was given every 2-3 days.

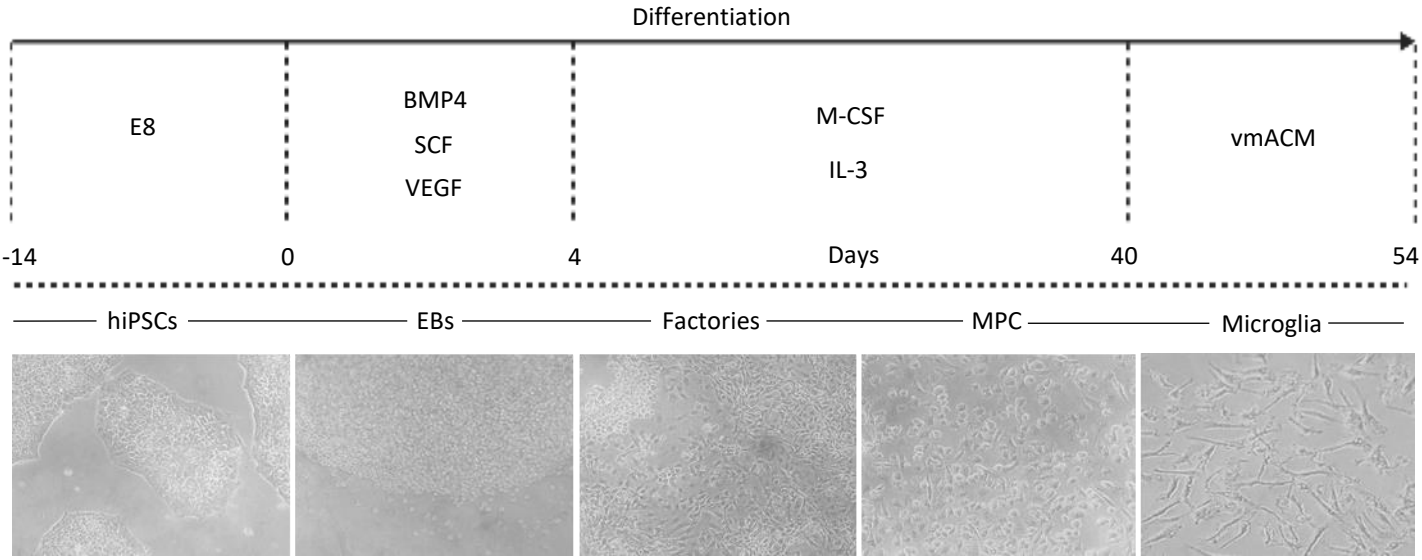

Figure 6. Protocol for generating microglia-like progenitor cells and microglia from hiPSCs.

2.1.12 vmMicroglia activation

Terminally differentiated vmMicroglia seeded in a 12 well format on fibronectin coated plates were treated with either (1) microglia maturation media (control) or (2) microglia maturation media supplemented with LPS for 24hrs at 37ºC 5% CO_2.

2.1.13 Short hair (sh)RNA gene silencing

Transformation

NEB stable Escherichia coli were thawed from -80°C and transformed with plasmids containing shRNAs for ATG14 (Sigma-Aldrich; TRCN0000145367) and Rubicon (Sigma-Aldrich; TRCN0000021543) via heat shock treatment (30 minutes ice; 30 seconds 42°C; 5 minutes ice). NEB outgrowth media was added to the mixture and incubated at 37°C for 1h on a 250rpm shaker. The mixture was steaked on LB agar + ampicillin resistant plates and incubated overnight at 37°C. The transformed colonies were picked and incubated in LB broth + ampicillin at 37°C overnight. The cultures were centrifuged at 4000 x*g* for 10 minutes and the pellet was used for mini prep using the QIAGEN QIAprep Spin Miniprep Kit as per the manufacturer's instructions. The concentration of purified plasmid was determined using NanoDrop Lite Spectrophometer (Thermo Fisher Scientific).

Lentiviral production

HEK293T cells were cultured at 37°C 5% CO_2 in DMEM/F12 with 10% FBS for lentiviral production. At 80% confluency, 7µg of plasmid-shRNA mixed with nuclease free water was added to HEK293T cells via Lenti-X Packaging Single Shots and incubated at 37°C 5% CO_2. After 48hrs, the spent media was collected and filtered through 0.45µM filters then mixed with 1/3 Lenti-X Concentrator and incubated at 4°C for 30 minutes. The mixture was then centrifuged at 1,500 x*g* for 45min at 4°C and the pellet was resuspended in ASTRO media. The virus was then used immediately or stored at -80°C.

Transduction

For viral transduction, cells were infected with viral media and 10µg/mL polybrene for 24hrs. The media was then replenished with fresh media containing 2µg/mL or 1µg/mL puromycin for selecting stably transduced cells across 3-5 days. Cells were then harvested for western blot and qRT-PCR analysis.

2.1.14 Short interfering (si)RNA gene silencing

siRNA targeting human Rubicon (Santa Cruz Biotechnology; sc-78326) or human ATG14 (OriGene technologies; SR307828) were suspended in RNAse buffer and transiently transfected according to the manufacturer's protocol. On the day of transfection, HEK293T cells or hiPSC-derived vmAstros were detached and resuspended in appropriate volumes of cell culture media. Cells were reverse transfected with 30nM Rubicon siRNA, ATG14 siRNA or scramble control mixed with Opti-MEM and Lipofectamine 2000 in 6-well or 12-well plate for 48hrs. Cells were then forward transfected with 30nM Rubicon siRNA, ATG14 siRNA or scramble control with Lipofectamine 2000 for 24hs. After the second transfection, HEK293T cells and hiPSC-derived vmAstros were harvested for western blot and qRT-PCR analysis.

2.2 Experimental and analytical procedures

2.2.1 Reagents

Reagent	Manufacturer	Catalogue number
1,4-diazabicylo[2.2.2]octane (DABCO)	Sigma-Aldrich	D27802
1000X Pathogreen Histoflourescent stain	Biotium	80027
4X ProtoGel Resolving Buffer	Thermo Fisher	EC892
Ammonium persulfate (APS)	Sigma-Aldrich	A3678
Bafilomycin A1 (BafA1)	Enzo	BML-CM110
Bovine serum albumin (BSA)	Sigma-Aldrich	5470
DAPI	Sigma-Aldrich	D9542
Ethanol	Sigma-Aldrich	64-17-5
Glycerol	Sigma-Aldrich	G5516
Glycine	Sigma-Aldrich	302160
Goat serum	Vector Labs	S-1000-20
Hanks balanced salt solution (HBSS)	Gibco	14175095
Human serum	Sigma-Aldrich	P2918
LumiGLO Peroxidase Chemiluminescent Substrate Kit	Seracare	5430-0040
Methanol	Sigma-Aldrich	67-56-1
Mowial	Sigma-Aldrich	324590
Non-fat dried milk	Millipore	70166
Paraformaldehyde (PFA)	Thermo Fisher	28908
Pierce BSA Protein Assay Kit	Thermo Scientific	23225
Protease inhibitor cocktail tablets	Sigma-Aldrich	65726900
Protogel Acrylamide	Thermo Fisher	EC890
ProtoGel Stacking buffer	Thermo Fisher	EC893
Sodium Dodecyl sulfate (SDS)	Sigma-Aldrich	151213
TaqMan Gene Expression Cells-to-C_T kit	Thermo Fisher	4399002
Tetramethylethylenediamine (TEMED)	Thermo Fisher	EC503
Tris HCL	Melford	PHG0002
Triton-X-100	Sigma-Aldrich	X100
Tween-20	Sigma-Aldrich	P7949
Zymosan A (*S. cerevisiae*) BioParticles™, Alexa Fluor™ 594 conjugate	Thermo Fisher	Z23374
Zymosan A *S. cerevisiae* BioParticles™, unlabeled	Thermo Fisher	Z2849

Table 3. List of reagents for analytical procedures.

2.2.2 Zymosan preparation and treatment

Zymosan was opsonized by 30-minute incubation with human serum at 37ºC. Opsonized zymosan was resuspended in PBS at a working concentration of 20mg/mL. YFP-LC3B RPE1 cells, vmAstros and vmMicroglia had their media replenished and supplemented with 30µg/mL opsonized zymosan particles for 4h or 24h and analyzed via western blotting, immunocytochemistry or qRT-PCR.

2.2.3 vmDAN UV treatment

vmDANs terminally differentiated on 1X Geltrex and laminin coated plates had their media replaced with non-redox media supplemented with 1000X Pathogreen Histofluorescent stain for 2hrs. The cells were washed thrice with PBS then exposed to 1000mJ of UV radiation. Neuronal fragments were harvested after 48hrs and 100ul was added to cultures of vmAstros or vmMicroglia and analysed via immunocytochemistry and qRT-PCR.

2.2.4 Immunocytochemistry

YFP-LC3 RPE1 cells, hiPSC-derived vmAstros, MPCs, vmMicroglia, and vmDANs were cultured on coverslips and fixed with ice cold methanol for 4 minutes or 4% PFA for 10 minutes at RT. If blocking was required, cells were blocked for 1h at RT in 10% goat serum and 1% BSA in 0.1% PBS with Triton X-100 (PBS-tx). Cells were then incubated in primary antibody for 20 minutes at RT or overnight at 4ºC (see table 4). Cells were washed thrice with PBS then incubated in secondary antibody for 20 minutes or 1h at RT (see table 4). Cells were washed thrice with PBS and incubated with DAPI for 10 minutes at RT before mounting onto coverslips with Mowiol containing 25mg/mL DABCO antifade and left to dry overnight. Cells were imaged by widefield fluorescence microscopy or confocal microscopy.

Antibody	Host species	Dilution	Supplier	Cat no.
Primary				
CD11b	Mouse	1:300	Invitrogen	2488586
CD14	Rabbit	1:300	Protein tech	17000-1-AP
FOXA2	Mouse	1:50	SCBT	NB600501
GLAST	Rabbit	1:300	Protein tech	20785-1-AP
IBA1	Rabbit	1:300	Antibodies	A82670
LC3	Mouse	1:300	Sigma	SAB200361
TH	Rabbit	1:300	Millipore	3328928
TUJ1	Mouse	1:500	Biolegend	B264428
Secondary				
Alexa Flour 488	Goat Anti-Mouse	1:500	ThermoFisher	A32723
Alexa Flour 488	Goat Anti-Rabbit	1:500	ThermoFisher	A32731
Alexa Flour 594	Goat Anti-Mouse	1:500	ThermoFisher	A21203
Alexa Flour 594	Goat Anti-Rabbit	1:500	ThermoFisher	A32740

Table 4. List of antibodies for immunocytochemistry.

2.2.5 Analysis and quantification of fixed cells

For fixed cell quantification of zymosan uptake and $LC3^{+ve}$ phagosomes, cells were imaged using the widefield microscope and analyzed on Metamorph software. Graphical data depict the mean and standard error of the mean (s.e.m) for two independent experiments of n=50. The measure of significance (*P* value) was determined by unpaired two-tailed Student's t-test with Welch's correction (GraphPad Prism version 9). Differences were considered significant if P<0.05; ***P<0.001; **P<0.01; *P<0.05; ns (non-significant).

2.2.6 qRT-PCR

TaqMan Gene Expression Cells-to-C_T kit was used to perform cDNA synthesis according to the manufacturer's instructions. Briefly, HEK293T cells, hiPSC-derived vmAstros, or hiPSC-

derived vmMicroglia were detached and resuspended in 1mL of media holding 100,000 cells. The cell suspension was washed once with ice-cold PBS then incubated for 5 minutes at RT with lysis solution followed by 2-minute incubation with stop solution. The Cells-to-CT lysates were stored at -20ºC for up to several months.

Cell lysates were synthesized to cDNA using 20X reverse transcription enzyme mix and 2X reverse transcription buffer by reverse transcription (37ºC; 60 minutes) followed by reverse transcription inactivation (95ºC; 5 minutes) and indefinite hold (4ºC) using the Bio-Rad T100 Thermal Cycler.

The cDNA was amplified by real time (q)PCR using Taqman gene expression master mix and TaqMan gene expression assays for the target of interest (see table 5) using the QuantStudio™ 3 Real-Time PCR System (Thermo Fisher Scientific). The qPCR cycling conditions were as follows: UDG incubation (1 rep; 50ºC for 2 min), enzyme activation (1 rep; 95ºC for 10 min), PCR cycle (40 reps; 95ºC for 15 seconds; 60ºC for 1 min).

Relative gene expression was calculated by the $2^{(-\Delta\Delta Ct)}$ method and results were graphed by $2^{(-\Delta\Delta Ct)}$ or Log2 fold change of $2^{(-\Delta\Delta Ct)}$ with results normalized to GAPDH. The measure of significance (*P* value) was determined by one-way ANOVA (GraphPad Prism version 9).

TaqMan Gene Assay	**Manufacturer**	**Catalogue number**
ATG14	Thermo Fisher Scientific	Hs00208732_m1
C3	Thermo Fisher Scientific	Hs00163811_m1
CCL2	Themro Fisher Scientific	Hs00234140_m1
GAPDH	Thermo Fisher Scientific	Hs02758991_m1
ICAM1	Thermo Fisher Scientific	Hs00164932_m1
IL-1β	Thermo Fisher Scientific	Hs01555410_m1
IL-6	Thermo Fisher Scientific	Hs00174131_m1
PTX3	Thermo Fisher Scientific	Hs00173615_m1
Rubicon	Thermo Fisher Scientific	Hs00943570_m1

Table 5. TaqMan gene expression assays for qPCR.

2.2.7 Autophagy and LAP induction

Starvation was performed using HBSS to induce autophagy, BafA1 to block late phase autophagy, and zymosan to induce LAP. YFP-LC3B RPE1s were seeded in a 6-well format and grown to 100% confluency. Briefly, the cell medium was aspirated and treated: (1) RPE1 media (control); (2) RPE1 media + 2µg/mL BafA1; (3) HBSS; (4) HBSS + 2µg/mL BafA1; (5) RPE1 media + 30µg/mL zymosan; (6) RPE1 media + 50µg/mL zymosan. YFP-LC3B cells were then incubated for 1h at 37ºC 5% CO2. Samples were analysed by protein quantification via western blotting.

2.2.8 Western blotting

1. Cells seeded in a 6-well format were washed twice with ice cold PBS then lysed with 100ul of radioimmunoprecipitation (RIPA) buffer consisting of 50mM Tris HCL (pH 7.4), 150nM NaCl, 1% Triton-X-100, 0.5% sodium Deoxycholate and 0.1% SDS supplemented with one tablet of protease inhibitor per 10mL.
2. The lysed cells were collected and sonicated for 5 minutes before centrifuging (12,000 x*g*, 15 minutes, 4ºC). The supernatant was transferred to ice-cold Eppendorf tubes and stored at -80ºC.
3. The concentration of protein samples were quantified using the Pierce BSA Protein Assay Kit. 30µg of protein from lysed samples was added to fresh Eppendorf tubes with 5X SDS sample loading buffer (50mM Tris HCL; pH 6.8, 100mM dithiothreitol (DTT), 2% SDS, 0.1% bromophenol blue and 10% glycerol).
4. Resolving gels (8-12%) consisting of lower buffer (pH8.8; 1.5M Tris-HCL and 0.4% SDS), 30% acrylamide, H_20, 10% APS and TEMED were prepared between two glass plates.
5. Once set, stacking gels consisting of upper buffer (0.5M Tris-HCL and 0.4% SDS; pH 6.8), 30% acrylamide, H_20, 10% APS and TEMED was prepared and a 1.0mm 10-well comb was inserted and allowed to set.

6. Gels were placed in a mini-PROTEAN-III tank in 1x SDS-PAGE running buffer (25mM Tris, 190mM glycine and 0.1% SDS in ddH_2O; pH 8.3). The prepared samples and pre-stained protein ladder were loaded, and electrophoresis was conducted at 120Vs until the bromophenol blue dye reached the bottom of the gel.
7. Protein samples were transferred from the gel to nitrocellulose membranes (Biolabs). The electrophoresis apparatus was deconstructed, and gels were added to transfer buffer (20% Biorad turbo buffer, 10% ethanol in ddH2O; pH 7.7) for 5 minutes. The transfer sandwich was constructed in a cassette as follows: 1 piece of foam, 2 filter papers, gel, nitrocellulose membrane, 3 filter papers and 1 piece of foam. The cassette was added to the transfer tank along with more transfer buffer. The transfer was carried out for 85 minutes at 110Vs.
8. The nitrocellulose membrane was blocked for 1h at RT in blocking solution (20mM Tris-HCL, 150mM NaCl, 0.1% Tween-20 and 5% non-fat dried milk in ddH20; pH 7.6).
9. The membranes were then incubated overnight at 4ºC in primary antibodies (see table 6) diluted at appropriate concentrations in blocking solution (5% BSA or 5% milk).
10. The following day the membranes were rinsed once then washed 3x5 minutes in 1xTBS-0.1% Tween 20 (TBS-Tw) (20mM Tris-HCl, 150nM NaCl, 0.1% Tween-20; pH7.5).
11. The membrane was then incubated for 1h at RT in the relevant horse-radish peroxidase (HRP)-conjugated secondary antibodies (see table 6).
12. The membranes were rinsed once then washed 3x5 minutes in 1xTBS-Tw.
13. Protein binding was detected via the enhanced ECL kit by mixing equal volumes of reagent A with reagent B and were applied to the membrane for 8 minutes.
14. The membranes were placed in a blotting cassette and exposed to autoradiography hyperfilm sheet (GE Healtcare) and developed in an AGFA Curix 60 film processor.

Antibodies	Host species	Dilution	Supplier	Cat no.
Primary				
ATG14	Rabbit	1:1000	Cell signalling	5504S
GAPDH	Mouse	1:5000	Sigma-Aldrich	MFCD01322099
LC3B	Mouse	1:1000	Cell signalling	83506S
P62	Mouse	1:5000	Abnova	H00008878
Rubicon	Rabbit	1:1000	Cell signalling	8465S
Secondary				
HRP	Goat Anti-Mouse	1:10,000	Sigma-Aldrich	32160702
HRP	Goat Anti-Rabbit	1:10,000	Sigma-Aldrich	MFCD00162788

Table 6. List of antibodies for western blotting.

3. Results

3.1 LAP induction with zymosan in YFP-LC3B RPE1 cells

Previously, the retinal pigment epithelium (RPE) has been shown to utilise LAP for the turnover of photoreceptor outer segments (POS) in the retina (Frost *et al*, 2015). Hence hTERT-RPE1 cells stably expressing YFP-LC3B (Antón et al, 2020) were employed for proof-of-study to monitor LAP induction using zymosan particles. Zymosan is isolated from the cell wall of yeast and induces phagocytosis via engagement with TLR2 (Allen & Aderem, 1995). In this study, LC3B recruitment to the phagosome membrane was monitored with YFP-LC3B labelling. Fluorescence analysis identified $LC3^{+}$ phagosomes (LAPosomes) 4h and 24h post-incubation with zymosan particles (Fig.7A). However, the proportion of cells that showed clear evidence of phagocytosed zymosan particles, and the number of those cells with confirmed LAPosomes were relatively low. This was supported by immunoblotting for LC3B during autophagy and LAP induction (Fig 7B). LC3B facilitates autophagosome maturation and lysosomal fusion, and its lipidation (conversion from LC3B-I to LC3-II) can be used to assess autophagic flux by virtue of increased migration following covalent attachment of a lipid (typically, PE). Autophagy induction by starvation increased the levels of lipidated LC3B-II, suggestive of an increased number of autophagosomes. Furthermore, BafA1, used to block late phase autophagy, led to an accumulation of LC3B-II; however, LAP induction with (non-opsonized) zymosan particles revealed no upregulation of LC3B-II levels, indicating that zymosan failed to sufficiently activate LAP.

Opsonization of zymosan particles has been previously shown to enhance phagocytosis. Consistent with these reports, the number of cells with phagocytosed opsonized zymosan particles significantly increased from 14.2% to 47.6% after 4hrs, and 16.8% to 30.9% after 24hrs (Fig.7C & D). Furthermore, the number of cells with LAPosomes significantly increased from 1.2% to 8.7% after 4hrs, and 0.8% to 2.4% after 24hrs (Fig.7C & E). Hence, opsonized zymosan particles were used for future monitoring of LAP. The significant

reduction in LAPosomes 24hrs post-exposure to opsonized zymosan suggests this timepoint was outside the active range to monitor LAP (Fig.7E). Overall, these results support the use of opsonized zymosan particles for monitoring LAP induction *in vitro*.

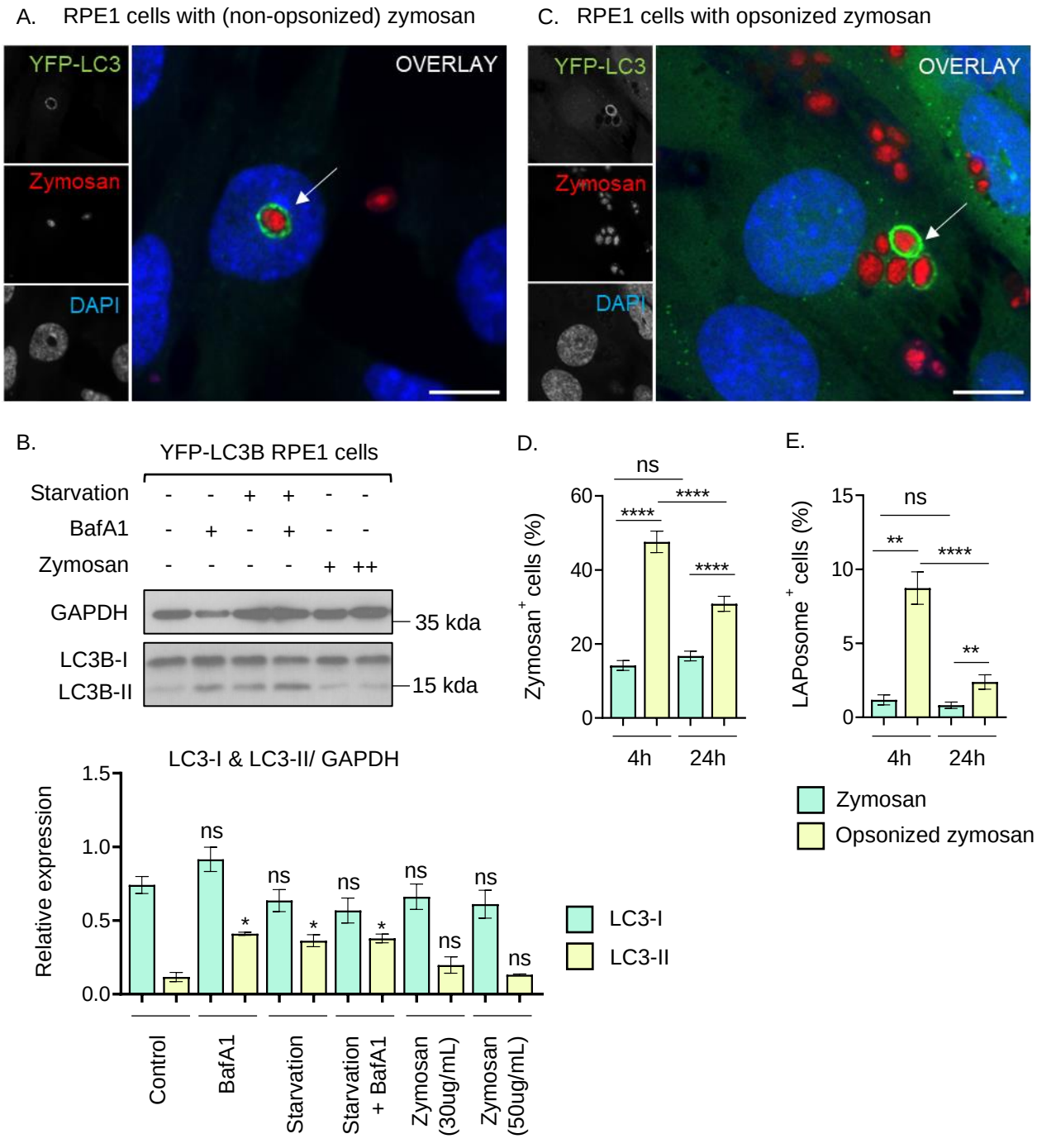

Figure 7. Zymosan induces LAP in RPE1-YFP-LC3B cells.

(A) Fluorescence of LAP induction with (non-opsonized) zymosan in YFP-LC3B RPE1 cells. (B) Immunoblot with quantification of autophagy and LAP manipulation for 1h in YFP-LC3B RPE1 cells. (C) Fluorescence of LAP induction with opsonized zymosan in YFP-LC3B RPE1 cells. Quantification of microscope images showing (D) the number of zymosan^{+} cells and (E) the number of cells with LC3^{+} LAPosomes following 4h and 24h incubation with zymosan or opsonized zymosan particles. Mean ± s.e.m, n = 2-3; students t-test with Welsh's correction; *P < 0.05, **P < 0.01 ****P < 0.0001; ns= not significant. Scale bar= 10µm.

3.2 LAP induction with opsonized zymosan in vmAstros

Astrocytes share functional properties with professional phagocytes. For example, astrocytes participate in phagocytosing pathological protein aggregates, synapses, and neuronal debris (Lee & Chung, 2021). We hypothesised that vmAstros would use LAP for specialist clearance of phagocytic substrates of relevance to brain (patho)physiology. HiPSCs were terminally differentiated to vmAstros via inclusion of CHIR99021 and sonic hedgehog (SHH) to initiate signalling for ventral midbrain patterning, alongside initiation of JAK/STAT, EGF, and BMP signalling for expansion and maturation of vmAstros (Crompton *et al*, 2021) (Fig.8A). This generated vmAstros which expressed the mature astrocyte marker GLAST and the midbrain marker FOXA2, as expected (Fig.8B). vmAstros were incubated with opsonized zymosan particles, with 29.0% and 26.7% of cells phagocytosing zymosan after 4h and 24h, respectively (Fig.C & F). Immunocytochemistry analysis of fixed cells labelled with anti-LC3B antibodies also identified that 6.8% of vmAstros after 4h and 3.5% of vmAstros after 24h possessed $LC3^{+}$ LAPosomes (Fig.8C & G). Therefore, our results indicate that LAP is engaged for assisted clearance of zymosan in vmAstros *in vitro*.

In PD, vmAstros become chronically reactive, exhibiting a switch in their phenotype from neuroprotective to neurotoxic (Liddelow & Barres, 2017). Reactive vmAstros are instrumental in the increased neuroinflammatory signalling events which has been shown to decrease the survival of vmDANs in mouse models (Koprich *et al*, 2008). Reactive vmAstros are triggered by exposure to pro-inflammatory cytokines IL-1α, TNF-α, and C1q (ITC) that are released by activated microglia (Liddelow *et al*, 2017). To mimic activation *in vitro*, hiPSC-derived vmAstros were incubated for 24hrs with ITC. Gene expression analysis by qRT-PCR confirmed an A1 neurotoxic phenotype by virtue of increased expression of the pro-inflammatory markers ICAM1 (38.3-fold) and C3 (624.9-fold) (Fig.8E). PTX3— a marker typically associated with the A2 neuroprotective phenotype— was also upregulated (20.2-fold) (Fig 8E). Therefore, ITC-treated vmAstros upregulated markers that are characteristic of both A1 (pro-inflammatory) and A2 (anti-inflammatory) activation.

When vmAstros are activated to a pro-inflammatory phenotype characteristic of PD, the ensuing regulation of phagocytosis is not well understood. In a mouse model infected with prions, phagocytic activity was significantly downregulated in reactive astrocytes (Sinha *et al*, 2021). Currently, the general relationships between vmAstro reactivity state and phagocytosis with or without LAP involvement has not been reported. We evaluated phagocytosis in reactive vmAstros by incubation with opsonized zymosan particles for 4hrs or 24hrs. This revealed comparable numbers of cells that had phagocytosed zymosan between resting and reactive vmAstros (Fig.8D & F). We also monitored $LC3^+$ LAPosomes, with no appreciable differences in the number of $LAPosome^+$ cells observed after 24h. By contrast, the number of $LAPosome^+$ vmAstros was significantly reduced between resting (6.8%) and reactive (1.3%) states at the earlier 4h timepoint (Fig.8D & G). Hence, while the non-specific phagocytosis rate was apparently not influenced by vmAstro reactive status, the incidence of LAP events was markedly reduced during the early, dynamic phase. This has important implications for the possible involvement of LAP in the acute phase of vmAstro responses to local pathology and the influence of vmAstro reactivity state.

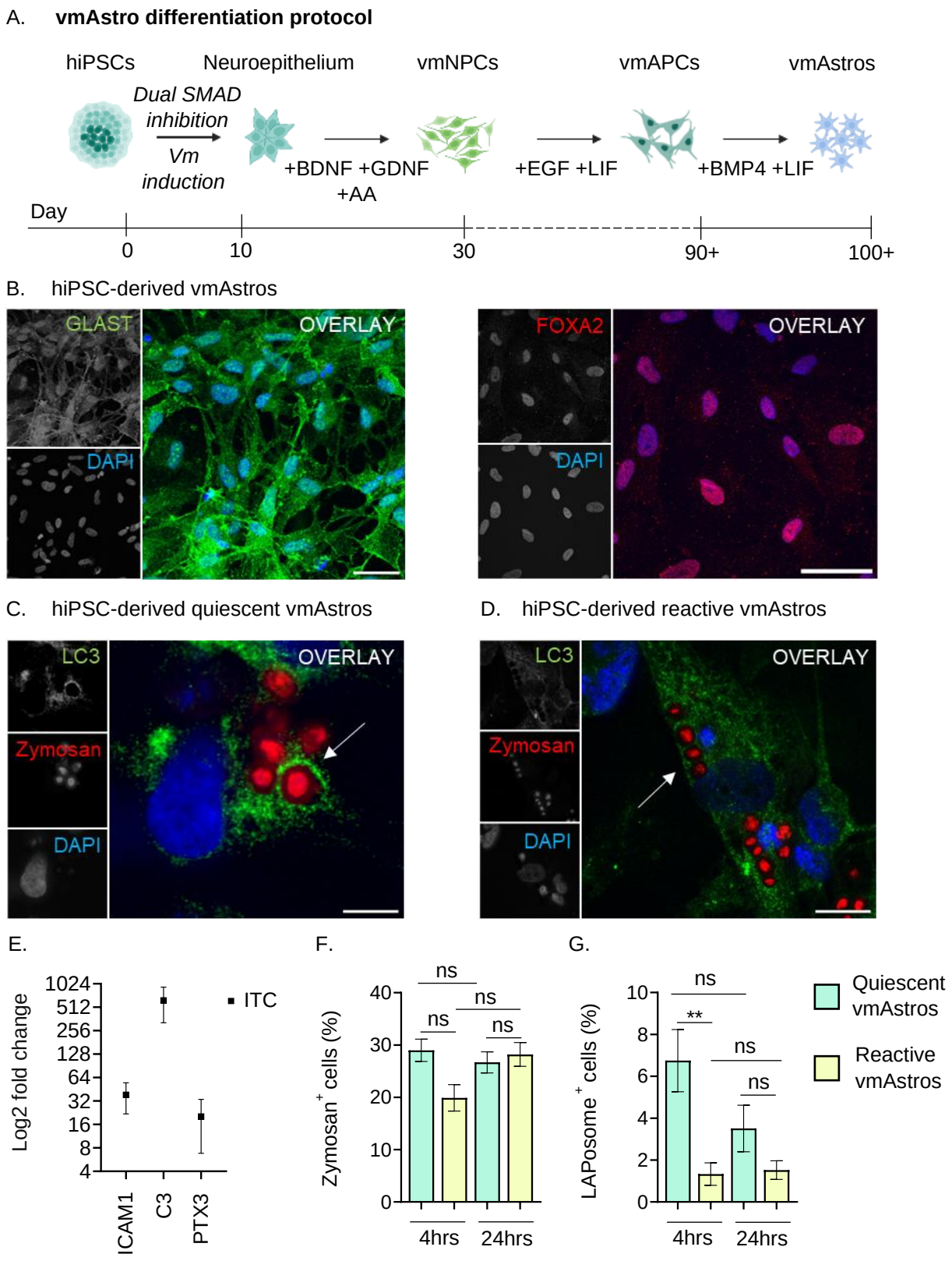

Figure 8. Zymosan clearance via LAP is abrogated in pro-inflammatory astrocytes.

(A) Schematic for the production of vmAstros from hiPSCs. (B) Characterisation of hiPSC-derived vmAstros with the mature astrocyte marker GLAST (left) and midbrain marker FOXA2 (right); Scale bar = 50μm. Immunofluorescence analysis of LAP induction with zymosan in (C) quiescent hiPSC-derived vmAstros and (D) reactive hiPSC-derived vmAstros; Scale bar = 10μm. (E) qRT-PCR of log2-fold change (normalised to GAPDH) in neuroinflammatory marker expression after 24h incubation with ITC in vmAstros. Quantification of (F) zymosan$^+$ cells (phagocytosis) and (G) LC3$^+$ LAPosomes following 4h and 24h incubation with opsonized zymosan. Mean ± s.e.m, n = 2-3; student's t-test with Welsh's correction; **P<0.01; ns (non-significant).

3.3 Generation and characterisation of midbrain microglia

In addition to astrocyte dysfunction in PD, microglia are critical players during neuroinflammatory-mediated toxicity and loss of vmDANs (McGeer *et al*, 1993). HiPSCs were differentiated to microglial progenitor cells (MPCs) using established protocols (Haenseler *et al*, 2017) (Fig.9A). This generated MPCs which expressed macrophage lineage markers CD14 and CD11b (Fig.9B). Currently, it is not well established whether the transcriptional and functional landscape differs between microglia resident in different areas of the brain. As regional variations in soluble factors derived from neighbouring cells is likely to influence microglial identity, we adapted previously published protocols that used cortical astrocyte-derived media (Haenseler *et al*, 2017) by treating MPCs with media obtained from vmAPC cultures, in an attempt to condition the maturing microglia to the region of the brain first affected in PD (Fig.9A). The generated microglia expressed CD11b and CD14, as well as the mature microglia marker IBA1 (Fig.9C & D). vmMicroglia were also stained for ventral midbrain markers FOXA2 and LMX1B (Fig.9E). Although all cells were positive for these markers, relatively few cells showed clear evidence of the expected nuclear expression (Fig.9E). This suggests that the microglia obtained using this adapted protocol are likely to be midbrain-conditioned, although further detailed characterisation will be needed to confirm their (midbrain) microglial identity.

To further characterise the functional properties of the hiPSC-derived vmMicroglia, cells were incubated with the bacterial endotoxin, LPS. Previously, LPS-primed microglia were shown to become activated to a M1 pro-inflammatory phenotype which amplified the degeneration of vmDANs in mouse models (Nakamura, Si & Kataoka, 1999; Subhramanyam *et al*, 2019; Gao *et al*, 2002). Hence, pro-inflammatory cytokines (IL-1β and IL-6) and chemokines (CCL2) previously reported to be preferentially upregulated during LPS treatment were used to assess reactivity induction in hiPSC-derived vmMicroglia (Lively & Schlichter, 2018; Speicher *et al*, 2019). After 24h LPS treatment, qRT-PCR revealed that microglia showed increased expression of the pro-inflammatory markers IL-6 (86.8-fold), IL-

1β (545.4-fold), and CCL2 (2.6-fold) (Fig.9F). Overall, these results help validate the generation of vmMicroglia for subsequent experimentation.

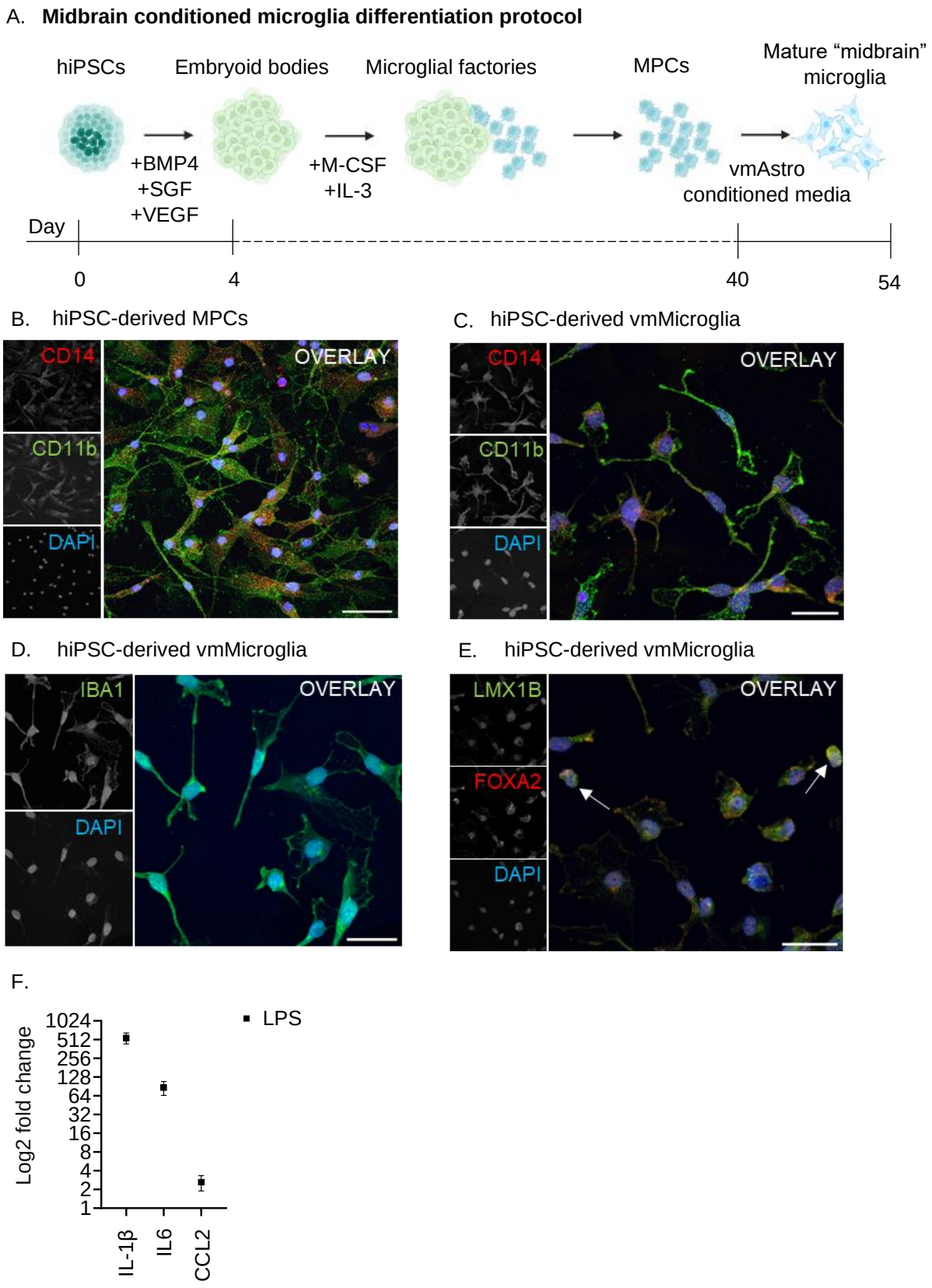

Figure 9. Characterisation of hiPSC-derived vmMicroglia.

(A) Schematic for the production of vmMicroglia from hiPSCs. Characterisation using the macrophage markers CD11b and CD14 in (B) MPCs and (C) vmMicroglia. Characterization of hiPSC-derived microglia with the mature microglia marker (D) IBA1 and (E) midbrain markers FOXA2 and LMX1B. (F) qRT-PCR of log2 fold change (normalised to GAPDH) in neuroinflammatory markers after 24h incubation with LPS in vmMicroglia. Mean ± s.e.m, n = 3, scale bar= 50µm.

3.4 LAP induction with opsonized zymosan in vmMicroglia

Microglia are immune competent cells that are regarded as the principal phagocytes in the CNS (Matejuk & Ransohoff, 2020). For example, microglia phagocytose synapses, dendrites, axons, myelin, and neurons under physiological and pathological conditions (Ho, 2019; Matejuk & Ransohoff, 2020). We hypothesised that vmMicroglia would engage LAP for assisted clearance of phagocytic substrates. To study the role of LAP in vmMicroglia, cells were cultured with opsonized zymosan particles for 4h or 24h, fixed and stained using anti-LC3B antibodies, revealing a large proportion of cells which phagocytosed zymosan into $LC3^+$ LAPosomes (Fig.10A). For the purposes of quantification, the amount of zymosan particles added in these assays was decreased 10-fold from the assays using RPE1 cells and vmAstros. Data revealed that 33.2% and 24.1% of cells had phagocytosed zymosan after 4h and 24h, respectively (Fig.10B). Furthermore, 16.1% (4h) and 2.2% (24h) of vmMicroglia contained $LC3^+$ LAPosomes (Fig.10C). Therefore, vmMicroglia engage LAP for supported clearance of zymosan *in vitro*.

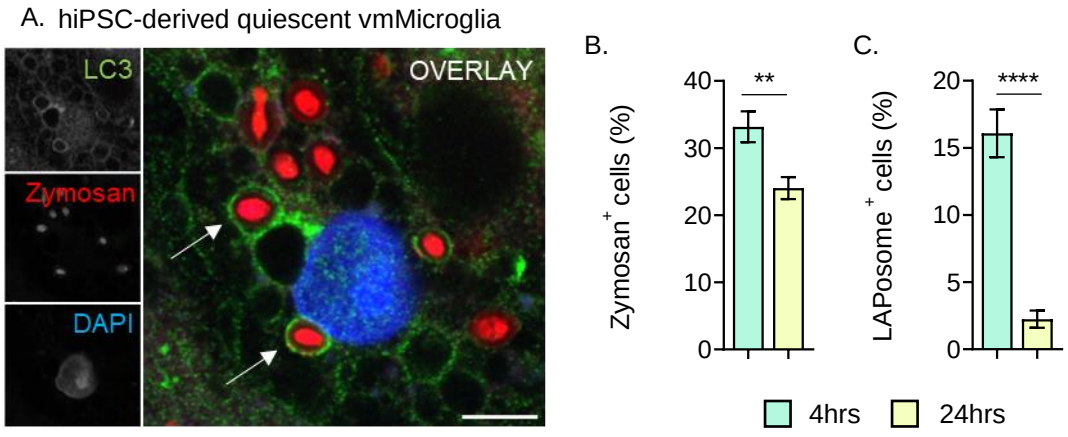

Figure 10. Opsonized zymosan induces LAP in hiPSC-derived vmMicroglia.

(A) Immunofluorescence analysis of LAP induction with zymosan in quiescent hiPSC-derived vmMicroglia. Quantification of (B) $zymosan^+$ cells (phagocytosis) and (C) $LC3^+$ LAPosomes following 4h and 24h incubation with opsonized zymosan. Mean ± s.e.m, n = 2; student's t-test with Welsh's correction; **P < 0.01 ****P < 0.0001. Scale bar= 50µm.

3.5 LAP induction with vmDAN fragments in vmAstros and vmMicroglia

A pathological hallmark of PD is the loss of vmDANs in the SNpc (Lotharius & Brudin, 2002). Hence, fragments of vmDANs were employed as a physiologically relevant phagocytic cargo to monitor the LAP response in our PD model. HiPSC-derived vmNPCs were terminally differentiated to vmDANs as previously described (Stathakos *et al*, 2019) (Fig.11A). Neural induction was achieved by dual SMAD inhibition, and ventral midbrain patterning via CHIR99021 and SHH signalling. This generated vmDANs which expressed the mature neuronal marker class III beta-tubulin (TUJ1), as well as the midbrain marker tyrosine hydroxylase (TH) (Fig.11B).

Astrocytes and microglia were previously found to employ LAP for the clearance of axon debris in a Drosophila model of nervous system injury (Szabo *et al*, 2023). Therefore, we hypothesised that hiPSC-derived vmAstros and vmMicroglia would engage LAP to clear vmDAN corpses. vmDANs were treated with Pathogreen Histoflourescent dye which stains degenerating neurons and their processes. vmDANs were induced to undergo apoptosis via UV-mediated DNA damage and the vmDAN fragments were then harvested and cultured with vmAstros and vmMicroglia for 4hrs or 24hrs (Fig.11C). Immunocytochemistry analysis revealed a small number of vmAstros and vmMicroglia that had phagocytosed vmDANs (Fig.11D & E). However, immunofluorescence staining could not detect LC3B localisation to vmDAN-containing phagosomes. Therefore, no LAPosomes were observed in this setting, and we were unable to provide evidence supporting whether LAP is recruited for safe clearance of vmDANs *in vitro*.

Neuroinflammation is a hallmark of PD, and dying vmDANs have been reported to activate glial cells and accelerate PD via neuroinflammation. Hence, the inflammatory consequence of phagocytosis induction with vmDAN fragments was assessed in hiPSC-derived glial cells. After 24h incubation with vmDAN debris, activation of pro-inflammatory glia was assessed by qRT-PCR. This revealed no upregulation of inflammatory markers in vmAstros (PTX3,

ICAM1, C3) or in vmMicroglia (IL-6, IL-1β, CCL2) (Fig.11F & G). Additionally, vmMicroglia-mediated vmAstro activation was assessed by adding the conditioned media from cultures of vmMicroglia cultured with vmDAN fragments to vmAstros. Similarly, qRT-PCR detected no upregulation of the pro-inflammatory markers in vmAstros (ICAM1, PTX3, C3) (Fig.11H). Therefore, vmDAN fragments did not appear to induce an A1 astrocyte or M1 microglia phenotype with the associated pro-inflammatory response in this setting.

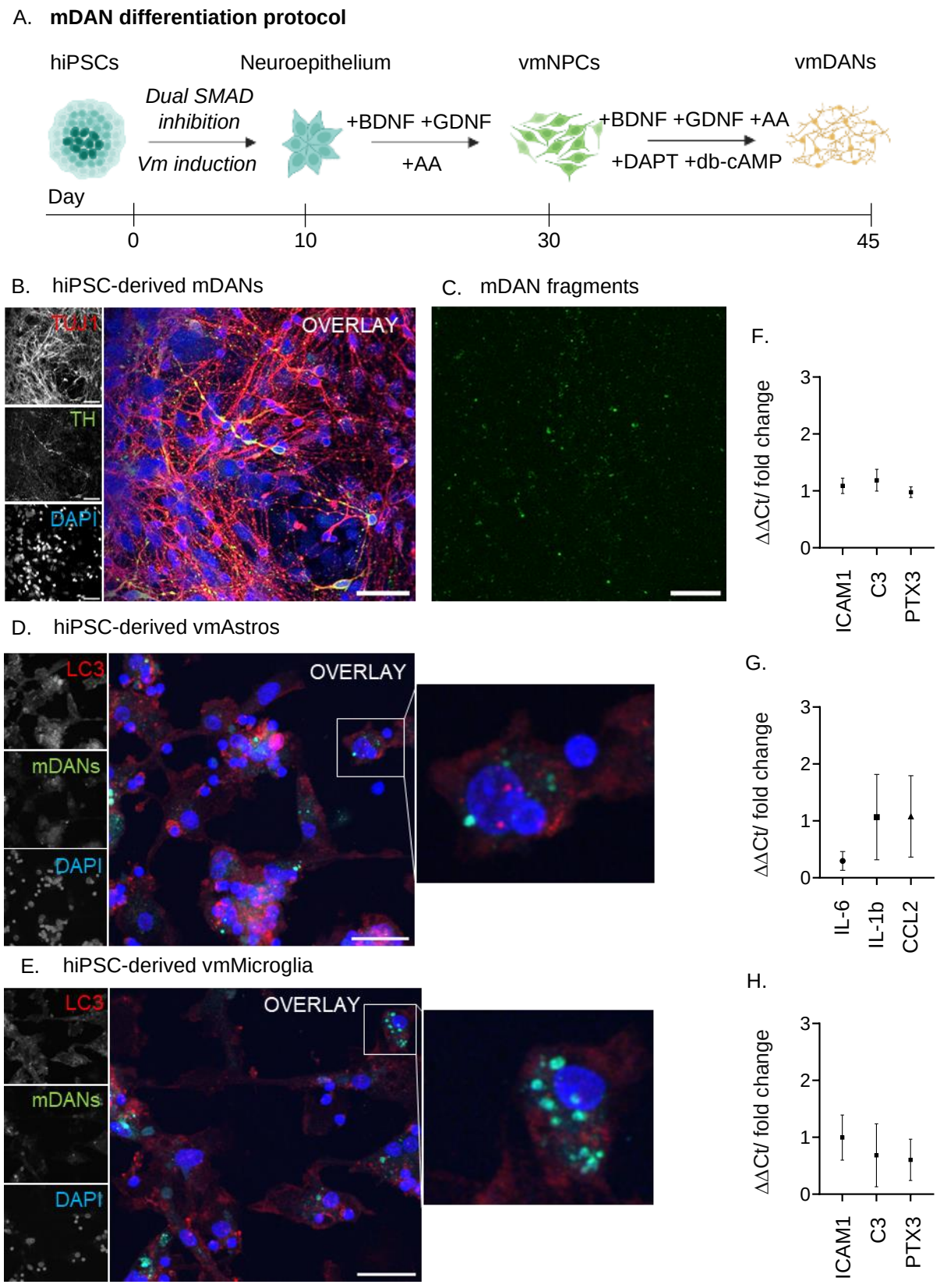

Figure 11. Phagocytosis induction with vmDAN fragments failed to induce an inflammatory response in hiPSC-derived vmAstros and vmMicroglia.

(A) Schematic for the production of vmDANs from hiPSCs. (B) Characterisation of hiPSC-derived vmDANs with the mature neuronal marker TUJ1 and midbrain marker TH. (C) Fluorescence showing pathogreen staining in vmDAN fragments after 1000mJ UV treatment. Immunofluorescence analysis of LAP induction with vmDAN fragments in (D) hiPSC-derived vmAstros and (E) hiPSC-derived vmMicroglia. qRT-PCR showing the change in expression of inflammatory markers when LAP was induced with vmDAN fragments in (F) hiPSC-derived vmAstros, (G) hiPSC-derived vmMicroglia and (H) media from microglia cultured with vmAstros. Mean ± s.e.m, n = 3.

3.6 Characterisation of shRNA targeting Rubicon and ATG14 in vmAstros

Inefficient clearance of dying cells has been implicated in inflammatory and neurodegenerative diseases (Sokolowski & Mandell, 2011). We hypothesised that LAP is required for non-inflammatory clearance of vmDAN debris, and that LAP-deficient hiPSC-derived vmAstros would consequently be unable to safely remove vmDAN fragments. Previously, LAP impairment has been achieved by targeting the essential protein, Rubicon, with Rubicon-deficient macrophages unable to initiate LAP in response to zymosan, TLR2 coated beads, or A. fumigatus infection (Martinez *et al*, 2015). Rubicon binds to VPS34 as part of the PI3KC3 complex required for the generation of PI3P on the phagosome membrane. Hence, Rubicon knockdown was employed to study LAP modulation of the neuroinflammatory response in hiPSC-derived vmAstros. In canonical autophagy, ATG14 plays a similar role to that provided by Rubicon during LAP; it binds to VPS34 and is essential for the generation of PI3P on the double-membraned autophagosome. Hence, ATG14 knockdown was selected to attenuate canonical autophagy for comparison of the neuroinflammatory response.

Lentiviral transduction of shRNA targeting Rubicon and ATG14 was first tested in HEK293T, cells as these cells are easy to manipulate genetically. The virus was incubated in HEK293T cells for 24 hours with polybrene added to enhance the efficiency of viral infection. HEK293T cells were then harvested for protein extraction at 48hrs and 72hrs post infection. Compared to HEK293T cells transduced with control-shRNA, no reduction in Rubicon or ATG14 expression was detected in Rubicon and ATG14-shRNA treated cells (Fig.12A). Subsequent experiments were conducted in hiPSC-derived vmAstros with the additional step of puromycin treatment to select for stably transduced cells. The shRNA-plasmid contains a puromycin resistant gene, so, non-transduced cells were excluded by culturing with 2 µg/mL puromycin, and the surviving transduced cells were lysed for RNA extraction. qRT-PCR detected evidence of shRNA-mediated knockdown of Rubicon and ATG14 in vmAstros (Fig.12B). However, the vmAstros presented with morphological changes indicative of

cellular stress following the 2µg/mL puromycin treatment. Therefore, lentiviral transduction was repeated with 1µg/mL puromycin. Compared to vmAstros transduced with control-shRNA, we paradoxically observed increased expression of Rubicon and ATG14 proteins in Rubicon and ATG14-specific shRNA treated cells (Fig.12C). Therefore, the lentiviral vector-based shRNA was unable to knockdown Rubicon or ATG14. Furthermore, qRT-PCR showed a fold change depletion in ATG14 mRNA (20.3%) whereas the fold change in Rubicon mRNA increased (58.3%) when transduced with their respective shRNA lentiviruses (Fig.12D). Overall, the lentiviral shRNA knockdown of Rubicon and ATG14 was determined to be inappropriate to explore neuroinflammatory changes during LAP induction, with further testing and validation required. Alternative knockdown methods were therefore explored.

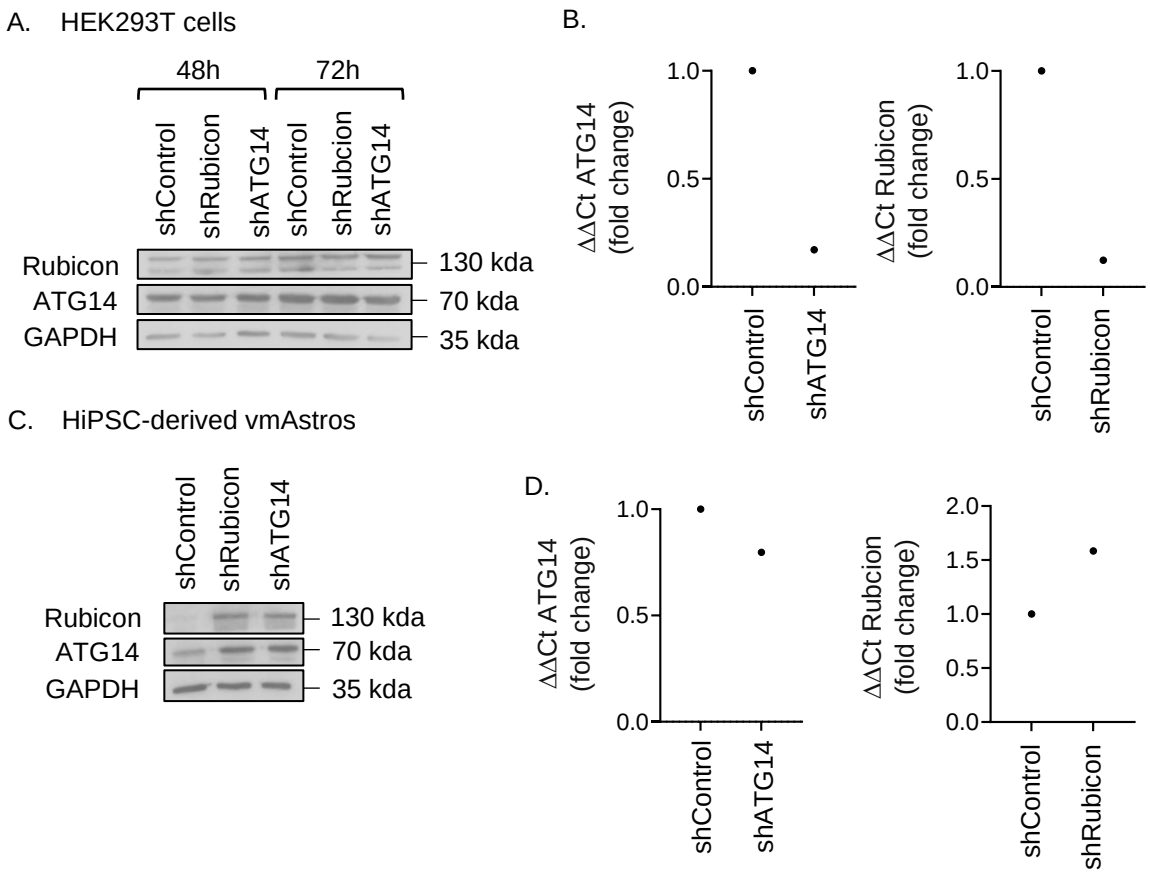

Figure 12. Characterisation of shRNA suppression of ATG14 and Rubicon.

(A) Immunoblot of protein levels following shRNA suppression of ATG14 or Rubicon in HEK293T cells. (B) qRT-PCR analysis of mRNA levels following shRNA suppression of ATG14 (left) or Rubicon (right) in hiPSC-derived vmAstros after 4 days of puromycin (2µg/mL). (C) Immunoblot of shRNA suppression of ATG14 or Rubicon in hiPSC-derived vmAstros after 4 days of puromycin (1µg/mL). (D) qRT-PCR analysis of mRNA levels following shRNA suppression of ATG14 (left) or Rubicon (right) in hiPSC-derived vmAstros after 4 days of puromycin (1µg/mL).

3.7 LAP induction with vmDANs in Rubicon and ATG14-deficient vmAstros

Lentiviral vector-based shRNA failed to introduce sufficient knockdown of Rubicon and ATG14 in HEK293T cells and hiPSC-derived vmAstros (Fig.12A-D). As an alternative approach, HEK293T cells were transiently transfected with siRNA targeting Rubicon, ATG14, or a scrambled control, using a sequential forward and reverse transfection protocol. Immunoblotting detected reasonable siRNA-mediated knockdown of Rubicon (73.5%) and ATG14 (42.0%) in HEK293T cells (Fig.13A). This was supported by qRT-PCR showing a reduction in mRNA levels of Rubicon (44.4%) and ATG14 (28.2%) (Fig.13B). The transient

infection of siRNA was next validated in hiPSC-derived vmAstros. Compared to vmAstros transduced with control-siRNA, Rubicon knockdown was detected by immunoblotting (56.4%) and qRT-PCR (42.3%) in Rubicon-siRNA treated vmAstros. Similarly, ATG14 knockdown was detected by immunoblotting (60.2%) and qRT-PCR (30.0%) in siATG14-siRNA treated vmAstros (Fig.13C & D). Overall, these results suggested that there was sufficient gene suppression and protein depletion to use this approach in subsequent experiments.

LAP supports an immunologically silent response in macrophages, via suppression of pro-inflammatory cytokines (Martinez *et al*, 2015). In contrast, LAP-deficient macrophages responded to A. fumigatus infection with increased pro-inflammatory cytokine release: specifically, IL-6, IL-1β, and TNFα (Martinez *et al*, 2015). Previously, we found that vmDAN fragments added to cultures of hiPSC-derived vmAstros failed to induce a pro-inflammatory response and did not stimulate A1-type activation (Fig.11F). We therefore assessed the neuroinflammatory consequences of LAP-deficient hiPSC-derived vmAstros upon exposure with vmDAN corpses. Using the siRNA transfection methods previously validated, Rubicon and ATG14-deficient vmAstros were challenged for 24hrs with vmDAN fragments and changes to neuroinflammatory gene expression were monitored by qRT-PCR. No significant change in expression of inflammatory markers C3, PTX3, or ICAM1 were detected in ATG14-siRNA or Rubicon-siRNA treated vmAstros (Fig.13E). Therefore, vmDAN fragments failed to induce an inflammatory response in LAP-deficient and autophagy-deficient vmAstros in this setting. Of note, PTX3 expression was downregulated in siRNA-control treated vmAstros (Fig.13E), proposing the siRNA could be modulating the neuroinflammatory response following its incorporation into the RNA-induced silencing (RISC) complex. This could be disrupting the comparative analysis of the inflammatory response during treatment with vmDAN fragments in the ATG14-siRNA and Rubicon-siRNA treated cells.

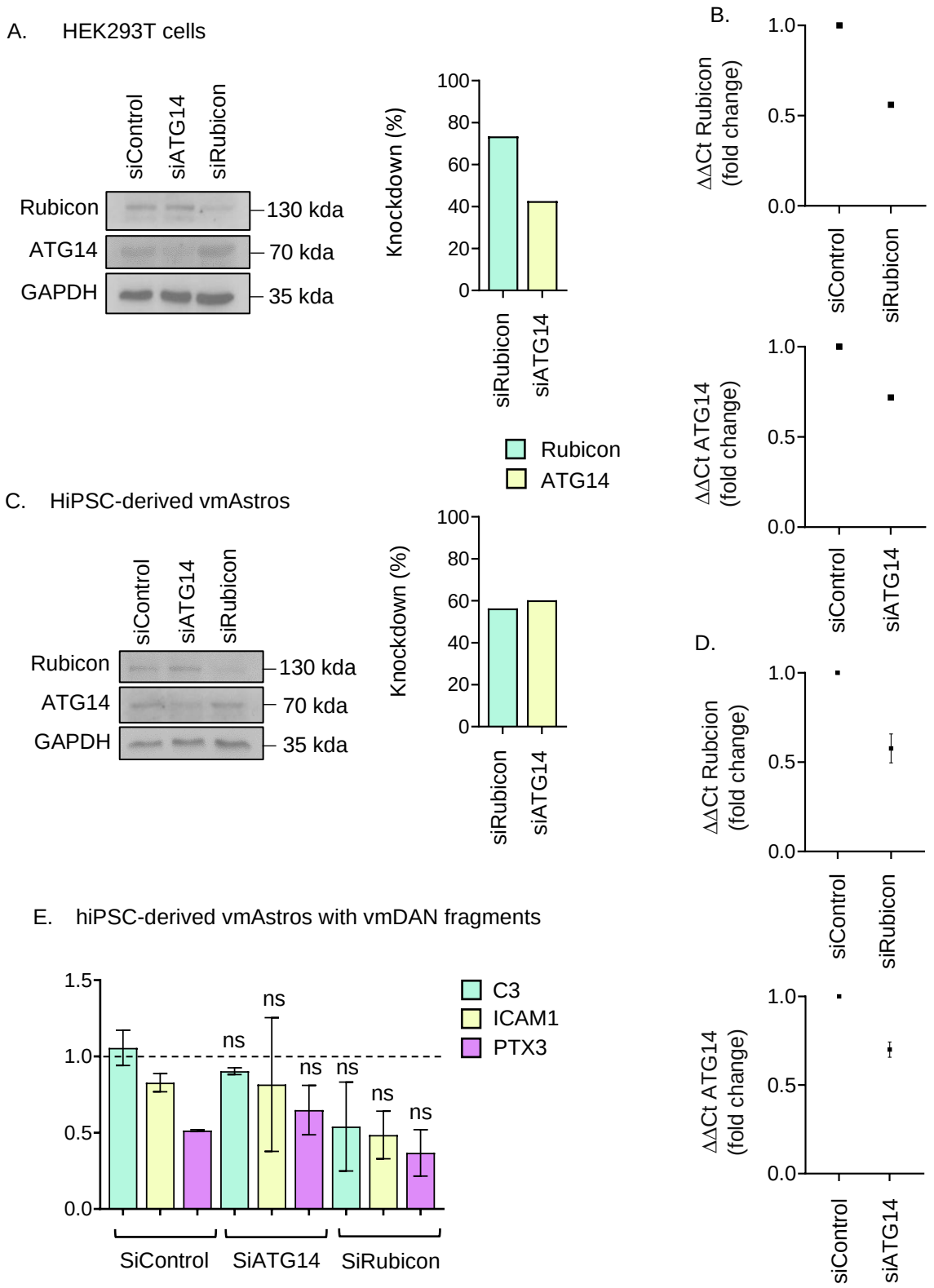

Figure 13. LAP-deficient hiPSC-derived vmAstros showed no neuroinflammatory response when LAP was induced with vmDAN fragments.

(A) Immunoblot of protein levels following siRNA suppression of ATG14 or Rubicon in HEK293T cells. (B) qRT-PCR analysis of gene expression following siRNA suppression of ATG14 or Rubicon in HEK293T cells. (C) Immunoblot of protein levels following siRNA suppression of ATG14 or Rubicon in hiPSC-derived vmAstros. (D) qRT-PCR analysis of gene expression following siRNA suppression of ATG14 or Rubicon in hiPSC-derived vmAstros. (E) qRT-PCR analysis of inflammatory gene expression following siRNA suppression of ATG14 or Rubicon in hiPSC-derived vmAstros cultured with vmDAN fragments (24h). Mean ± s.e.m, n = 3; one way ANOVA; ns= not significant.

3.8 LAP modulation of the neuroinflammatory response with AST23 vmDANs

Previous experiments were performed using neuronal cells derived from NAS2 hiPSCs which are wild-type for α-syn. Accumulation and aggregation of α-syn is a hallmark of PD (Ray *et al*, 2020), and α-syn is the major constituent of Lewy bodies and a potent inflammatory stimulus for neighbouring glial cells (Roodveldt, Christodoulou & Dobson, 2008). Furthermore, overexpression of α-syn in mouse models triggers vmDAN degeneration (Xu *et al*, 2002). Subsequent experiments therefore used AST23 hiPSCs derived from a PD patient with a triplication in the α-syn gene (SCNA), providing an *in vitro* model more closely recapitulating PD-related pathology.

Whereas vmDAN fragments derived from NAS2 hiPSCs were unable to induce an inflammatory response in vmAstros (Fig.11F), we hypothesised that fragments from AST23-derived vmDANs would stimulate a pro-inflammatory response due to the combinatorial presence of elevated α-syn. AST23 hiPSCs were terminally differentiated to vmDANs as previously described (Fig.11A). qRT-PCR analysis detected no substantial upregulation of pro-inflammatory markers 4hrs or 24hrs post-incubation with AST23 vmDANs (Fig.14A-B).

To determine whether LAP-deficient vmAstros were more vulnerable to neuroinflammatory activation with AST23 vmDANs, the siRNA transfection methods that were previously validated were employed to suppress Rubicon and ATG14 expression (Fig.13A-C). Compared to control-siRNA treated vmAstros, there was no significant up- or down-regulation in inflammatory markers in Rubicon and ATG14-deficient vmAstros (Fig.14C). Therefore, no modulation of the inflammatory response was observed during vmAstro-mediated clearance of PD-like vmDAN corpses.

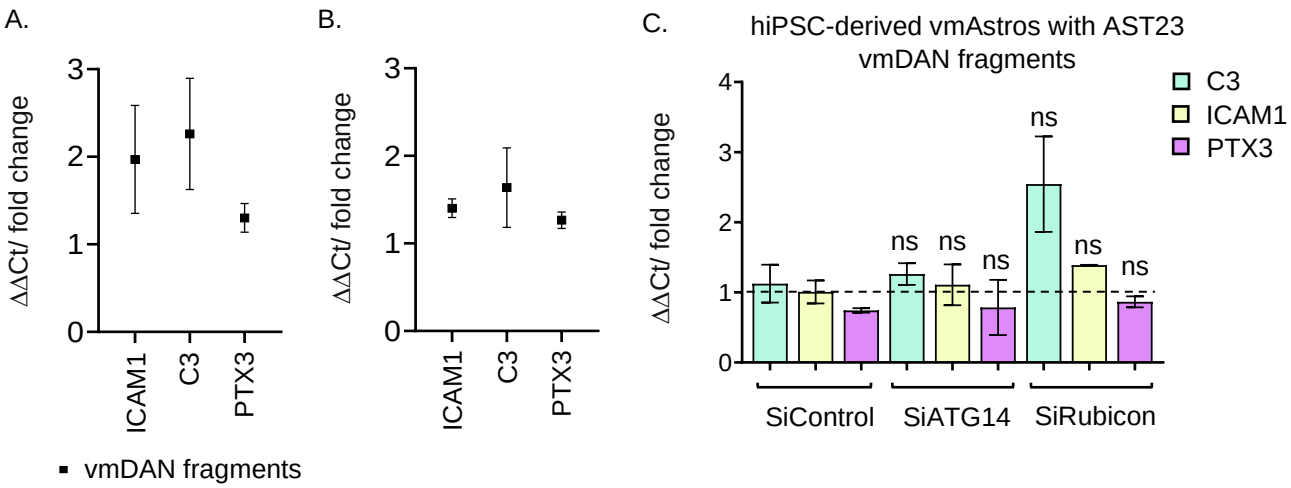

Figure 14. LAP-deficient hiPSC-derived vmAstros showed no neuroinflammatory response when LAP was induced with AST23 hiPSC-derived vmDAN fragments.

qRT-PCR showing the change in expression of inflammatory markers when LAP was induced with AST23 hiPSC-derived vmDAN fragments in hiPSC-derived vmAstros after (A) 4hrs and (B) 24hrs. (C) qRT-PCR analysis of change in expression of inflammatory markers following siRNA suppression of ATG14 or Rubicon in hiPSC-derived vmAstros cultured with AST23 hiPSC-derived vmDAN fragments (24h). Mean ± s.e.m, n = 2-3; one way ANOVA; ns= not significant.

4. Discussion

The motor symptoms of PD are initiated by the preferential loss of vmDANs in the SNpc (Forno, 1996). To preserve the function of the CNS and prevent propagation of PD-related pathology, the efficient and safe removal of vmDAN debris is crucial. However, the exact clearance pathways utilised in the brain at the early stages of PD are not known, and the possible participation of LAP during this inherent process has not previously been reported. Of note, LAP activity diminishes with age, with LAP-deficiency concomitantly causing elevated inflammation in macrophages of the peripheral immune system (Inomata *et al*, 2020). Given that chronic neuroinflammation is hallmark of PD suggested to accelerate the loss of vmDANs (Gelders, Baekelandtan & Van der Perren, 2018), the potential involvement of LAP in neuroinflammatory PD pathophysiology merits detailed analysis.

In this study, hTERT-RPE1 cells were first employed as an amenable cell-type to optimise LAP induction with zymosan particles, prior to their use in hiPSC-derived glial models. Frequent $LC3^+$ phagosomes were detected in RPE1 cells 4hrs and 24hrs post-incubation with opsonized zymosan particles; however, only 1/6 cells (4hrs) or 1/13 cells (24hrs) that had phagocytosed zymosan possessed $LC3^+$ LAPosomes. Possible explanations include RPE1 cells which have powerful antioxidant pathways are effectively LAP defective (since ROS generation is essential for the progression of LAP), or alternatively, given that LAP is an active and dynamic process, RPE1 cells might be highly efficient such that at steady state few LAP profiles can be seen in fixed cells. Overall, these results provided proof-of-study for our *in vitro* measurement of LAP induction with zymosan.

4.1 hiPSC-derived vmAstros

4.1.1 Generation of vmAstros

Astrocytes are the most abundant glial cell in the CNS, residing close to neurons and required for maintaining metabolic homeostasis and synaptic integrity (Linnerbauer &

Rothhammer, 2020). In PD, vmAstro dysfunction has been closely linked to vmDAN degeneration, highlighting the importance of understanding the mechanisms mediating vmAstro neurotoxicity. Astrocytes are heterogenous cells with distinct developmental origins, with their gene expression profiles, physiology, and function dependent on the surrounding subtypes of neuronal populations (Zhang & Barres, 2010). In a process resembling astrocyte generation in the brain, hiPSC-derived vmNPCs were differentiated to vmAPCs, and these cells were matured to functional human vmAstros: with confirmed expression of the mature astrocyte marker (GLAST) as well as midbrain markers (FOXA2), as expected.

4.1.2 vmAstro reactive phenotype

The activated phenotypes of astrocytes are described as A1 (pro-inflammatory) or A2 (anti-inflammatory), with chronic A1 activation being associated with PD (Linnerbauer & Rothhammer, 2020). In the present study, A1 astrocyte activation was achieved through the administration of an inflammatory cocktail comprising IL-1α, TNF-α, and C1q, which mimics conditions that are initiated following microglial activation in the brain (Liddelow *et al*, 2017). This generated reactive vmAstros which secreted a variety of pro-inflammatory markers implicated in CNS pathologies (including ICAM1 and C3). ICAM1 is a transmembrane glycoprotein expressed in astrocytes, and its stimulation induces expression of pro-inflammatory cytokines such as IL-1α, IL-1β, IL-6, and TNF-α (Lee *et al*, 2000). Of note, PTX3, a pattern recognition molecule with roles in tissue repair via its involvement in forming the glial scar, was also upregulated. PTX3 is a marker typically associated with A2 astrocytes (Rodriguez *et al*, 2014), so its upregulation in ITC-treated vmAstros presents conflicting evidence on their activation state. Interestingly, ITC treatment of murine astrocytes caused suppression of PTX3 expression, with elevated PTX3 expression reported only in the presence of IL-1β (Liddelow *et al*, 2017). It is possible that there are species-specific differences in the reactive profiles of astrocytes, or that ventral midbrain astrocytes behave differently to the forebrain subtype analysed in Liddelow et al, (2017). It is also possible that autocrine signalling in our *in vitro* setting finetunes the vmAstro inflammatory

response, although absence of secreted IL-1β in our assay system (Crompton *et al*, 2023) would possibly argue against this.

In the context of the above, it is perhaps significant that glial-derived PTX3 has been found to stimulate microglial phagocytosis of zymosan particles, suggesting that astrocyte-derived PTX3 enables reciprocal regulation of microglia function in the brain immune setting (Jeon *et al,* 2010). In our system, whilst the fold increase in PTX3 gene expression (20.18-fold) was notable, it was substantially lower than the change in C3 expression (624.85-fold increase). C3 is a marker specific for the A1 phenotype (Liddelow et al, 2017). C3 is a component of the complement system and its increased expression in A1 activated astrocytes is associated with impairing neuronal morphology and function (Lawrence *et al*, 2023). Furthermore, activation of the transcription factor nuclear factor-κB (NF-κB) increases C3 complement release from astrocytes and C3/NF-κB activation induces the expression of pro-inflammatory cytokines and adhesion molecules (Fan & Huo, 2021; Yates, 2015; Kempuraj *et al*, 2016). IL-10, an anti-inflammatory cytokine, suppresses inflammation via inhibiting NF-κB and suppresses microglia activation which is neuroprotective in populations of vmDANs *in vitro* and *in vivo* (Kempuraj *et al*, 2016). Overall, dual upregulation of C3 and ICAM1 supports the generation of A1 vmAstros. In addition to looking at changes to inflammatory gene expression, future experiments should investigate alterations in protein secretion via enzyme-linked immunosorbent assay (ELISA) to provide more accurate interpretation on the corresponding changes to the phenotype of the cell after ITC treatment.

4.1.3 LAP induction in quiescent and reactive vmAstros

Astrocytes are important for immune regulation and for phagocytic removal of pathological substrates and cell debris (Lee & Chung, 2021; Jensen, Massie & De Keyser, 2013). Astrocytes are non-professional phagocytes, but their essential role in phagocytosing harmful CNS substrates has been reported over recent years. This is perhaps best supported by data showing that astrocytes can compensate for phagocytic activities when

microglia are impaired (Konishi *et al*, 2020). To explore the potential involvement of LAP in midbrain glial debris clearance, vmAstros were incubated with opsonized zymosan particles revealing numerous cells which had phagocytosed opsonized zymosan into $LC3^+$ vacuoles. This supports recent findings that astrocytes can recruit LAP for clearing a variety of cellular debris in the CNS (Zhou *et al*, 2022; Wakida *et al*, 2022; Szabó *et al*, 2023).

PD has been linked to autophagy dysfunction and defects in the machinery that regulates both canonical autophagy and LAP (Martinez, 2018). Recent data suggested that HD striatal astrocytes were LAP-deficient compared to WT astrocytes (Wakida *et al*, 2022). This proposes a negative relationship between LAP and HD pathology. To test whether this relationship applied to our *in vitro* system of inflammatory vmAstros, the number of $LC3^+$ LAPosomes were quantified in quiescent and ITC-treated vmAstros. In quiescent vmAstros, 1/4 of cells with phagocytosed zymosan possessed $LC3^+$ vesicles, in contrast, 1/15 of cells with phagocytosed zymosan possessed $LC3^+$ vesicle in ITC-treated vmAstros. The significant reduction in detected LAP profiles suggests that our pro-inflammatory vmAstros were LAP-deficient. Of note, phagocytosis of zymosan was comparable between the two treatments, suggesting the significant reduction in $LC3^+$ vesicles was specific to changes in the mediators regulating LAP rather than canonical phagocytosis. Given that our ITC-treated vmAstros phenotypically mimic A1 activated vmAstros characteristic of PD, this generates interest into whether LAP is defective in neurodegenerative diseases, like PD. Future experiments should explore how increased neuroinflammatory signalling interferes with the machinery governing LAP, for example, via immunoblotting different components responsible for phagosome maturation and membrane lipidation.

4.2 hiPSC-derived vmMicroglia

4.2.1 Generation of vmMicroglia

Microglia are ubiquitously dispersed in the CNS and are principally neuroprotective under physiological conditions (Reemst *et al*, 2016). Microglia can have opposing roles during

injury, infection, or disease, and can readily switch to a neurotoxic phenotype in CNS pathologies (Gao *et al*; 2002; Hickman *et al*, 2018). The present study derived vmMicroglia from hiPSCs, generating cells with strong expression of macrophage lineage markers (CD11b and CD14) as well as the mature microglial markers (IBA1). For future direction of this project, hiPSC-derived vmMicroglia should undergo further characterisation and more vigorous study in order to discriminate microglia from other myeloid cells. For example, the transmembrane protein, TMEM119, has been reported to be more specific to microglia than IBA1, a calcium binding protein which has also been identified in macrophages (Bennett *et al*, 2016). Furthermore, microglia are characterised as $CD11b^{+}CD45^{low}$ whereas macrophages are $CD11b^{+}CD45^{+}$ (Martin *et al*, 2017). Hence, fluorescent activated cell sorting (FACS) could be employed to categorise heterogenous populations of cells with these important molecular phenotypes.

Generating hiPSC-derived vmDANs and vmAstros has been well described (Stathakos *et al*, 2021; Crompton *et al*, 2021), whereas methods to derive vmMicroglia from hiPSCs have not been reported. Several studies have presented conflicting findings on whether microglia residing in different regions of the CNS possess unique transcriptional and functional signatures (De Biase *et al*, 2017; Grabert *et al*, 2016; Li *et al*, 2019). However, it is well understood that microglia are critically influenced by their environment, particularly important when their progenitor cells migrate to the CNS during mid-embryonic development: preventing the maturation of peripheral myeloid cells and promoting the maturation of microglia (Ginhoux *et al*, 2010). The present study generated vmMicroglia by maturing the MPCs in vmAPC conditioned media to recapitulate the environment in the ventral midbrain: the area of the brain first susceptible to vmDAN loss in PD. Interestingly, only a few cells appeared to express classical midbrain markers (FOXA2 and LMX1B). Future experiments should attempt to evaluate how the transcriptional landscape of microglia changes when their progenitor cells are cultured in vmAstro conditioned media compared to cortical

astrocyte media. This will assess whether microglia are primed by different environments and display regional heterogeneity *in vitro*.

4.2.2 vmMicroglia reactive phenotype

During ageing, microglia exit their resting state and become 'primed' to a low level of activation (Cornell *et al*, 2022; Koss *et al*, 2019). In PD, microglia become chronically activated to an M1 pro-inflammatory phenotype (Liddelow & Barres, 2017). This study aimed to test the functional properties of the hiPSC-derived vmMicroglia via the use of the M1 pro-inflammatory stimulus, LPS. Microglia upregulated several pro-inflammatory markers including IL-6, IL-1β, and CCL2 during LPS stimulation of TLR signalling. These pro-inflammatory cytokines and chemokines are classically upregulated in neurodegenerative diseases including PD:

- **IL-1β**; elevated levels of IL-1β have been reported in the SNpc in PD patient-post mortem studies (Przedborski, 2007). In the SNpc of MPTP-induced animal models, IL-1β levels were increased, and interfering with IL-1β signalling in this setting reduced vmDAN neurotoxicity (Yan *et al*, 2014; Jackson-Lewis *et al*, 2002). Autocrine signalling of IL-1β in microglia can stimulate the macrophage glycoprotein receptor CD23 inducing the expression of iNOS leading to the accumulation of NO exacerbating neuroinflammation (Phani, Loike & Przedborski, 2012).
- **IL-6**; IL-6 activates classical Jak/Stat signalling cascades required for neuronal development, growth, and survival (Kummer *et al*, 2021; Lashgari *et al*, 2021). Alternatively, increased serum levels of IL-6 have been reported in PD patients, and high plasma concentrations of IL-6 have been associated with increased risk of developing PD (Scalzo *et al*, 2010; Yan *et al*, 2014). Accordingly, dysregulated or over-production of IL-6 is detrimental to vmDAN health and survival.
- **CCL2**; CCL2 is a member of the monocyte chemoattractant protein (MCP) family constitutively expressed in neurons and glia (Bose & Cho, 2013). Its receptor, CCR2,

has been identified in vmDANs of the SNpc and increased levels of CCL2 have been reported in PD patient studies (Qu *et al*, 2023). CCL2 is involved in recruiting monocytes and T cells to sites of inflammation and has extensive links to chronic neuroinflammation (Bose & Cho, 2013).

It is worth noting that based on comparison with current literature, the upregulation of these pro-inflammatory cytokines and chemokines was lower than predicted (Lively & Schlichter, 2018). Hence, future experiments should attempt to optimise the concentration of LPS or add additional inflammatory supplements such as IFN-γ and Nigericin to maximise the inflammatory response (Lively & Schlichter, 2018). Microglia activation is also strongly promoted by fibronectin, a glycoprotein in the extracellular matrix utilised for adhering vmMicroglia in culture (Milner & Campbell, 2003). Therefore, culturing the vmMicroglia on fibronectin-coated plates may have interfered with the comparison of the inflammatory response between the activated (LPS-treated) and quiescent (non-LPS treated) vmMicroglia. Of note, whilst monitoring inflammatory activation during LPS treatment assists in testing the functional properties of the vmMicroglia, macrophages also respond to LPS-treatment (Rossol *et al*, 2011); therefore, this does not facilitate the distinction between these two cell types.

4.2.3 LAP induction in vmMicroglia

As microglia are considered to have related immune functions and inflammatory regulation to macrophages, characterising LAP in these cells was of paramount importance. vmMicroglia were cultured with opsonized zymosan particles to induce LAP revealing a considerable dependence of LAP in vmMicroglia: demonstrated by 1/2 of cells that had phagocytosed zymosan possessed $LC3^{+}$ LAPosomes. This data supports novel findings that microglia recruit LAP in models of CNS injury (Szabó *et al*, 2023).

Dysregulated phagocytosis in microglia may lead to an accumulation of neuronal corpses and accelerated neuronal degeneration, and this has been suggested to participate in

neurodegenerative disease progression (Tremblay, Cookson & Civiero, 2019). Several studies have sought to investigate whether the phagocytic activities of microglia are up- or down-regulated during inflammation. In a mouse model infected with prions, microglia phagocytosis was upregulated (Sinha *et al*, 2021). Alternatively, microglia phagocytic activity was downregulated in an AD model, triggering neuronal damage and the presence of plagues (Fu *et al*, 2016; Lee *et al*, 2018). In models of infection, treatment with TLR agonists significantly increased microglial phagocytosis of bacteria (Kochan *et al*, 2012). In contrast, LPS stimulation of TLRs suppressed ATG expression and impaired phagocytosis and degradation via LAP in primary microglia cultures (Lee *et al*, 2019). TLRs have been linked to PD pathology, α-syn has been reported to activate microglia and alter the expression of TLRs, for example (Béraud *et al*, 2011). Given the recruitment of LAP was significantly reduced in A1 vmAstros, future experiments should monitor LAP during vmMicroglia M1 activation induced by LPS-mediated TLR signalling.

4.3 vmDAN fragments as novel LAP cargo in ventral midbrain glia

vmDANs are the first class of neurons susceptible to degeneration in PD, and by the time the clinical symptoms of PD are apparent, and the diagnosis made, up to 70% of vmDANs have been lost (Simon, Tanner & Brundin, 2020). Engulfment of neuronal fragments by phagocytic glia has been demonstrated *in vitro* and *in vivo* (Raiders *et al*, 2021). Astrocytes and microglia play orchestrated roles when phagocytosing neuronal corpses: astrocytes engulfed small dendritic apoptotic bodies and microglia engulfed soma and apical dendrites (Damisah *et al*, 2020). To study whether LAP was recruited for supported clearance of vmDANs by ventral midbrain glial cells, hiPSCs were differentiated toward vmDANs, and these cells expressed the mature neuronal marker TUJ1 as well as the midbrain marker TH, as expected. Fragments of cells were obtained via UV-mediated DNA damage which was used to deduce whether LAP was involved during their phagocytic clearance. However, when the vmDAN fragments were cultured with vmAstros and vmMicroglia, no $LC3^{+}$ LAPosomes were detected. One explanation for these results is the methodological

limitation of monitoring $LC3^+$ LAPosomes with anti-LC3B antibody staining in fixed cells, since LAP is a highly active and dynamic process. Still, a recent study demonstrated that astrocytes recruit LAP during the removal of microglia debris (Zhou *et al*, 2022), and astrocytes and microglia recruit LAP for the clearance of axonal debris in models of CNS injury (Szabó *et al*, 2023). Accordingly, the requirement of LAP during this essential housekeeping process should not yet be dismissed. Future studies should attempt time-lapse imaging on fluorescent LC3-labelled cells in attempt to capture LC3 conjugation to vmDAN-containing phagosomes.

A variety of pro-inflammatory stimuli have been reported to activate glial cells. For example, increased permeability of the BBB can promote glial activation via infiltrating components of the adaptive immune system including $CD4^+$ T lymphocytes: found in the SNpc of PD patients (Brochard et al, 2008). Furthermore, degenerating vmDANs release ROS, α-syn, and cell debris leading to lasting stimulation and activation of neighbouring glia (Castillo-Rangel *et al*, 2023). Therefore, a detrimental positive feedback loop exists between activated glial cells, chronic neuroinflammation and loss of vmDANs in PD. The present study aimed to test whether vmDAN fragments cultured with quiescent ventral midbrain glial cells would stimulate an inflammatory response *in vitro*. After 24hrs in culture with vmDAN fragments, no upregulation of neuroinflammatory cytokines or chemokines were detected in vmAstros or vmMicroglia. Therefore, vmDAN fragments did not drive an A1/A2 or M1/M2 inflammatory phenotype in our hiPSC-derived glial models. Several explanations could account for these results. Firstly, the low level of activation common with *in vitro* cultures of microglia (discussed in section 4.2.2) could have perturbed comparison of the neuroinflammatory response with vmDAN corpses. Though, a recent study found synaptosomes, myelin debris, apoptotic neurons, or synthetic amyloid-beta fibrils drove the formation of different transcriptional states in hiPSC-derived microglia including that of neurotoxic M1 phenotype (Dolan *et al*, 2023). This data supports the idea that changes in the active state of microglia can be detected *in vitro*. Given that both vmMicroglia and vmAstros were not activated to

their respective pro- or anti-inflammatory phenotype, a more likely explanation could be assigned to the properties of the vmDAN fragments. Post-UV damage, the vmDAN fragments may not phenotypically resemble vmDAN debris in the midbrain. Therefore, alternative methods to induce neuronal death might be beneficial for future analysis.

4.4 LAP modulation of the neuroinflammatory response

Interestingly, several studies have identified that cells that are LAP defective (via silencing the protein, Rubicon) cultured with apoptotic cells stimulate increased expression and release of pro-inflammatory cytokines (IL-1β, IL-6) and chemokines (CXCL-10) (Heckmann & Green, 2019). In this study, Rubicon and ATG14 knockdown was used to assess the neuroinflammatory outcome of LAP and autophagy-deficient hiPSC-derived vmAstros in a PD-like model. Lentiviral transduction of shRNA was first selected to suppress protein expression. Cells that internalized the virus containing the shRNA-plasmid construct were tested for the reduction in ATG14 and Rubicon expression. However, no suppression in either protein was observed when vmAstros were transduced with their respective shRNA lentiviruses compared to shRNA-control treated cells. Therefore, the shRNA-plasmid failed to sufficiently knockdown the proteins of interest. Subsequent experiments transiently transfected siRNA targeting ATG14 or Rubicon; concluding protein expression was adequately suppressed following siRNA treatment in hiPSC-derived vmAstros. vmDAN fragments were next cultured with the Rubicon and ATG14 deficient cells; however, no significant upregulation in inflammatory markers (ICAM1, C3, and PTX3) was observed (discussed in section 4.5).

Most PD cases are sporadic, emerging from an interaction between genetic susceptibility and environmental factors such as ageing, infections, and toxins. Alternatively, 5-10% are familial cases (Simon, Tanner & Brundin, 2020; Matheoud *et al*, 2019). To date, over 20 genetic loci (PARK) have been linked to PD found on genes such as SCNA (α-syn gene), LRRK2 (leucine-rich repeat kinase 2), VPS35 (vacuolar protein sorting 35 retromer complex

component), and PINK1 (PTEN-induced kinase 1). Inflammation plays a major role in both the sporadic and inherited forms of PD, and many inherited mutant genes associated with PD have been linked to regulating inflammatory responses (Deleidi & Gasser, 2013). Previous experiments were performed using NAS2 hiPSCs which possess no PD-specific mutations in the SNCA. However, hiPSCs provide a unique opportunity for generating cells derived from patients with disease-associated mutations. The final experiments used AST23 hiPSCs which contain a triplication in the SNCA which is typically associated with early-onset PD (Lee & Trojanowski, 2006). Importantly, SCNA gene triplication has been reported to increase α-syn in terminally differentiated hiPSC-derived cells (Tagliafierro & Chiba-Falek, 2016). α-syn is an abundant pre-synaptic protein found in proximity with synaptic vesicles in neurons (Sulzer & Edwards, 2019). Physiologically, α-syn is thought to regulate neurotransmitter release and synaptic transmission via chaperoning the assembly of the soluble NSF attachment protein receptor (SNARE) complex (Sulzer & Edwards, 2019). α-syn aggregation and the formation of amyloid fibrils is closely linked with PD pathology, and α-syn makes up the major constituent of Lewy bodies (Ray *et al*, 2020; Ohgita *et al*, 2022). In mouse models, overexpression of α-syn induced nigrostriatal dopaminergic denervation (Kirik *et al*, 2002), and α-syn has been identified as a potent inflammatory stimulus for neighbouring glia (Roodveldt, Christodoulou & Dobson, 2008). Therefore, we reasoned that while the NAS2 vmDAN fragments did not stimulate glial activation, dual action of vmDAN fragments and increased levels of α-syn would stimulate a pro-inflammatory response. For this study, AST23 hiPSCs were differentiated toward vmDANs and fragmented via UV-mediated damage. After 4hrs and 24hrs incubation of AST23 vmDAN fragments with vmAstros, no upregulation of pro-inflammatory markers (ICAM1 and C3) or anti-inflammatory markers (PTX3) was observed. Next, we sought to test whether Rubicon and ATG14-deficient vmAstros were more prone to activation and stimulation of the neuroinflammatory response when in culture with AST23-derived vmDAN fragments. However, similar findings to the NAS2 experiments were concluded, whereby no upregulation in pro- and anti-

inflammatory mediators were found using the AST23 vmDAN fragments (discussed in section 4.5).

4.5 Future refinements to the experimental design

Previously, stimulation of vmAstros with vmDAN fragments significantly upregulated the anti-inflammatory molecule PTX3 (Trainer, 2021). This supports the motivation for investigating the neuroinflammatory consequence in glial cells challenged with vmDAN fragments. Furthermore, this generates interest into the consequence of LAP-deficiency on the A2 neuroprotective vmAstro phenotype. The results presented in this report could not identify any changes to the neuroinflammatory response when phagocytosis was induced with vmDAN corpses in quiescent or Rubicon-deficient glial cells. To this end, future research could optimise and refine the experimental design by adjusting several different parameters:

1. Improved suppression of Rubicon and ATG14 expression.

Unsuccessful modulation of the neuroinflammatory response during LAP attenuation with siRNA could be resolved by improving the knockdown efficacy of Rubicon and ATG14 expression. Approximately, 50% Rubicon expression may have been sufficient for immunologically silent phagocytic clearance of vmDANs. Therefore, future experiments should explore alternative gene silencing mechanisms. For example, shRNA gene silencing may provide greater protein depletion for more vigorous testing of LAP deficiency in hiPSC-derived vmAstros. Furthermore, shRNA is generally preferred over siRNA due to fewer off-target affects, lower concentrations and the opportunity for inducible applications (Rao *et al*, 2009).

Of note, the current study identified siRNA modulation of the inflammatory response in siRNA-control treated cells. This suggests that siRNA acting via the RISC complex could be altering inflammation i.e. via IFN signalling and stimulating viral-like host responses (Sioud, 2005). This represents a major challenge in siRNA knockdown experiments and future

research could benefit from employing CRISPR interference(i)-based gene knockdowns to circumvent viral-like host responses and provide highly efficient gene knockdowns (Larson *et al*, 2013).

2. Alternative methods for generating vmDAN fragments.

As discussed previously, the methods in this study to generate vmDAN fragments via UV-mediated cell damage may have altered the molecular and chemical properties of the fragments so that they no longer recapitulate degenerating dopaminergic neurons in the ventral midbrain. Future experiments should explore (patho)physiologically relevant approaches to induce apoptosis in cultures of vmDANs. For example, transfection of wild-type or mutant α-syn selectively induced apoptosis in cultures of vmDANs, but not cortical neurons (Xu *et al*, 2002). Given α-syn dysregulation is intrinsically involved in pathogenesis of PD, this may provide a model for cell death more appropriate for PD studies. This method could also improve the characterization of vmDAN fragments and increase the proportion of fragments derived from $TUJ1^{+}TH^{+}$ cells.

3. Optimising the timepoints to monitor LAP modulation of the neuroinflammatory response.

The results presented in this report monitored neuroinflammatory induction in wild-type and Rubicon deficient vmAstros 24hrs post-incubation with vmDAN fragments. However, the optimal time point to study LAP modulation of the neuroinflammatory response has not been adequately tested. The present study found the number of $LC3^{+}$ vesicles were significantly higher 4hrs post-incubation with opsonized zymosan compared to 24hrs in cultures of glial cells. Furthermore, literature reports suggest that LAP peaks at 30 min to 1h after phagocytosis (Romao & Münz, 2014), and the inflammatory response in LAP-deficient macrophages was monitored after 1.5hrs (Inomata *et al*, 2020). Therefore, this suggests that investigation of LAP modulation is preferential during the early dynamic phase of LAP. In contrast, *in vitro* studies monitoring glial activation typically monitor the neuroinflammatory

response after 24hrs or across several days (Liddelow *et al*, 2017). Therefore, future research should characterise how neuroinflammatory markers change over time following LAP induction.

4. Monitor the neuroinflammatory response with opsonized zymosan.

$LC3^+$ LAPosomes were detected in cultures of hiPSC-derived vmAstros and vmMicroglia post-exposure to opsonized zymosan. However, whether vmDAN fragments are phagocytosed into $LC3^+$ vacuoles in ventral midbrain glial cells is uncertain, as current measurements failed to detect profiles of LAP. For this reason, the present study would benefit from examining the neuroinflammatory response with zymosan (i.e., cargo known to engage LAP in our vmAstros). This would provide a critical comparison to the expected changes during neuroinflammatory activation in wild-type and LAP-deficient vmAstros.

5. Use of exogenous α-syn.

AST23 vmDAN fragments did not provoke an inflammatory response in vmAstros after 4hrs or 24hrs. Therefore, alternative sources of α-syn supplementation could be employed. For example, exogenous administration of α-syn can activate microglia, and this was found to be toxic in cultures of vmDANs (Zhang *et al*, 2005). Furthermore, α-syn has been reported to increase GFAP levels in astrocytes, traditionally a marker used to assess astrocyte reactivity (Cavaliere *et al*, 2017). Therefore, the use of exogenous forms of α-syn in combination with vmDAN fragments may stimulate altered neuroinflammatory signalling to allow comparison of the neuroinflammatory response in wild-type and LAP-deficient vmAstros.

6. LAP suppression in hiPSC-derived vmMicroglia.

Immunocytochemistry analysis suggested vmMicroglia had a greater dependence on LAP for the removal of zymosan than vmAstros. Accordingly, vmMicroglia could be more susceptive to inflammatory activation during LAP-deficiency. However, the intra- and inter-culture variability of EBs and MPC-producing factories hindered the opportunity to further

explore the importance of LAP in vmMicroglia. Before subsequent experimentation, work should try to optimise the differentiation protocol for more efficient and scalable generation of vmMicroglia from hiPSCs.

7. Exploring alternative methods for attenuating the progression of LAP.

Molecular characterization of the protein Rubicon was made within the last decade, with studies reporting an essential and specific requirement of Rubicon for the progression of LAP. However, in recent years, our understanding of LAP and non-canonical autophagy (e.g., CASM) has expanded, uncovering new targets which could be more specific to study LAP-deficiency. For example, V-ATPase has been shown to be a master regulator of LAP and CASM: the association of V-ATPase V0-V1 subunits is required for ATG16L recruitment and ATG8 lipidation (Hooper *et al*, 2022). Therefore, alternative methods for targeting LAP and non-canonical autophagy should be explored.

Refining the experimental procedures with the suggestions made above would offer new avenues to explore LAP-deficiency in the ventral midbrain and in the context of PD. Given that glial dysfunction has been reported to induce neuronal damage and potentiate vmDAN degeneration (Phani, Loike & Przedborski, 2012), future research could also establish co-culture systems to explore the neurotoxic effects of LAP-deficient glial cells in culture with vmDANs (i.e., by measuring changes to neurite length or quantifying γ-H2AX staining: a marker specific for DNA damage) (Clements *et al*, 2022; De Miranda *et al*, 2015).

To date, there are no PD treatments available to halt the degeneration of vmDANs. Dopamine-based therapies (e.g., levodopa) have become a popular choice for alleviating dopamine depletion and improving prognosis in PD patients (Armstrong & Okun, 2020). Furthermore, nonsteroidal anti-inflammatory drugs (NSAIDs) have been suggested to be neuroprotective in neurodegenerative disorders via dampening neuroinflammation (Kempuraj *et al*, 2016). This typifies the contribution of neuroinflammation to PD-pathology and supports the need to understand the (patho)physiological mechanisms that mediate

neuroinflammation. This could provide new treatment strategies and opportunities to improve early preventative measures.

Overall, there is emerging evidence implicating the requirement of LAP in health and disease. For example, LAP has been identified in phagocytes (Inomata *et al*, 2020; Masud *et al*, 2019) and non-professional phagocytes (Frost *et al*, 2015; Zhou *et al*, 2022) in models of injury (Szabó *et al*, 2023), infection (Inomata *et al*, 2020; Masud *et al*, 2019), and disease (Wakida et al, 2022; Wan *et al*, 2020). However, the importance of LAP and the consequences of LAP-deficiency remains largely unknown. For example, it was first suggested that mice deficient in LAP, but not canonical autophagy, showed increased inflammatory cytokine and autoantibody production, and when injected with dying cells, stimulated the development of systemic lupus erythematosus (SLE)-like disease (Martinez *et al*, 2016). However, it was later shown that the reverse was true: Rubicon-deficiency was advantageous in an SLE mouse model (Gordon *et al*, 2022). Therefore, further research is needed to fully understand and characterise the important roles of LAP.

4.6 Concluding remarks

The present study has shown that vmAstros and vmMicroglia recruit LAP for assisted clearance of conventional LAP stimulants such as zymosan. Furthermore, the current study demonstrated that when vmAstros are activated to a pro-inflammatory phenotype resembling PD-like pathology, the rate of canonical phagocytosis was not influenced by vmAstro reactive status, whereas the incidence of LAP profiles was markedly reduced during the early, dynamic phase. This could have important implications for the possible involvement of LAP in vmAstro responses to local pathology. Future experiments should priorities optimising the experimental design during phagocytosis induction with vmDAN fragments in our hiPSC-derived glial model of human neuroinflammation. This would enable more vigorous assessment on the contribution of LAP during glial phagocytic clearance and allow changes to the neuroinflammatory response during LAP-deficiency to be monitored.

5. References

Allen, L. and Aderem, A. (1995) ‘A role for MARCKS, the alpha isozyme of protein kinase C and myosin I in zymosan phagocytosis by macrophages’, *The Journal of Experimental Medicine*, *182*(3), pp. 829-840.

Anderson, M. Burda, J. Ren, Y. Ao, Y. O’Shea, T. Kawaguchi, R. Coppola, G. Khakh, B. Deming, T. and Sofroniew, M. (2016) ‘Astrocyte scar formation aids central nervous system axon regeneration’, *Nature*, *532*(7598), pp. 195-200.

Antón, Z. Betin, V. Simonetti, B. Traer, C. Attar, N. Cullen, P. and Lane, J. (2020) ‘A heterodimeric SNX4–SNX7 SNX-BAR autophagy complex coordinates ATG9A trafficking for efficient autophagosome assembly’, *Journal of Cell Science*, *133*(14), p. jcs246306.

Arena, G. Sharma, K. Agyeah, G. Krüger, R. Grünewald, A. and Fitzgerald, J. (2022) ‘Neurodegeneration and neuroinflammation in Parkinson’s disease: a self-sustained loop’, *Current Neurology and Neuroscience Reports*, *22*(8), pp. 427-440.

Armstrong, M. and Okun, M. (2020) ‘Diagnosis and treatment of Parkinson disease: a review’, *Jama*, *323*(6), pp. 548-560.

Backer, J. (2016) ‘The intricate regulation and complex functions of the Class III phosphoinositide 3-kinase Vps34’, *Biochemical Journal*, *473*(15), pp. 2251-2271.

Ball, N. Teo, W. Chandra, S. and Chapman, J. (2019) ‘Parkinson's disease and the environment’, *Frontiers in Neurology*, *10*, p. 218.

Barbin, G. Katz, D. Chamak, B. Glowinski, J. and Prochiantz, A. (1988) ‘Brain astrocytes express region-specific surface glycoproteins in culture’, *Glia*, *1*(1), pp. 96-103.

Barz, S. Kriegenburg, F. Sánchez-Martín, P. and Kraft, C. (2021) ‘Small but mighty: Atg8s and Rabs in membrane dynamics during autophagy’, *Biochimica et Biophysica Acta (BBA)-Molecular Cell Research*, *1868*(9), p. 119064.

Batter, D. and Kessler, J. (1991) ‘Region-specific regulation of preproenkephalin mRNA in cultured astrocytes’, *Molecular Brain Research*, *11*(1), pp. 65-69.

Bennett, M. Bennett, F. Liddelow, S. Ajami, B. Zamanian, J. Fernhoff, N. Mulinyawe, S. Bohlen, C. Adil, A. Tucker, A. and Weissman, I. (2016) ‘New tools for studying microglia in the mouse and human CNS’, *Proceedings of the National Academy of Sciences*, *113*(12), pp. 1738-1746.

Béraud, D. Twomey, M. Bloom, B. Mittereder, A. Ton, V. Neitzke, K. Chasovskikh, S. Mhyre, T. and Maguire-Zeiss, K. (2011) ‘α-Synuclein alters toll-like receptor expression’, *Frontiers in Neuroscience*, *5*, p. 80.

Berglund, R. Guerreiro-Cacais, A. Adzemovic, M. Zeitelhofer, M. Lund, H. Ewing, E. Ruhrmann, S. Nutma, E. Parsa, R. Thessen-Hedreul, M. and Amor, S. (2020) ‘Microglial autophagy–associated phagocytosis is essential for recovery from neuroinflammation’, *Science Immunology*, *5*(52), p. eabb5077.

Blesa, J. Trigo-Damas, I. Quiroga-Varela, A. and Jackson-Lewis, V. (2015) ‘Oxidative stress and Parkinson’s disease’, *Frontiers in Neuroanatomy*, *9*, p. 91.

Bloem, B. Okun, M. and Klein, C. (2021) ‘Parkinson's disease’, *The Lancet*, *397*(10291), pp. 2284-2303.

Booth, H. Hirst, W. and Wade-Martins, R. (2017) ‘The role of astrocyte dysfunction in Parkinson’s disease pathogenesis’, *Trends in Neurosciences*, *40*(6), pp. 358-370.

Bose, S. and Cho, J. (2013) ‘Role of chemokine CCL2 and its receptor CCR2 in neurodegenerative diseases’, *Archives of Pharmacal Research*, *36*, pp. 1039-1050.

Boyle, K. and Randow, F. (2015) ‘Rubicon swaps autophagy for LAP’, *Nature Cell Biology*, *17*(7), pp. 843-845.

Brochard, V. Combadière, B. Prigent, A. Laouar, Y. Perrin, A. Beray-Berthat, V. Bonduelle, O. Alvarez-Fischer, D. Callebert, J. Launay, J. and Duyckaerts, C. (2008) ‘Infiltration of CD4+ lymphocytes into the brain contributes to neurodegeneration in a mouse model of Parkinson disease’, *The Journal of Clinical Investigation*, *119*(1), pp. 182-192.

Burbulla, L. Song, P. Mazzulli, J. Zampese, E. Wong, Y. Jeon, S. Santos, D. Blanz, J. Obermaier, C. Strojny, C. and Savas, J. (2017) ‘Dopamine oxidation mediates mitochondrial and lysosomal dysfunction in Parkinson’s disease’, *Science*, *357*(6357), pp. 1255-1261.

Cahoy, J. Emery, B. Kaushal, A. Foo, L. Zamanian, J. Christopherson, K. Xing, Y. Lubischer, J. Krieg, P. Krupenko, S. and Thompson, W. (2008) ‘A transcriptome database for astrocytes, neurons, and oligodendrocytes: a new resource for understanding brain development and function’, *Journal of Neuroscience*, *28*(1), pp. 264-278.

Castillo-Rangel, C. Marin, G. Hernández-Contreras, K. Vichi-Ramírez, M. Zarate-Calderon, C. Torres-Pineda, O. Diaz-Chiguer, D. De la Mora González, D. Gómez Apo, E. Teco-Cortes, J. and Santos-Paez, F. (2023) ‘Neuroinflammation in Parkinson’s Disease: From Gene to Clinic: A Systematic Review’, *International Journal of Molecular Sciences*, 24(6), p. 5792.

Cavaliere, F. Cerf, L. Dehay, B. Ramos-Gonzalez, P. De Giorgi, F. Bourdenx, M. Bessede, A. Obeso, J. Matute, C. Ichas, F. and Bezard, E. (2017) ‘In vitro α-synuclein neurotoxicity and spreading among neurons and astrocytes using Lewy body extracts from Parkinson disease brains’, *Neurobiology of Disease*, *103*, pp. 101-112.

Chen, X. Tao, T. Liu, X. Wu, W. Wang, J. Yue, T. Li, X. Zhou, Y. Gao, S. Sheng, B. and Peng, Z. (2023) ‘P38-DAPK1 axis regulated LC3-associated phagocytosis (LAP) of microglia

in an in vitro subarachnoid hemorrhage model', *Cell Communication and Signaling*, *21*(1), pp. 1-15.

Chinta, S. and Andersen, J. (2005) 'Dopaminergic neurons', *The international Journal of Biochemistry & Cell Biology*, *37*(5), pp. 942-946.

Chung, W. Clarke, L. Wang, G. Stafford, B. Sher, A. Chakraborty, C. Joung, J. Foo, L. Thompson, A. Chen, C. and Smith, S. (2013) 'Astrocytes mediate synapse elimination through MEGF10 and MERTK pathways', *Nature*, *504*(7480), pp. 394-400.

Clements, R. Fuller, L. Kraemer, K. Radomski, S. Hunter-Chang, S. Hall, W. Kalantar, A. and Kraemer, B. (2022) 'Quantification of Neurite Degeneration with Enhanced Accuracy and Efficiency in an In Vitro Model of Parkinson's Disease', *Eneuro*, *9*(2).

Cornell, J. Salinas, S. Huang, H. and Zhou, M. (2022) 'Microglia regulation of synaptic plasticity and learning and memory', *Neural Regeneration Research*, *17*(4), p. 705.

Crompton, L. McComish, S. Stathakos, P. Cordero-Llana, O. Lane, J. and Caldwell, M. (2021) 'Efficient and scalable generation of human ventral midbrain astrocytes from human-induced pluripotent stem cells', *JoVE (Journal of Visualized Experiments)*, *2*(176), p. e62095.

Crompton, L. McComish, S. Steward, T. Whitcomb, D. Lane, J. and Caldwell, M. (2023) 'Human stem cell-derived ventral midbrain astrocytes exhibit a region-specific secretory profile', *Brain Communications*, *5*(2), p. fcad114.

Cross, J. Durgan, J. McEwan, D. and Florey, O. (2023) 'Lysosome damage triggers direct ATG8 conjugation and ATG2 engagement via CASM', *BioRxiv*, p. e113105

Cunha, L. Yang, M. Carter, R. Guy, C. Harris, L. Crawford, J. Quarato, G. Boada-Romero, E. Kalkavan, H. Johnson, M. and Natarajan, S. (2018) 'LC3-associated phagocytosis in myeloid cells promotes tumor immune tolerance', *Cell*, *175*(2), pp. 429-441.

Damisah, E. Hill, R. Rai, A. Chen, F. Rothlin, C. Ghosh, S. and Grutzendler, J. (2020) ‘Astrocytes and microglia play orchestrated roles and respect phagocytic territories during neuronal corpse removal in vivo’, *Science Advances*, *6*(26), p. eaba3239.

De Biase, L. Schuebel, K. Fusfeld, Z. Jair, K. Hawes, I. Cimbro, R. Zhang, H. Liu, Q. Shen, H, Xi, Z. and Goldman, D. (2017) ‘Local cues establish and maintain region-specific phenotypes of basal ganglia microglia’, *Neuron*, *95*(2), pp. 341-356.

De Miranda, B. Popichak, K. Hammond, S. Miller, J. Safe, S. and Tjalkens, R. (2015) ‘Novel para-phenyl substituted diindolylmethanes protect against MPTP neurotoxicity and suppress glial activation in a mouse model of Parkinson’s disease’, *Toxicological Sciences*, *143*(2), pp. 360-373.

Decressac, M. Volakakis, N. Björklund, A. and Perlmann, T. (2013) ‘NURR1 in Parkinson disease—from pathogenesis to therapeutic potential’, *Nature Reviews Neurology*, *9*(11), pp. 629-636.

Dehay, B. Bové, J. Rodríguez-Muela, N. Perier, C. Recasens, A. Boya, P. and Vila, M. (2010) ‘Pathogenic lysosomal depletion in Parkinson's disease’, *Journal of Neuroscience*, *30*(37), pp. 12535-12544.

Deleidi, M. and Gasser, T. (2013) ‘The role of inflammation in sporadic and familial Parkinson’s disease’, *Cellular and Molecular Life Sciences*, *70*, pp. 4259-4273.

Dias, V. Junn, E. and Mouradian, M. (2013) ‘The role of oxidative stress in Parkinson's disease’, *Journal of Parkinson's Disease*, *3*(4), pp. 461-491.

Dietrich, J. (2002) ‘The adhesion molecule ICAM-1 and its regulation in relation with the blood–brain barrier’, *Journal of Neuroimmunology*, *128*(1-2), pp. 58-68.

Dolan, M. Therrien, M. Jereb, S. Kamath, T. Gazestani, V. Atkeson, T. Marsh, S. Goeva, A. Lojek, N. Murphy, S. and White, C. (2023) ‘Exposure of iPSC-derived human microglia to

brain substrates enables the generation and manipulation of diverse transcriptional states in vitro', *Nature Immunology*, *24*, pp. 1382–1390.

D'Souza, G. Rose, S. Knupp, A. Nicholson, D. Keene, C. and Young, J. (2021) 'The application of in vitro-derived human neurons in neurodegenerative disease modeling', *Journal of Neuroscience Research*, *99*(1), pp. 124-140.

Durgan, J. and Florey, O. (2022) 'Many roads lead to CASM: Diverse stimuli of noncanonical autophagy share a unifying molecular mechanism', *Science Advances*, *8*(43), p. eabo1274.

Durgan, J. Lystad, A. Sloan, K. Carlsson, S. Wilson, M. Marcassa, E. Ulferts, R. Webster, J. Lopez-Clavijo, A. Wakelam, M. and Beale, R. (2021) 'Non-canonical autophagy drives alternative ATG8 conjugation to phosphatidylserine', *Molecular Cell*, *81*(9), pp. 2031-2040.

Elmore, M. Hohsfield, L. Kramár, E. Soreq, L. Lee, R. Pham, S. Najafi, A. Spangenberg, E. Wood, M. West, B. and Green, K. (2018) 'Replacement of microglia in the aged brain reverses cognitive, synaptic, and neuronal deficits in mice', *Aging Cell*, *17*(6), p. e12832.

Fan, Y. and Huo, J. (2021) 'A1/A2 astrocytes in central nervous system injuries and diseases: Angels or devils?', *Neurochemistry International*, *148*, p. 105080.

Fazeli, G. and Wehman, A. (2017) 'Safely removing cell debris with LC3-associated phagocytosis', *Biology of the Cell*, *109*(10), pp. 355-363.

Fearnley, J. and Lees, A. (1991) 'Ageing and Parkinson's disease: substantia nigra regional selectivity', *Brain*, *114*(5), pp. 2283-2301.

Fernández, Á. and López-Otín, C. (2015) 'The functional and pathologic relevance of autophagy proteases', *The Journal of Clinical Investigation*, *125*(1), pp. 33-41.

Festa, B. Siddiqi, F. Jimenez-Sanchez, M. Won, H. Rob, M. Djajadikerta, A. Stamatakou, E. and Rubinsztein, D. (2023) ‘Microglial-to-neuronal CCR5 signaling regulates autophagy in neurodegeneration’, *Neuron*, *111*, pp. 2021–2037

Fimia, G. Kroemer, G. and Piacentini, M. (2013) ‘Molecular mechanisms of selective autophagy’, *Cell Death & Differentiation*, *20*(1), pp. 1-2.

Forno, L. (1996) ‘Neuropathology of Parkinson's disease’, *Journal of Neuropathology & Experimental Neurology*, *55*(3), pp. 259-272.

Friedman, L. Lachenmayer, M. Wang, J. He, L. Poulose, S. Komatsu, M. Holstein, G. and Yue, Z. (2012) ‘Disrupted autophagy leads to dopaminergic axon and dendrite degeneration and promotes presynaptic accumulation of α-synuclein and LRRK2 in the brain’, *Journal of Neuroscience*, *32*(22), pp. 7585-7593.

Frost, L. Lopes, V. Bragin, A. Reyes-Reveles, J. Brancato, J. Cohen, A. Mitchell, C. Williams, D. and Boesze-Battaglia, K. (2015) ‘The contribution of melanoregulin to microtubule-associated protein 1 light chain 3 (LC3) associated phagocytosis in retinal pigment epithelium’, *Molecular Neurobiology*, *52*, pp. 1135-1151.

Fu, A. Hung, K. Yuen, M. Zhou, X. Mak, D. Chan, I. Cheung, T. Zhang, B. Fu, W. Liew, F. and Ip, N. (2016) ‘IL-33 ameliorates Alzheimer’s disease-like pathology and cognitive decline’, *Proceedings of the National Academy of Sciences*, *113*(19), pp. 2705-2713.

Fujita, N. Itoh, T. Omori, H. Fukuda, M. Noda, T. and Yoshimori, T. (2008) ‘The Atg16L complex specifies the site of LC3 lipidation for membrane biogenesis in autophagy’, *Molecular Biology of the Cell*, *19*(5), pp. 2092-2100.

Gandhi, S. and Abramov, A. (2012) ‘Mechanism of oxidative stress in neurodegeneration’, *Oxidative Medicine and Cellular Longevity*, *2012*, p. 428010.

Gao, H. Jiang, J. Wilson, B. Zhang, W. Hong, J. and Liu, B. (2002) ‘Microglial activation-mediated delayed and progressive degeneration of rat nigral dopaminergic neurons: relevance to Parkinson's disease’, *Journal of Neurochemistry*, *81*(6), pp. 1285-1297.

Garcia-Abreu, J. Neto, V. Carvalho, S. and Cavalcante, L. (1995) ‘Regionally specific properties of midbrain glia: I. Interactions with midbrain neurons’, *Journal of Neuroscience Research*, *40*(4), pp. 471-477.

Gelders, G. Baekelandt, V. and Van der Perren, A. (2018) ‘Linking neuroinflammation and neurodegeneration in Parkinson’s disease’, *Journal of Immunology Research*, *2018*, p. 4784268.

Ginhoux, F. Greter, M. Leboeuf, M. Nandi, S. See, P. Gokhan, S. Mehler, M. Conway, S. Ng, L. Stanley, E. and Samokhvalov, I. (2010) ‘Fate mapping analysis reveals that adult microglia derive from primitive macrophages’*, Science, 330*(6005), pp. 841-845.

Glick, D. Barth, S. and Macleod, K. (2010) ‘Autophagy: cellular and molecular mechanisms’, *The Journal of Pathology*, *221*(1), pp. 3-12.

Gordon, R. Giannouli, C. Raparia, C. Bastacky, S. Marinov, A. Hawse, W. Cattley, R. Tilstra, J. Campbell, A. Nickerson, K. and Davidson, A. (2022) ‘Rubicon promotes rather than restricts murine lupus and is not required for LC3-associated phagocytosis’, *JCI insight*, *7*(7), p. e155537.

Grabert, K. Michoel, T. Karavolos, M. Clohisey, S. Baillie, J. Stevens, M. Freeman, T. Summers, K. and McColl, B. (2016) ‘Microglial brain region− dependent diversity and selective regional sensitivities to aging’, *Nature Neuroscience*, *19*(3), pp. 504-516.

Gray, M. and Woulfe, J. (2015) ‘Striatal blood–brain barrier permeability in Parkinson's disease’, *Journal of Cerebral Blood Flow & Metabolism*, *35*(5), pp. 747-750.

Guo, Y. Duan, W. Lu, D. Ma, X. Li, X. Li, Z. Bi, W. Kurihara, H. Liu, H. Li, Y. and He, R. (2021) ‘Autophagy-dependent removal of α-synuclein: a novel mechanism of GM1 ganglioside neuroprotection against Parkinson’s disease’, *Acta Pharmacologica Sinica*, *42*(4), pp. 518-528.

Haenseler, W. Sansom, S. Buchrieser, J. Newey, S. Moore, C. Nicholls, F. Chintawar, S. Schnell, C. Antel, J. Allen, N. and Cader, M. (2017) ‘A highly efficient human pluripotent stem cell microglia model displays a neuronal-co-culture-specific expression profile and inflammatory response’, *Stem Cell Reports*, *8*(6), pp. 1727-1742.

Hall, S. Janelidze, S. Surova, Y. Widner, H. Zetterberg, H. and Hansson, O. (2018) ‘Cerebrospinal fluid concentrations of inflammatory markers in Parkinson’s disease and atypical parkinsonian disorders’, *Scientific Reports*, *8*(1), p. 13276.

Han, X. Sun, S. Sun, Y. Song, Q. Zhu, J. Song, N. Chen, M. Sun, T. Xia, M. Ding, J. and Lu, M. (2019) ‘Small molecule-driven NLRP3 inflammation inhibition via interplay between ubiquitination and autophagy: implications for Parkinson disease’, *Autophagy*, *15*(11), pp. 1860-1881.

Heckmann, B. and Green, D. (2019) ‘LC3-associated phagocytosis at a glance’, *Journal of Cell Science*, *132*(5), p. jcs222984.

Henault, J. Martinez, J. Riggs, J. Tian, J. Mehta, P. Clarke, L. Sasai, M. Latz, E. Brinkmann, M. Iwasaki, A. and Coyle, A. (2012) ‘Noncanonical autophagy is required for type I interferon secretion in response to DNA-immune complexes’, *Immunity*, *37*(6), pp. 986-997.

Hickman, S. Izzy, S. Sen, P. Morsett, L. and El Khoury, J. (2018) ‘Microglia in neurodegeneration’, *Nature Neuroscience*, *21*(10), pp. 1359-1369.

Hooper, K. Jacquin, E. Li, T. Goodwin, J. Brumell, J. Durgan, J. and Florey, O. (2022) 'V-ATPase is a universal regulator of LC3-associated phagocytosis and non-canonical autophagy', *Journal of Cell Biology*, *221*(6), p. e202105112.

Ichimura, Y. Kirisako, T. Takao, T. Satomi, Y. Shimonishi, Y. Ishihara, N. Mizushima, N. Tanida, I. Kominami, E. Ohsumi, M. and Noda, T. (2000) 'A ubiquitin-like system mediates protein lipidation', *Nature*, *408*(6811), pp. 488-492.

Inomata, M. Xu, S. Chandra, P. Meydani, S. Takemura, G. Philips, J. and Leong, J. (2020) 'Macrophage LC3-associated phagocytosis is an immune defense against Streptococcus pneumoniae that diminishes with host aging', *Proceedings of the National Academy of Sciences*, *117*(52), pp. 33561-33569.

Jackson-Lewis, V. Vila, M. Tieu, K. Teismann, P. Vadseth, C. Choi, D. Ischiropoulos, H. and Przedborski, S. (2002) 'Blockade of microglial activation is neuroprotective in the 1-methyl-4-phenyl-1, 2, 3, 6-tetrahydropyridine mouse model of Parkinson disease', *Journal of Neuroscience*, *22*(5), pp. 1763-1771.

Jensen, C. Massie, A. and De Keyser, J. (2013) 'Immune players in the CNS: the astrocyte', *Journal of Neuroimmune Pharmacology*, *8*, pp. 824-839.

Jeon, H. Lee, S. Lee, W. and Suk, K. (2010) 'Analysis of glial secretome: the long pentraxin PTX3 modulates phagocytic activity of microglia', *Journal of Neuroimmunology*, *229*(1-2), pp. 63-72.

Jin, M. Wang, F. Qi, D. Liu, W. Gu, C. Mao, C. Yang, Y. Zhao, Z. Hu, L. and Liu, C. (2018) 'A critical role of autophagy in regulating microglia polarization in neurodegeneration', *Frontiers in Aging Neuroscience*, *10*, p. 378.

Kam, T. Hinkle, J. Dawson, T. and Dawson, V. (2020) 'Microglia and astrocyte dysfunction in Parkinson's disease', *Neurobiology of Disease*, *144*, p. 105028.

Karavanova, I. Vasudevan, K. Cheng, J. and Buonanno, A. (2007) ‘Novel regional and developmental NMDA receptor expression patterns uncovered in NR2C subunit-β-galactosidase knock-in mice’, *Molecular and Cellular Neuroscience*, *34*(3), pp. 468-480.

Kaushik, S. and Cuervo, A. (2018) ‘The coming of age of chaperone-mediated autophagy’, *Nature Reviews Molecular Cell Biology*, *19*(6), pp. 365-381.

Kempuraj, D. Thangavel, R. Natteru, P. Selvakumar, G. Saeed, D. Zahoor, H. Zaheer, S. Iyer, S. and Zaheer, A. (2016) ‘Neuroinflammation induces neurodegeneration’, *Journal of Neurology, Neurosurgery and Spine*, *1*(1), p. 1003.

Kirik, D. Rosenblad, C. Burger, C. Lundberg, C. Johansen, T. Muzyczka, N. Mandel, R. and Björklund, A. (2002) ‘Parkinson-like neurodegeneration induced by targeted overexpression of α-synuclein in the nigrostriatal system’, *Journal of Neuroscience*, *22*(7), pp. 2780-2791.

Kish, S. Tong, J. Hornykiewicz, O. Rajput, A. Chang, L. Guttman, M. and Furukawa, Y. (2008) ‘Preferential loss of serotonin markers in caudate versus putamen in Parkinson's disease’, *Brain*, *131*(1), pp. 120-131.

Kochan, T. Singla, A. Tosi, J. and Kumar, A. (2012) ‘Toll-like receptor 2 ligand pretreatment attenuates retinal microglial inflammatory response but enhances phagocytic activity toward Staphylococcus aureus’, *Infection and Immunity*, *80*(6), pp. 2076-2088.

Konishi, H. Okamoto, T. Hara, Y. Komine, O. Tamada, H. Maeda, M. Osako, F. Kobayashi, M. Nishiyama, A. Kataoka, Y. and Takai, T. (2020) ‘Astrocytic phagocytosis is a compensatory mechanism for microglial dysfunction’, *The EMBO Journal*, *39*(22), p. e104464.

Koprich, J. Reske-Nielsen, C. Mithal, P. and Isacson, O. (2008) ‘Neuroinflammation mediated by IL-1β increases susceptibility of dopamine neurons to degeneration in an animal model of Parkinson's disease’, *Journal of Neuroinflammation*, *5*(1), pp. 1-12.

Koss, K. Churchward, M. Tsui, C. and Todd, K. (2019) ‘In vitro priming and hyper-activation of brain microglia: an assessment of phenotypes’, *Molecular Neurobiology*, *56*, pp. 6409-6425.

Kumar, S. Jia, J. and Deretic, V. (2021) ‘Atg8ylation as a general membrane stress and remodeling response’, *Cell Stress*, *5*(9), p. 128.

Kummer, K. Zeidler, M. Kalpachidou, T. and Kress, M. (2021) ‘Role of IL-6 in the regulation of neuronal development, survival and function’, *Cytokine*, *144*, p. 155582.

Kwon, H. and Koh, S. (2020) ‘Neuroinflammation in neurodegenerative disorders: The roles of microglia and astrocytes’, *Translational Neurodegeneration*, *9*, pp. 1-12.

Lamb, C. Yoshimori, T. and Tooze, S. (2013) ‘The autophagosome: origins unknown, biogenesis complex’, *Nature reviews Molecular Cell Biology*, *14*(12), pp. 759-774.

Larson, M. Gilbert, L. Wang, X. Lim, W. Weissman, J. and Qi, L. (2013) ‘CRISPR interference (CRISPRi) for sequence-specific control of gene expression’, *Nature Protocols*, *8*(11), pp. 2180-2196.

Lashgari, N. Roudsari, N. Momtaz, S. Sathyapalan, T. Abdolghaffari, A. and Sahebkar, A. (2021) ‘The involvement of JAK/STAT signaling pathway in the treatment of Parkinson's disease’, *Journal of Neuroimmunology*, *361*, p. 577758.

Lawrence, J. Schardien, K. Wigdahl, B. and Nonnemacher, M. (2023) ‘Roles of neuropathology-associated reactive astrocytes: A systematic review’, *Acta Neuropathologica Communications*, *11*(1), pp. 1-28.

Lawson, L. Perry, V. Dri, P. and Gordon, S. (1990) ‘Heterogeneity in the distribution and morphology of microglia in the normal adult mouse brain’, *Neuroscience, 39*(1), pp. 151-170.

Lee, C. Daggett, A. Gu, X. Jiang, L. Langfelder, P. Li, X. Wang, N. Zhao, Y. Park, C. Cooper, Y. and Ferando, I. (2018) 'Elevated TREM2 gene dosage reprograms microglia responsivity and ameliorates pathological phenotypes in Alzheimer's disease models', *Neuron*, *97*(5), pp. 1032-1048.

Lee, J. Nam, H. Kim, L. Jeon, Y. Min, H. Ha, S. Lee, Y. Kim, S. Lee, S. Kim, E. and Yu, S. (2019) 'TLR4 (toll-like receptor 4) activation suppresses autophagy through inhibition of FOXO3 and impairs phagocytic capacity of microglia', *Autophagy*, *15*(5), pp. 753-770.

Lee, S. and Chung, W. (2021) 'The roles of astrocytic phagocytosis in maintaining homeostasis of brains', *Journal of Pharmacological Sciences*, *145*(3), pp. 223-227.

Lee, S. Drabik, K. Van Wagoner, N. Lee, S. Choi, C. Dong, Y. and Benveniste, E. (2000) 'ICAM-1-induced expression of proinflammatory cytokines in astrocytes: involvement of extracellular signal-regulated kinase and p38 mitogen-activated protein kinase pathways', *The Journal of Immunology*, *165*(8), pp. 4658-4666.

Lee, V. and Trojanowski, J. (2006) 'Mechanisms of Parkinson's disease linked to pathological α-synuclein: new targets for drug discovery', *Neuron*, *52*(1), pp. 33-38.

Li, Q. Cheng, Z. Zhou, L. Darmanis, S. Neff, N. Okamoto, J. Gulati, G. Bennett, M. Sun, L. Clarke, L. and Marschallinger, J. (2019) 'Developmental heterogeneity of microglia and brain myeloid cells revealed by deep single-cell RNA sequencing', *Neuron*, *101*(2), pp. 207-223.

Li, W. Li, J. and Bao, J. (2012) 'Microautophagy: lesser-known self-eating', *Cellular and Molecular Life Sciences*, *69*, pp. 1125-1136.

Liddelow, S. and Barres, B. (2017) 'Reactive astrocytes: production, function, and therapeutic potential', *Immunity*, *46*(6), pp. 957-967.

Liddelow, S. Guttenplan, K. Clarke, L. Bennett, F. Bohlen, C. Schirmer, L. Bennett, M. Münch, A. Chung, W. Peterson, T. and Wilton, D. (2017) 'Neurotoxic reactive astrocytes are induced by activated microglia', *Nature*, *541*(7638), pp. 481-487.

Linnerbauer, M. and Rothhammer, V. (2020) 'Protective functions of reactive astrocytes following central nervous system insult', *Frontiers in Immunology, 11*, p. 573256.

Lively, S. and Schlichter, L. (2018) 'Microglia responses to pro-inflammatory stimuli (LPS, IFNγ+ TNFα) and reprogramming by resolving cytokines (IL-4, IL-10)', *Frontiers in Cellular Neuroscience*, *12*, p. 215.

Lotharius, J. and Brundin, P. (2002) 'Pathogenesis of Parkinson's disease: dopamine, vesicles and α-synuclein', *Nature Reviews Neuroscience*, *3*(12), pp. 932-942.

MacDonald, V. and Halliday, G. (2002) 'Selective loss of pyramidal neurons in the pre-supplementary motor cortex in Parkinson's disease', *Movement disorders: Official Journal of the Movement Disorder Society*, *17*(6), pp. 1166-1173.

Maday, S. and Holzbaur, E. (2016) 'Compartment-specific regulation of autophagy in primary neurons', *Journal of Neuroscience*, *36*(22), pp. 5933-5945.

Martin, E. El-Behi, M. Fontaine, B. and Delarasse, C. (2017) 'Analysis of microglia and monocyte-derived macrophages from the central nervous system by flow cytometry', *JoVE (Journal of Visualized Experiments)*, *124*, p. e55781.

Martinez, J. (2018) 'LAP it up, fuzz ball: a short history of LC3-associated phagocytosis', *Current opinion in Immunology*, *55*, pp. 54-61.

Martinez, J. Almendinger, J. Oberst, A. Ness, R. Dillon, C. Fitzgerald, P. Hengartner, M. and Green, D. (2011) 'Microtubule-associated protein 1 light chain 3 alpha (LC3)-associated phagocytosis is required for the efficient clearance of dead cells', *Proceedings of the National Academy of Sciences*, *108*(42), pp. 17396-17401.

Martinez, J. Cunha, L. Park, S. Yang, M. Lu, Q. Orchard, R. Li, Q. Yan, M. Janke, L. Guy, C. and Linkermann, A. (2016) 'RETRACTED ARTICLE: Noncanonical autophagy inhibits the autoinflammatory, lupus-like response to dying cells', *Nature*, *533*(7601), pp. 115-119.

Martinez, J. Malireddi, R. Lu, Q. Cunha, L. Pelletier, S. Gingras, S. Orchard, R. Guan, J. Tan, H. Peng, J. and Kanneganti, T. (2015) 'Molecular characterization of LC3-associated phagocytosis reveals distinct roles for Rubicon, NOX2 and autophagy proteins', *Nature Cell Biology*, *17*(7), pp. 893-906.

Martinez-Vicente, M. Talloczy, Z. Kaushik, S. Massey, A. Mazzulli, J. Mosharov, E. Hodara, R. Fredenburg, R. Wu, D. Follenzi, A. and Dauer, W. (2008) 'Dopamine-modified α-synuclein blocks chaperone-mediated autophagy', *The Journal of Clinical Investigation*, *118*(2), pp. 777-788.

Masud, S. Prajsnar, T. Torraca, V. Lamers, G. Benning, M. Van Der Vaart, M. and Meijer, A. (2019) 'Macrophages target Salmonella by Lc3-associated phagocytosis in a systemic infection model', *Autophagy*, *15*(5), pp. 796-812.

Matejuk, A. and Ransohoff, R. (2020) 'Crosstalk between astrocytes and microglia: an overview', *Frontiers in Immunology*, *11*, p. 1416.

Matheoud, D. Cannon, T. Voisin, A. Penttinen, A. Ramet, L. Fahmy, A. Ducrot, C. Laplante, A. Bourque, M. Zhu, L. and Cayrol, R. (2019) 'Intestinal infection triggers Parkinson's disease-like symptoms in Pink1−/− mice', *Nature*, *571*(7766), pp. 565-569.

McGeer, P. Itagaki, S. Boyes, B. and McGeer, E. (1988) 'Reactive microglia are positive for HLA-DR in the substantia nigra of Parkinson's and Alzheimer's disease brains', *Neurology*, *38*(8), pp. 1285-1285.

McGeer, P. Kawamata, T. Walker, D. Akiyama, H. Tooyama, I. and McGeer, E. (1993) 'Microglia in degenerative neurological disease', *Glia*, *7*(1), pp. 84-92.

Mertens, J. Reid, D. Lau, S. Kim, Y. and Gage, F. (2018) ‘Aging in a dish: iPSC-derived and directly induced neurons for studying brain aging and age-related neurodegenerative diseases’, *Annual Review of Genetics*, *52*, pp. 271-293.

Metcalf, D. García-Arencibia, M. Hochfeld, W. and Rubinsztein, D. (2012) ‘Autophagy and misfolded proteins in neurodegeneration’, *Experimental Neurology*, *238*(1), pp. 22-28.

Milner, R. and Campbell, I. (2003) ‘The extracellular matrix and cytokines regulate microglial integrin expression and activation’, *The Journal of Immunology*, *170*(7), pp. 3850-3858.

Miyazaki, I. and Asanuma, M. (2020) ‘Neuron-astrocyte interactions in Parkinson’s disease’, *Cells*, *9*(12), p. 2623.

Mizushima, N. (2007) ‘Autophagy: process and function’, *Genes & Development*, *21*(22), pp. 2861-2873.

Mizushima, N. (2010) ‘The role of the Atg1/ULK1 complex in autophagy regulation’, *Current Opinion in Cell Biology*, *22*(2), pp. 132-139.

Molofsky, A. and Deneen, B. (2015) ‘Astrocyte development: a guide for the perplexed’, *Glia, 63*(8), pp. 1320-1329.

Montgomery, D. (1994) ‘Astrocytes: form, functions, and roles in disease’, *Veterinary Pathology*, *31*(2), pp. 145-167.

Moore, J. Mistry, J. Hellmich, C. Horton, R. Wojtowicz, E. Jibril, A. Jefferson, M. Wileman, T. Beraza, N. Bowles, K. and Rushworth, S. (2022) ‘LC3-associated phagocytosis in bone marrow macrophages suppresses acute myeloid leukemia progression through STING activation’, *The Journal of Clinical Investigation*, *132*(5), p. e153157.

Moore, R. (2003) ‘Organization of midbrain dopamine systems and the pathophysiology of Parkinson's disease’, *Parkinsonism & Related Disorders*, *9*, pp. 65-71.

Müller, M. and Bohnen, N. (2013) ‘Cholinergic dysfunction in Parkinson’s disease’. *Current Neurology and Neuroscience Reports*, *13*, pp. 1-9.

Nahimi, A. Sommerauer, M. Kinnerup, M. Østergaard, K. Wintherdahl, M. Jacobsen, J. Schacht, A. Johnsen, B. Damholdt, M. Borghammer, P. and Gjedde, A. (2018) ‘Noradrenergic deficits in Parkinson disease imaged with 11C-MeNER’, *Journal of Nuclear Medicine*, *59*(4), pp. 659-664.

Nakatogawa, H. (2013) ‘Two ubiquitin-like conjugation systems that mediate membrane formation during autophagy’, *Essays in Biochemistry*, *55*, pp. 39-50.

Nguyen, M. Wong, Y. Ysselstein, D. Severino, A. and Krainc, D. (2019) ‘Synaptic, mitochondrial, and lysosomal dysfunction in Parkinson’s disease’, *Trends in Neurosciences*, *42*(2), pp. 140-149.

Nishida, Y. Arakawa, S. Fujitani, K. Yamaguchi, H. Mizuta, T. Kanaseki, T. Komatsu, M. Otsu, K. Tsujimoto, Y. and Shimizu, S. (2009) ‘Discovery of Atg5/Atg7-independent alternative macroautophagy’, *Nature*, *461*(7264), pp. 654-658.

Nishikawa, S. Goldstein, R. and Nierras, C. (2008) ‘The promise of human induced pluripotent stem cells for research and therapy’, *Nature Reviews Molecular Cell Biology*, *9*(9), pp. 725-729.

Noelker, C. Morel, L. Lescot, T. Osterloh, A. Alvarez-Fischer, D. Breloer, M. Henze, C. Depboylu, C. Skrzydelski, D. Michel, P. and Dodel, R. (2013) ‘Toll like receptor 4 mediates cell death in a mouse MPTP model of Parkinson disease’, *Scientific Reports*, *3*(1), p. 1393.

Ohgita, T. Namba, N. Kono, H. Shimanouchi, T. and Saito, H. (2022) ‘Mechanisms of enhanced aggregation and fibril formation of Parkinson’s disease-related variants of α-synuclein’, *Scientific Reports*, *12*(1), p. 6770.

Phani, S. Loike, J. and Przedborski, S. (2012) ‘Neurodegeneration and inflammation in Parkinson's disease’, *Parkinsonism & Related Disorders*, *18*, pp. 207-209.

Polymeropoulos, M. Lavedan, C. Leroy, E. Ide, S. Dehejia, A. Dutra, A. Pike, B. Root, H. Rubenstein, J. Boyer, R. and Stenroos, E. (1997) ‘Mutation in the α-synuclein gene identified in families with Parkinson's disease’, *Science*, *276*(5321), pp. 2045-2047.

Proikas-Cezanne, T. Takacs, Z. Dönnes, P. Kohlbacher, O. (2015) ‘WIPI proteins: essential PtdIns3 P effectors at the nascent autophagosome’, *Journal of Cell Science*, *128*(2), pp. 207-217.

Przedborski, S. (2007) ‘Neuroinflammation and Parkinson's disease’, *Handbook of Clinical Neurology*, *83*, pp. 535-551.

Qu, Y. Li, J. Qin, Q. Wang, D. Zhao, J. An, K. Mao, Z. Min, Z. Xiong, Y. Li, J. and Xue, Z. (2023) ‘A systematic review and meta-analysis of inflammatory biomarkers in Parkinson’s disease’, *npj Parkinson's Disease*, *9*(1), p. 18.

Raiders, S. Han, T. Scott-Hewitt. N, Kucenas, S. Lew, D. Logan, M. and Singhvi, A. (2021) ‘Engulfed by glia: glial pruning in development, function, and injury across species’, *Journal of Neuroscience*, *41*(5), pp. 823-833.

Nakamura, Y. Si, Q. and Kataoka, K. (1999) ‘Lipopolysaccharide-induced microglial activation in culture: temporal profiles of morphological change and release of cytokines and nitric oxide’, *Neuroscience Research*, *35*(2), pp. 95-100.

Rao, D. Senzer, N. Cleary, M. and Nemunaitis, J. (2009) ‘Comparative assessment of siRNA and shRNA off target effects: what is slowing clinical development’, *Cancer Gene Therapy*, *16*(11), pp. 807-809.

Ray, S. Singh, N. Kumar, R. Patel, K. Pandey, S. Datta, D. Mahato, J. Panigrahi, R. Navalkar, A. Mehra, S. and Gadhe, L. (2020) ‘α-Synuclein aggregation nucleates through liquid–liquid phase separation’. *Nature Chemistry*, *12*(8), pp. 705-716.

Reemst, K. Noctor, S. Lucassen, P. and Hol, E. (2016) ‘The indispensable roles of microglia and astrocytes during brain development’, *Frontiers in Human Neuroscience*, *10*, p. 566.

Reggiori, F.(2006) ‘Membrane origin for autophagy’, *Current Topics in Developmental Biology*, *74*, pp. 1-30.

Reuss, B. Leung, D. Ohlemeyer, C. Kettenmann, H. and Unsicker, K. (2000) ‘Regionally distinct regulation of astroglial neurotransmitter receptors by fibroblast growth factor 2’, *Molecular and Cellular Neuroscience*, *16*(1), pp. 42-58.

Rodriguez-Grande, B. Swana, M. Nguyen, L. Englezou, P. Maysami, S. Allan, S. Rothwell, N. Garlanda, C. Denes, A. and Pinteaux, E. (2014) ‘The acute-phase protein PTX3 is an essential mediator of glial scar formation and resolution of brain edema after ischemic injury’, *Journal of Cerebral Blood Flow & Metabolism*, *34*(3), pp. 480-488.

Romao, S. and Münz, C. (2014) ‘LC3-associated phagocytosis’, *Autophagy*, *10*(3), pp. 526-528.

Roodveldt, C. Christodoulou, J. and Dobson, C. (2008) ‘Immunological features of α-synuclein in Parkinson's disease’, *Journal of Cellular and Molecular Medicine*, *12*(5b), pp. 1820-1829.

Rossol, M. Heine, H. Meusch, U. Quandt, D. Klein, C. Sweet, M. and Hauschildt, S. (2011) ‘LPS-induced cytokine production in human monocytes and macrophages’, *Critical Reviews™ in Immunology*, *31*(5).

Sahoo, S. Padhy, A. Kumari, V. and Mishra, P. (2022) ‘Role of Ubiquitin–Proteasome and Autophagy-Lysosome Pathways in α-Synuclein Aggregate Clearance’, *Molecular Neurobiology*, *59*(9), pp. 5379-5407.

Sanjuan, M. Dillon, C. Tait, S. Moshiach, S. Dorsey, F. Connell, S. Komatsu, M. Tanaka, K. Cleveland, J. Withoff, S. and Green, D. (2007) ‘Toll-like receptor signalling in macrophages links the autophagy pathway to phagocytosis’, *Nature*, *450*(7173), pp. 1253-1257.

Sato, S. Uchihara, T. Fukuda, T. Noda, S. Kondo, H. Saiki, S. Komatsu, M. Uchiyama, Y. Tanaka, K. and Hattori, N. (2018) ‘Loss of autophagy in dopaminergic neurons causes Lewy pathology and motor dysfunction in aged mice’, *Scientific Reports*, *8*(1), p. 2813.

Scalzo, P. Kümmer, A. Cardoso, F. and Teixeira, A. (2010) ‘Serum levels of interleukin-6 are elevated in patients with Parkinson's disease and correlate with physical performance’, *Neuroscience Letters*, *468*(1), pp. 56-58.

Schapira, A. Chaudhuri, K. and Jenner, P. (2017) ‘Non-motor features of Parkinson disease’, *Nature Reviews Neuroscience*, *18*(7), pp. 435-450.

Sevenich, L. (2018) ‘Brain-resident microglia and blood-borne macrophages orchestrate central nervous system inflammation in neurodegenerative disorders and brain cancer’, *Frontiers in Immunology*, *9*, p. 697.

Simon, D. Tanner, C. and Brundin, P. (2020) ‘Parkinson disease epidemiology, pathology, genetics, and pathophysiology’, *Clinics in Geriatric Medicine*, *36*(1), pp. 1-12.

Sinha, A. Kushwaha, R. Molesworth, K. Mychko, O. Makarava, N. and Baskakov, I. (2021) ‘Phagocytic activities of reactive microglia and astrocytes associated with prion diseases are dysregulated in opposite directions’, *Cells*, *10*(7), p. 1728.

Sioud, M. (2005) ‘Induction of inflammatory cytokines and interferon responses by double-stranded and single-stranded siRNAs is sequence-dependent and requires endosomal localization’, *Journal of Molecular Biology*, *348*(5), pp. 1079-1090.

Sokolowski, J. and Mandell, J. (2011) ‘Phagocytic clearance in neurodegeneration’, *The American Journal of Pathology*, *178*(4), pp. 1416-1428.

Speicher, A. Wiendl, H. Meuth, S. and Pawlowski, M. (2019) ‘Generating microglia from human pluripotent stem cells: novel in vitro models for the study of neurodegeneration’, *Molecular Neurodegeneration*, *14*(1), pp. 1-16.

Spillantini, M. Crowther, R. Jakes, R. Hasegawa, M. Goedert, M. (1998) ‘alpha-Synuclein in filamentous inclusions of Lewy bodies from Parkinson's disease and dementia with lewy bodies’, *Proceedings of the National Academy of Sciences*, *95*(11), pp. 6469-6473.

Stathakos, P. Jiménez-Moreno, N. Crompton, L. Nistor, P. Badger, J. Barbuti, P. Kerrigan, T. Randall, A. Caldwell, M. and Lane, J. (2021) ‘A monolayer hiPSC culture system for autophagy/mitophagy studies in human dopaminergic neurons’, *Autophagy*, *17*(4), pp. 855-871.

Stokholm, M. Iranzo, A. Østergaard, K. Serradell, M. Otto, M. Svendsen, K. Garrido, A. Vilas, D. Borghammer, P. Santamaria, J. and Møller, A. (2017) ‘Assessment of neuroinflammation in patients with idiopathic rapid-eye-movement sleep behaviour disorder: a case-control study’, *The Lancet Neurology*, *16*(10), pp. 789-796.

Subhramanyam, C. Wang, C. Hu, Q. and Dheen, S. (2019) ‘Microglia-mediated neuroinflammation in neurodegenerative diseases’, *Seminars in Cell & Developmental Biology*, *94*, pp. 112-120.

Sulzer, D. and Edwards, R. (2019) ‘The physiological role of α-synuclein and its relationship to Parkinson’s Disease’, *Journal of Neurochemistry*, *150*(5), pp. 475-486.

Sveinbjornsdottir, S. (2016) ‘The clinical symptoms of Parkinson's disease’, *Journal of Neurochemistry*, *139*, pp. 318-324.

Szabó, Á. Vincze, V. Chhatre, A. Jipa, A. Bognár, S. Varga, K. Banik, P. Harmatos-Ürmösi, A. Neukomm, L. and Juhász, G. (2023) ‘LC3-associated phagocytosis promotes glial degradation of axon debris after injury in Drosophila models’, *Nature Communications*, *14*(1), p. 3077.

Tagliafierro, L. and Chiba-Falek, O. (2016) ‘Up-regulation of SNCA gene expression: implications to synucleinopathies’, *Neurogenetics*, *17*, pp. 145-157.

Tasdemir-Yilmaz, O. and Freeman, M. (2014) ‘Astrocytes engage unique molecular programs to engulf pruned neuronal debris from distinct subsets of neurons’, *Genes & Developmen*t, *28*(1), pp. 20-33

Tay, T. Savage, J. Hui, C. Bisht, K. and Tremblay, M. (2017) ‘Microglia across the lifespan: from origin to function in brain development, plasticity and cognition’, *The Journal of Physiology*, *595*(6), pp. 1929-1945.

Torper, O. Pfisterer, U. Wolf, D. Pereira, M. Lau, S. Jakobsson, J. Björklund, A. Grealish, S. and Parmar, M. (2013) ‘Generation of induced neurons via direct conversion in vivo’, *Proceedings of the National Academy of Sciences*, *110*(17), pp. 7038-7043.

Trainer, T. (2021) ‘Glial autophagy capability and the control of neuroinflammatory signalling in Parkinson’s disease’, University of Bristol.

Tremblay, M. Cookson, M. and Civiero, L. (2019) ‘Glial phagocytic clearance in Parkinson’s disease’, *Molecular Neurodegeneration*, *14*, pp. 1-14.

Truban, D. Hou, X. Caulfield, T. Fiesel, F. and Springer, W. (2017) ‘PINK1, Parkin, and mitochondrial quality control: what can we learn about Parkinson’s disease pathobiology?’, *Journal of Parkinson's disease*, *7*(1), pp. 13-29.

Tu, H. Yuan, B. Hou, X. Zhang, X. Pei, C. Ma, Y. Yang, Y. Fan, Y. Qin, Z. Liu, C. and Hu, L. (2021) ‘α-synuclein suppresses microglial autophagy and promotes neurodegeneration in a mouse model of Parkinson’s disease’, *Aging Cell*, *20*(12), p. e13522.

Wakida, N. Lau, A. Nguyen, J. Cruz, G. Fote, G. Steffan, J. Thompson, L. and Berns, M. (2022) ‘Diminished LC3-associated phagocytosis by Huntington’s disease striatal astrocytes’, *Journal of Huntington's Disease*, *11*(1), pp. 25-33.

Wan, J. Weiss, E. Ben Mkaddem, S. Mabire, M. Choinier, P. Thibault-Sogorb, T. Hegde, P. Bens, M. Broer, L. Gilgenkrantz, H. and Moreau, R. (2020) ‘LC3-associated phagocytosis in myeloid cells, a fireman that restrains inflammation and liver fibrosis, via immunoreceptor inhibitory signaling’, *Autophagy*, *16*(8), pp. 1526-1528.

Williams-Gray, C. Wijeyekoon, R. Yarnall, A. Lawson, R. Breen, D. Evans, J. Cummins, G. Duncan, G. Khoo, T. Burn, D. and Barker, R. (2016) ‘Serum immune markers and disease progression in an incident Parkinson's disease cohort (ICICLE-PD)’, *Movement Disorders*, *31*(7), pp. 995-1003.

Xu, J. Kao, S. Lee, F. Song, W. Jin, L. and Yankner, B. (2002) ‘Dopamine-dependent neurotoxicity of α-synuclein: a mechanism for selective neurodegeneration in Parkinson disease’, *Nature Medicine*, *8*(6), pp. 600-606.

Yamamoto, H. Kakuta, S. Watanabe, T. Kitamura, A. Sekito, T. Kondo-Kakuta, C. Ichikawa, R. Kinjo, M. and Ohsumi, Y. (2012) ‘Atg9 vesicles are an important membrane source during early steps of autophagosome formation’, *Journal of Cell Biology*, *198*(2), pp. 219-233.

Yan, J. Fu, Q. Cheng, L. Zhai, M. Wu, W. Huang, L. and Du, G. (2014) ‘Inflammatory response in Parkinson's disease’, *Molecular Medicine Reports*, *10*(5), pp. 2223-2233.

Yates, D. (2015) ‘Factoring in astrocytes’, *Nature Reviews Neuroscience*, *16*(2), pp. 67-67.

Yun, S. Kam, T. Panicker, N. Kim, S. Oh, Y. Park, J. Kwon, S. Park, Y. Karuppagounder, S. Park, H. and Kim, S. (2018) 'Block of A1 astrocyte conversion by microglia is neuroprotective in models of Parkinson's disease', *Nature Medicine*, *24*(7), pp. 931-938.

Zaffagnini, G. and Martens, S. (2016) 'Mechanisms of selective autophagy', *Journal of Molecular Biology*, *428*(9), pp. 1714-1724.

Zhang, W. Wang, T. Pei, Z. Miller, D. Wu, X. Block, M. Wilson, B. Zhang, W. Zhou, Y. Hong, J. and Zhang, J. (2005) 'Aggregated α-synuclein activates microglia: a process leading to disease progression in Parkinson's disease', *The FASEB Journal*, *19*(6), pp. 533-542.

Zhang, Y. and Barres, B. (2010) 'Astrocyte heterogeneity: an underappreciated topic in neurobiology', *Current Opinion in Neurobiology*, *20*(5), pp. 588-594.

Zhong, Y. Wang, Q. Li, X. Yan, Y. Backer, J. Chait, B. Heintz, N. and Yue, Z. (2009) 'Distinct regulation of autophagic activity by Atg14L and Rubicon associated with Beclin 1–phosphatidylinositol-3-kinase complex', *Nature Cell Biology*, *11*(4), pp. 468-476.

Zhou, T. Li, Y. Li, X. Zeng, F. Rao, Y. He, Y. Wang, Y. Liu, M. Li, D. Xu, Z. and Zhou, X. (2022) 'Microglial debris is cleared by astrocytes via C4b-facilitated phagocytosis and degraded via RUBICON-dependent noncanonical autophagy in mice', *Nature Communications*, *13*(1), p. 6233.